



THE HONG KONG
POLYTECHNIC UNIVERSITY

香港理工大學

Pao Yue-kong Library

包玉剛圖書館

Copyright Undertaking

This thesis is protected by copyright, with all rights reserved.

By reading and using the thesis, the reader understands and agrees to the following terms:

1. The reader will abide by the rules and legal ordinances governing copyright regarding the use of the thesis.
2. The reader will use the thesis for the purpose of research or private study only and not for distribution or further reproduction or any other purpose.
3. The reader agrees to indemnify and hold the University harmless from and against any loss, damage, cost, liability or expenses arising from copyright infringement or unauthorized usage.

If you have reasons to believe that any materials in this thesis are deemed not suitable to be distributed in this form, or a copyright owner having difficulty with the material being included in our database, please contact lbsys@polyu.edu.hk providing details. The Library will look into your claim and consider taking remedial action upon receipt of the written requests.

Development of Recombinant Human Augmenter of Liver
Regeneration (ALR) for Treatment of Liver Diseases

A thesis submitted

to

Department of Applied Biology and Chemical Technology

and

Research Degree Committee

The Hong Kong Polytechnic University

In partial fulfillment of the requirement for the degree of

MASTER OF PHILOSOPHY

by

Chan Chi Leong

December 2005

Certificate of Originality

I hereby declare that this thesis is my own work and that, to the best of my knowledge and belief, it reproduces no material previously published or written, nor material that has been accepted for the award of any other degree or diploma, except where due acknowledgment has been made in the text.

Chan Chi Leong

December 2005

Abstract

Augmenter of liver regeneration (ALR; Hepatopoietin) is a novel hepatotrophic growth factor that stimulates hepatocyte proliferation by two pathways. Human ALR (hALR) is a protein that consists of 125 amino acids and its gene has been mapped on chromosome 16 next to the Polycystic Kidney Disease gene (*PKD1*). ALR belongs to Erv1p/ALR protein family, whose members have essential functions in the biogenesis of mitochondria. ALR has also been identified as a FAD-linked sulfhydryl oxidase. As ALR has the ability to stimulate hepatocyte proliferation and protect the liver in a liver specific manner, it is a potential drug for liver diseases.

In this project, we have successfully produced several polyhistidine-tagged hALR proteins in *Escherichia coli* expression system. This approach allows single-step affinity purification. The result demonstrated that addition of 12 histidines molecules to the C-terminus of ALR is the best design by which about 330 mg/L of hALR was obtained from 2-L fermentation culture with 95% purity. The *in vitro* specificity and biological activity of the modified hALR in promoting liver cell growth were found to be similar to those of hepatocyte

growth-promoting factor (pHGF), a commercially available drug in China to treat liver failure. Moreover, the modified hALR protein also possesses the sulfhydryl oxidase activity.

Recombinant hALR proteins are not very soluble and readily precipitated in phosphate buffer saline (PBS) or elution buffer. To overcome this problem, the ALR was buffer exchanged into a special solution. The solubility of protein was increased by 50 times from 0.02 mg/ml to 1 mg/ml. Another solution to increase its solubility in MilliQ water was to modify the protein with polyethylene glycol (PEG) to produce pegylated hALR. The pegylated protein was fully active in terms of biological activity and sulfhydryl oxidase activity. These data suggest that modified ALR proteins are effective in hepatocyte regeneration.

Table of contents

Abstract		
Acknowledgments	iv	
Abbreviations	vi	
List of figures and tables	ix	
<u>Chapter One: Introduction</u>		
1.1	Liver diseases	2
1.2	Liver regeneration	5
1.3	Hepatic stimulator substance (HSS)	10
1.3.1	Human augments of liver regeneration (rALR)	14
1.3.1.1	Proposed working mechanism of ALR	17
1.3.2	HPO-205	21
1.3.3	Hepatocyte growth-promoting factor (pHGF)	24
1.4	Epidermal growth factor (EGF)	26
1.5	ERV/ALR protein family	
1.5.1	<i>Saccharomyces cerevisiae</i> ERV1 protein	31
1.6	Polyhistidine tag	33
1.7	Protein pegylation technology	34
1.8	Objectives	36
<u>Chapter Two: Methodology</u>		
2.1	Construction of recombinant hALR	38
2.2	Small scale production of recombinant ALR proteins	
2.2.1	Shake flask culture	41
2.2.2	Purification of recombinant human ALR	
2.2.2.1	Purification of 0ALR0	42
2.2.2.2	Purification of 0ALR6, 0ALR12 and 0ALR18	43
2.2.3	Buffer exchange	44
2.2.4	Freeze-drying	45
2.3	Characterizations of recombinant ALR	
2.3.1	Solubility test	
2.3.1.1	Sodium Dodecyl Sulfate Polyacrylamide Gel Electrophoresis (SDS/PAGE)	46
2.3.1.2	Western blotting	48
2.3.2	Protein assay	50
2.3.3	Far-UV circular dichroism (CD) analysis	50

2.3.4	Mass spectrometry analysis	51
2.3.5	Isoelectric focusing	53
2.3.6	FAD content measurement	
2.3.6.1	Spectroscopy of recombinant ALR	54
2.3.6.2	Release of protein-bound FAD by heat and acid treatment	54
2.3.7	Solubility of 0ALR12 in various buffers	55
2.3.8	Activity assay	
2.3.8.1	Enzyme assay for sulfhydryl oxidase activity	56
2.3.8.2	Cell proliferation activity test of recombinant ALR	57
2.4	Pegylation of recombinant ALR	58
2.4.1	Pegylation of ALR with different PEG molecules	59
2.4.2	Pegylation of ALR with mPEG-MAL in different mole ratios	61
2.5	Pilot scale production of recombinant ALR	
2.5.1	Fed-batch fermentation	62
2.5.2	Purification of ALR	63

Chapter Three: Results

3.1	Small scale production of recombinant ALR in <i>Escherichia coli</i>	
3.1.1	Expression of recombinant ALR	65
3.1.2	Purification of recombinant ALR	
3.1.2.1	Purification of 0ALR0	72
3.1.2.2	Purification of 0ALR6	75
3.1.2.3	Purification of 0ALR12	78
3.1.2.4	Purification of 0ALR18	81
3.2	Characterizations of recombinant human ALR	
3.2.1	Solubility test	84
3.2.2	Dimer formation	86
3.2.3	Far-UV circular dichroism (CD) analysis	88
3.2.4	Isoelectric focusing	90
3.2.5	FAD content measurement	
3.2.5.1	Spectroscopy of recombinant ALR	92
3.2.5.2	Release of protein-bound FAD by heat and acid treatment	94
3.2.6	Mass-spectrometry analysis	97
3.2.7	Solubility of 0ALR12 in various buffers	100
3.2.8	Activity assay	
3.2.8.1	Sulfhydryl oxidase activity	102
3.2.8.2	Cell proliferation activity test	105
3.3	Pegylation of recombinant ALR	

3.3.1	Pegylation of ALR with different PEG molecules	112
3.3.2	Pegylation of ALR with mPEG-MAL in different mole ratios	117
3.4	Pilot scale production of recombinant ALR	121
3.4.1	Fed-batch fermentation	121
 <u>Chapter Four: Discussion</u>		
4.1	Small scale production and purification of ALR	127
4.2	Optimization of ALR production	129
4.3	ALR solubility	130
4.4	Dimer formation	132
4.5	Pegylation of ALR	133
4.6	Characterization of the recombinant human ALR	
4.6.1	Far-UV circular dichroism (CD) analysis	138
4.6.2	Spectroscopy of recombinant ALR	139
4.6.3	Sulfhydryl oxidase activity	140
4.6.4	Cell proliferation activity test	141
4.7	Summary of the properties of ALR proteins	143
4.8	Pilot scale production of ALR in fed-batch fermentation	145
 <u>Chapter Five: Future work</u>		147
 <u>Chapter Six: Conclusion</u>		150
 <u>References</u>		153

Acknowledgments

I am deeply indebted to my supervisor, Dr. Y. C. Leung, Thomas, for his support, guidance and valuable discussion. He has been patient to help me and gave advice for solving problems about my project. I am very grateful to my co-supervisor Dr. W. H. Lo, Thomas, for his helpful suggestions and supervision throughout the course of my study.

I would like to express my heartfelt gratitude to Dr. W. N. Ye for his excellent idea and the grant for this project. Without his help and guidance, this project would not have been possible.

I am thankful to Dr. H. B. Liu for the early development and his support in this project. I would like to thank Kareena Tsang for constructing the ALR proteins and her excellent assistance and suggestion. I also want to thank Johnson Choi for doing the fermentation as well as giving help in this project. Finally, I would like to acknowledge all my friends in the laboratory, including Law Kin Ho, Alan Lam, Alex Tsang, Anthony Cheng, Sammi Tsui, Lam Wai Man, Emily Tsang, Kelvin Chung, Yap Hong Kin, So Pui Kin and Panda Au for their help and support. I would like to thank all the laboratory technicians, Mr. Cheng, Sarah

Yeung, Ivy Toa, Sharon Chan and especially Mabel Yau for their assistance in the laboratory.

Abbreviations

ABC	ATP-binding cassette
ALR	Augmenter of liver regeneration
ALT	alanine transferase
Arg	Arginine
AP-1	Activating protein 1
AqpZ	Aquaporin Z
ATP	Adenosine triphosphate
Ax	Absorbance at a wavelength of x nm
BSA	Bovine serum albumin
CD	Circular dichroism
DG	Diacylglycerol
DMEM	Dulbecco's modified Eagle's medium
DNA	Deoxyribonucleic acid
DTNB	5,5'-dithiobis(2-nitrobenzoic acid)
<i>E. coli</i>	<i>Escherichia coli</i>
ECM	Extra-cellular matrix
EGF	Epidermal growth factor
EGFR	Epidermal growth factor receptor
ERV1	Essential for respiration and vegetative growth
FAD	Flavin adenine dinucleotide
Gln	Glutamine
h	Hour/ Hours
HBV	Hepatitis B virus

HCC	Hepatocellular carcinoma
HGF	Hepatocyte growth factor
His	Histidine
HPLC	High Performance Liquid Chromatography
HPO	Hepatopoietin
HSC	Hepatic stellate cells
HSS	Hepatic stimulator substance
IEF	Isoelectric focusing
IL-6	Interleukin-6
IP-3	Inositol 1,4,5-trisphosphate
ISC	Iron-sulfur cluster
JAB1	Jun activation domain-binding protein 1
MAPK	Mitogen-activated protein kinase
mAU	Absorbance units
MEK	Mitogen-activated, ERK-activated kinase
min	Minute/ Minutes
mPEG-ALD	Methoxy-polyethylene glycol-propionaldehyde
mPEG-MAL	Methoxy-polyethylene glycol-maleimide
mPEG-NHS	Methoxy-polyethylene glycol-N-hydroxysuccinimide
mPEG-SPA	Methoxy-polyethylene glycol succinimidyl propionate
MW	Molecular weight
NASH	Non-alcoholic Steatohepatitis
NK	Natural killer
OD	Optical density
PBS	Phosphate buffer saline

PCR	Polymerase chain reaction
PCS	Porta-cava shunt
PEG	Polyethylene glycol
PH	Partial-hepatectomy
pHGF	Hepatocyte growth-promoting factor
PLC γ	phospholipase C γ
PKC	Protein kinase C
<i>PKD1</i>	Polycystic Kidney Disease gene
rpm	Revolution per minute
s	Second/ Seconds
SB	Serum bilirubin
SDS-PAGE	Polyacrylamide gel electrophoresis in the presence of SDS
STAT3	Signal transducer and activator of transcription 3
TEMED	N, N, N', N' - Tetramethyl- ethylenediamine
TFF	Tangential flow filtration
TGF- α	Transforming growth factor-alpha
Tris-HCl	Tris(hydroxymethyl)aminomethane, pH adjusted with HCl
TNF	Tumor necrosis factor
UV	Ultra-violet light

List of figures and tables

List of figures

Fig. 1.1	Liver regeneration after two-thirds surgical partial-hepatectomy (PH)	6
Fig. 1.2	Diagrammatic outline of the key cellular elements and their location in the histological architecture of the hepatic lobule	9
Fig. 1.3	The three-dimensional structure of the rat ALR	13
Fig. 1.4	Sequence alignment of yeast (sc) and the putative human (h) ERV1 or named ALR proteins	16
Fig. 1.5	Amino acid sequence alignment of HPO-205 and ALR	23
Fig. 1.6	The protein sequence of human epidermal growth factor	27
Fig. 1.7	The EGFR signaling mechanism	30
Fig. 2.1	Structure of polyethylene glycol (PEG) molecules with different derivatives	60
Fig. 3.1	Growth of the <i>E.coli</i> strain BL21(DE3)pLysS in shake-flask	67
Fig. 3.2	12% SDS-PAGE analysis showing the protein (0ALR0) expression at different time point	68
Fig. 3.3	12% SDS-PAGE analysis showing the protein (0ALR6) expression at different time point	69
Fig. 3.4	12% SDS-PAGE analysis showing the protein (0ALR12) expression at different time point	70
Fig. 3.5	12% SDS-PAGE analysis showing the protein (0ALR18) expression at different time point	71
Fig. 3.6	Elution profile of 0ALR0 from the gel filtration column	73
Fig. 3.7	12% SDS-PAGE analysis showing fraction eluted from the gel filtration column	74
Fig. 3.8	Elution profile of 0ALR6 from the HiTrap chelating chromatography column	76
Fig. 3.9	12% SDS-PAGE analysis showing fractions eluted from the HiTrap chelating chromatography column	77

Fig. 3.10	Elution profile of 0ALR12 from the HiTrap chelating chromatography column	79
Fig. 3.11	12% SDS-PAGE analysis showing fractions eluted from the HiTrap chelating chromatography column	80
Fig. 3.12	Elution profile of 0ALR18 from the HiTrap chelating chromatography column	82
Fig. 3.13	12% SDS-PAGE analysis showing fractions eluted from the HiTrap chelating chromatography column	83
Fig. 3.14	The relationship between number of histidine in C-terminus and the percentage of solubility	85
Fig. 3.15	Denatured SDS-PAGE analysis showing the dimer formation of 0ALR12	87
Fig. 3.16	Far-UV circular dichroism analysis showing the CD spectrum of 0ALR0, 0ALR6 and 0ALR12	89
Fig. 3.17	The result of the isoelectric focusing of ALR	91
Fig. 3.18	The calibration curve of pI calibration kit (pH3-10)	91
Fig. 3.19	Spectroscopy of the purified 0ALR0, 0ALR6, 0ALR12 and pure FAD	93
Fig. 3.20	The visible spectroscopy of non-covalently bound FAD after heat and acid treatment	95
Fig. 3.21	The standard curve of the free FAD at A ₄₅₀	96
Fig. 3.22	The mass spectroscopy (ESI-MS) of polyhistidine-tagged (a) 0ALR6 and (b) 0ALR12	98
Fig. 3.23	Sulfhydryl oxidase activity assay of different ALR	103
Fig. 3.24	Sulfhydryl oxidase activity assay of pegylated ALR (0ALR12-MAL5K) and native ALR	104
Fig. 3.25	Effect of polyhistidine-tagged ALR on proliferation of different cell lines	107
Fig. 3.26	Effect of pHGF on proliferation of HepG2	110
Fig. 3.27	Effect of the pegylated ALR and native ALR on proliferation of HepG2 cells	111
Fig. 3.28	Purified 0ALR12 was modified with mPEG-NHS	114

Fig. 3.29	Purified 0ALR12 was modified with mPEG-ALD	114
Fig. 3.30	Purified 0ALR12 was modified with mPEG-SPA	115
Fig. 3.31	Purified 0ALR12 was modified with mPEG-MAL	115
Fig. 3.32	Western blot analysis of purified 0ALR12 and its pegylated products (0ALR12-MAL5K)	116
Fig. 3.33	Time course profile of pegylation products of 0ALR12 using different mole ratio of mPEG-MAL were analyzed by Coomassie blue stain and iodine stain	118
Fig. 3.34	Growth of the <i>E.coli</i> strain BL21(DE3)pLysS in a 2-L Fermentor	122
Fig. 3.35	Elution profile of 0ALR12 from a Chelating Sepharose FF column	123
Fig. 4.1	The chemical structure of histidine and imidazole	135
Fig. 4.2	The coupling reaction between 0ALR12 and mPEG-MAL	135
Fig. 4.3	The coupling reaction between 0ALR12 and mPEG-SPA	135

List of tables

Table 2.1	The primers used for ALR preparation	40
Table 2.2	The list of different buffer used in buffer test	55
Table 3.1	The yield of purified soluble ALR proteins with different length of polyhistidine tag	83
Table 3.2	The result of Jasco secondary structure estimation	89
Table 3.3	Calculated isoelectric points of polyhistidine tagged ALR	90
Table 3.4	Results of buffer test	101
Table 4.1	Summary of the properties of 0ALR0, 0ALR6 and 0ALR12	144
Table 4.2	Summary of the cell density and yield of 0ALR12 from batch and fed-batch fermentation trials	146

Chapter One: Introduction

1.1 Liver diseases

Liver is the largest organ in our body and is positioned at the lower right part of the ribs. Many important functions are partly mediated by the liver such as body growth, disease fighting, nutrient supply, metabolizing harmful substances, energy supply, and reproduction. These myriad functions are performed by liver cells, which are called hepatocytes. However, these processes especially the detoxication reactions often generate electrophilic toxic free radicals of relatively long half life, which can react with cellular nucleophiles such as DNA and proteins, and cause hepatocytes damage. In addition to the toxic substance, viruses can also cause liver disease.

Liver disease can cause acute or chronic damage to the liver. There are several major types of liver disease and causes. They are: 1) Viral liver disease represents one large category, caused by hepatitis A, B, C and others; 2) Alcoholic liver disease is another important type of liver disease, caused by chronic alcohol intake over many years. Cirrhosis and decompensated liver disease can be resulted; 3) Non-alcoholic Steatohepatitis, or NASH, is a rapidly increasing form of liver disease. This has many features similar to alcoholic

type, but occurred in mild alcohol drinkers. Typically, patients have one or more of the following property: obesity, diabetes, abnormal blood lipids, or high blood pressure; 4) The autoimmune type of liver disease. This represents a situation in which the body reacted against itself causing damage to the liver. Although this form of liver disease is less common, it is the major cause for liver transplantation; 5) Drug induced liver disease. This is caused by abnormal liver enzymes and liver injury because many drugs are metabolized through the liver; 6) Genetic defect caused by abnormal copy or disorder of the gene that lead to liver disease. Hemochromatosis, for example, is an inherited disorder that induces absorption of excessive amount of iron into the body.

Liver disease is a major killer in China, in which hepatitis B is the major cause. There are about 170 million Chinese infected with hepatitis B virus (HBV), within which 10% are chronic hepatitis sufferers (Sun *et al.*, 2002). Furthermore, hepatitis B can cause hepatocellular carcinoma (HCC) and end-stage cirrhosis. The liver cancer ranks second among the total cancer mortality. It causes the death of more than 300,000 people die each year. The end-stage of cirrhosis causes the death of another 150,000 people. Every year, a total of a half million people are killed by this disease.

Liver disease is a very serious problem in China, which may be due to the unhealthy living style. People in major cities, such as Shanghai and Beijing, are prone to this disease due to over-eating and excess drinking, which can lead to fatty liver (major cause of hepatitis and hepatocirrhosis). Medical studies showed that drinking 40 millilitres of alcohol a day, equivalent to two bottles of beer, can harm the liver of an average Chinese person. The incidence rate of fatty liver has increased rapidly in recent years, reaching 10-15% in some major Chinese cities including Shanghai and Guangzhou, according to Minde Zeng from the Shanghai Medical Association. Up till now, there are several methods to treat the liver disease, including surgical and medical methods. Even though after the surgical treatment, the patient still need to take medicine to speed up liver recovery. Thus, developing a new drug for liver disease is very demanding and important in China.

1.2 Liver regeneration

The term “regeneration” is used to describe the restoration of total liver mass. In humans, liver regeneration occurs frequently after liver damage by hepatitis, which is an inflammation of the liver. This amazing regenerative capacity of the liver was first described in Greek mythology of Prometheus (Michalopoulos *et al.*, 1997) and was demonstrated by the Higgins and Anderson (Higgins *et al.*, 1931) by using two-thirds partial-hepatectomy models in rodents. It is a simply surgical procedure in which 70 % of liver mass (three of the five lobes) is removed. The residual lobes enlarge and grow to restore the organ back to its original size, though the resected lobes never grow back (Fig. 1.1).

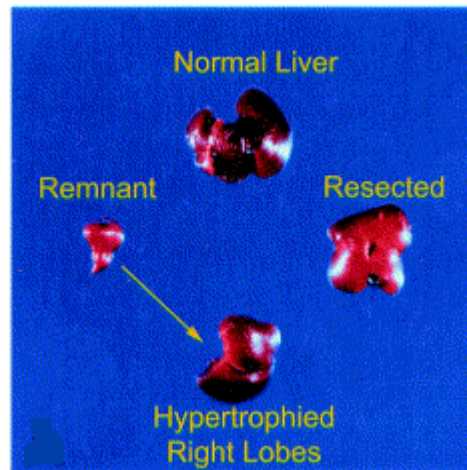


Fig. 1.1. Liver regeneration after two-thirds surgical partial-hepatectomy (PH).

The normal mouse livers before and after two-thirds PH, and hypertrophied remnant 6 days after two-thirds PH.

In addition, the liver mass is precisely regulated and the signals from the body can have negative as well as positive effects on the liver mass until the correct size is reached. When liver from large dog is transplanted into small dog, the liver size will gradually decrease until the size of the liver becomes proportional to the new body size (Francavilla. *et al.*, 1988).

Liver regeneration includes three phases; namely initiation, expansion and termination (Zimmermann *et al.*, 2004). During the initiation, hepatocytes are primed for subsequent replication. Priming factors comprise of interleukin-6

(IL-6) and tumor necrosis factor (TNF). They are produced by non-parenchymal cells, such as sinusoidal endothelia and Kupffer cells (Fig 1.2), and secreted in response to gut-derived lipopolysaccharide after PH (Koniaris *et al.*, 2003). IL-6 and TNF trigger the G₀/G₁ transition of the cell cycle. During the expansion phase, the growth factors allow the competent hepatocytes to progress through the cell cycle (G₁ to S), so the hepatocytes population is expanded. This is chiefly regulated by hepatocytes growth factor (HGF), transforming growth factor- α (TGF- α), epithelial growth factor (EGF) and augmenter of liver regeneration (ALR). The mechanism will be discussed later. When the growth overshoots, the superfluous hepatocytes will be eliminated through apoptosis. TNF takes the role of doing this. It not only induces regeneration, but also apoptosis. TNF is modulated by acidic sphingomyelinase (ASMase) (Garcia-Ruiz *et al.*, 2003). Subsequent to the expansion phase, the growth is about to progress to termination phase. There are two major factors contributing to this phase. They are TGF- β 1 and activin A. They regulate hepatic organ mass and tonically inhibit DNA synthesis in hepatocytes. TGF- β 1 inhibits hepatocyte proliferation and induces hepatocyte apoptosis by a c-Jun-independent mechanism while activin A is an autocrine inhibitor of initiation of hepatocyte DNA synthesis. It can also induce a reduction of liver mass, and

promotes apoptosis in hepatocytes, blocked by follistatin. In parallel to the termination phase, insinuation of vascular channels, formation of the perisinusoidal space of Disse, re-equipment of Disse's space by hepatic stellate cells (HSC) and the re-synthesis of the perisinusodial extra-cellular matrix (ECM) take place (Zimmermann *et al.*, 2004).

Since sinusoidal and littoral cells are the principle sources of the termination signals, these processes are crucial for the reconstruction of the regenerated lobule as well as for the termination of regeneration.

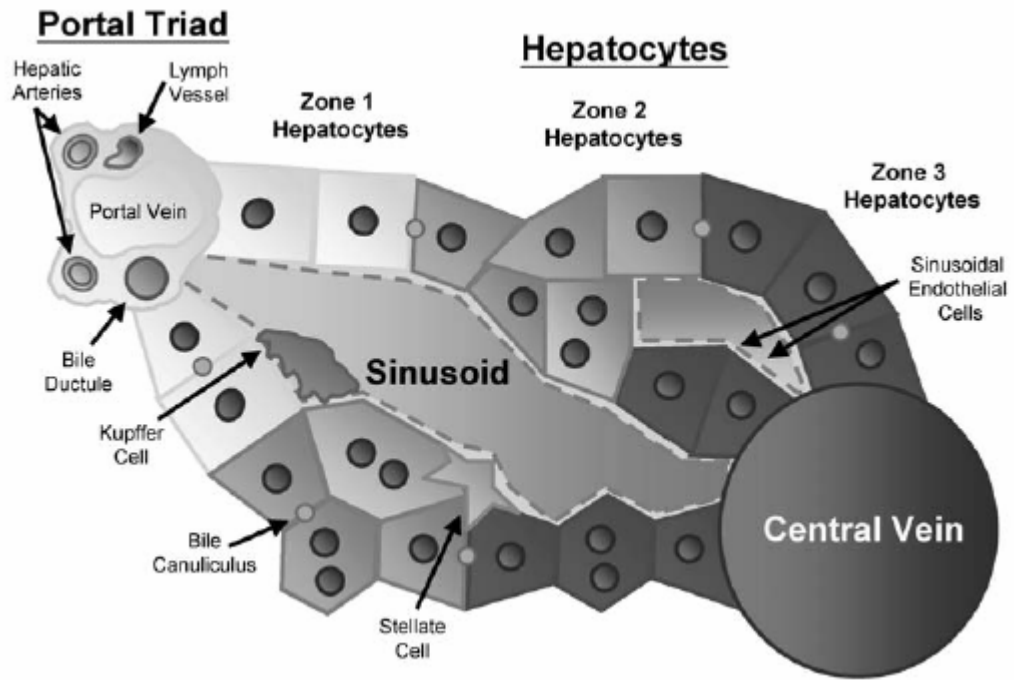


Fig. 1.2 Diagrammatic outline of the key cellular elements and their location in the histological architecture of the hepatic lobule (Michalopoulos *et al.*, 2005).

1.3 Hepatic stimulator substance

Hepatic stimulator substance (HSS), the first growth factor discovered and reported in the liver of weanling rat or partially hepatectomized rat, can specifically stimulate DNA synthesis of hepatic cells and induce liver growth (LaBrecque., 1991). The HTC hepatoma cell line was particularly responsive, showing up to 30-fold increase in [³H] thymidine incorporation into DNA in a dose-dependent manner. It also shows specificity for the liver but not kidney, spleen and bone marrow (LaBrecque & Bachur, 1982). Moreover, the HSS was not species restricted (Francavilla *et al.*, 1987) but organ specific. HSS is stable over a wide range of pH and temperatures. The stimulator activity is stable at 100 °C for 15 min (LaBrecque & Pesch, 1975). Further studies indicate that HSS is a highly negatively charged protein and that disulfide bonds or a complex tertiary structure are not essential for its activity (LaBrecque *et al.*, 1987). Some research showed that HSS has synergistic effect with a growth factor, EGF, on normal and regenerating hepatocytes (Fleig *et al.*, 1989). Although the HSS has been purified over 100,000-fold, the molecular weight of HSS cannot be confirmed. Because of the different purification schemes, LaBrecque *et al* (1987) found that the molecular weight was between 12,000

and 18,000 daltons while Francavilla *et al* (1987) found that the molecular weight was in the range of 14,000-50,000 daltons. Since, most characteristics and responses of these substances are very similar, so they probably represent the same molecule.

Francavilla *et al.* (1994) further purified and isolated the peptide from HSS, and finally indicated that the HSS protein itself is the rat augmenter of liver regeneration (rALR) (Hagiya *et al.*, 1994) or called hepatopoietin (HPO) (He *et al.*, 1993). Fig. 1.3 shows the three-dimensional structure of rALR. The rALR has two related forms, truncated (or 'short' rALR) and 'long' rALR. The former one has 125 amino acid and molecular weight of about 15 kDa while the later one contains 73 additional residues in the N-terminal segment of rALR with molecular weight of about 22 kDa (Giorda *et al.*, 1996, Rose *et al.*, 1997). The rALR gene was also mapped to the mouse chromosome 17. The rALR was synthesized and stored in the hepatocytes, which is the predominant liver cell (Gandhi *et al.*, 1999). Gandhi *et al.* (1999) found that the rALR was constitutively expressed in hepatocytes in an inactive form and was released from the cells in an active form by unknown means in response to partial hepatectomy and liver maturation or regeneration. In the meanwhile, the 'short'

rALR has been shown to be active *in vivo* using Eck's fistule assay (Hagiya *et al.*, 1994).

Giord *et al.* published the cDNA sequence of human ALR in 1996. At the same time, Yang *et al.* (1997) cloned the cDNA of human HPO by functional screening of a human fetal liver cDNA library and found that the human HPO is identical to human ALR. They found out that there are 87 % homology with rALR in nuclei acid sequence and 85 % homology in amino acid sequence.

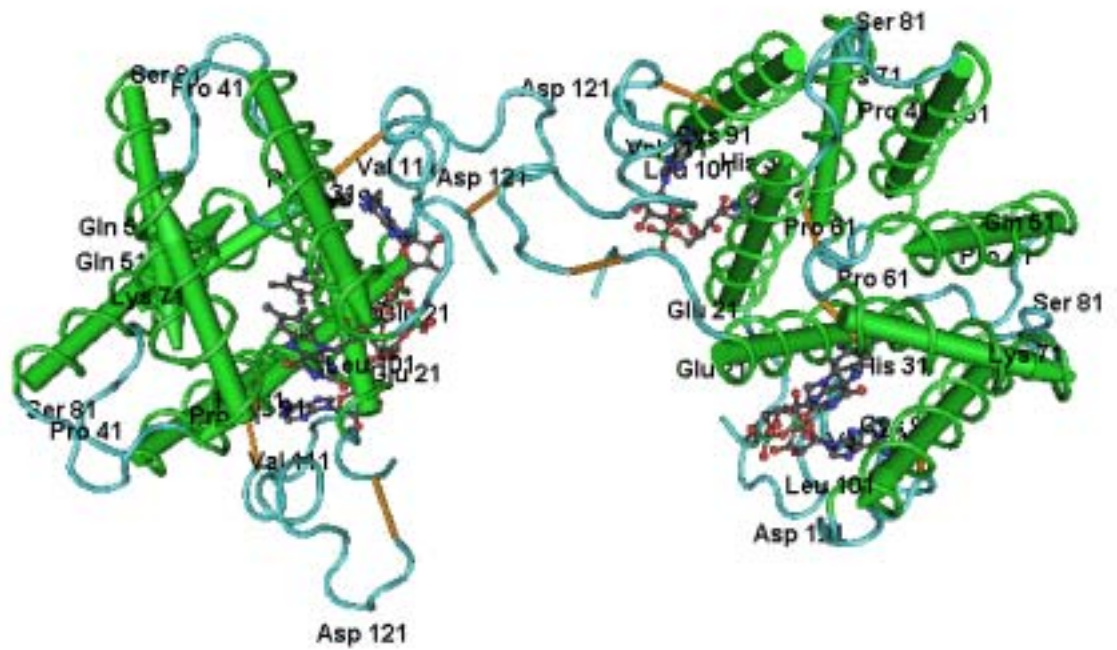


Fig. 1.3 The three-dimensional structure of the rat ALR (Wu *et al.*, 2003). The ALR monomer (32 x 26 x 20 Å), is cone-shaped with the FAD (in ball-and-stick formation) isoalloxazine moiety sitting in the mouth of the cone, forming the novel helix-bundle FAD-binding motif. The dimer is stabilized in part by two intersubunit disulfide bonds (yellow line) that are formed between the amino- and carboxy-terminal cysteines from each molecule that link the monomers in a head-to-tail fashion.

1.3.1 Human augments of liver regeneration (hALR)

Human ALR (hALR) is a protein of 125 amino acids. The length of the cDNA is 1.2 kb, which contains a 375-bp open reading frame. The hALR is constitutively expressed in the nuclear fraction of the liver parenchymal cells like the rALR dose (Li *et al.*, 2002). Fig 1.4 shows the amino acid sequence of the ALR. The human ALR has been mapped on chromosome 16 next to the Polycystic Kidney Disease gene (*PKDI*) (Hofhaus *et al.*, 1999). The sequences of rat and human ALR are highly homologous and show no homology to any known vertebrate protein (Rose *et al.*, 1997). However, the hALR does show a 50 % sequence homology with the dual-function nuclear gene ERV1 (essential for respiration and viability) product ERV1 from *Saccharomyces cerevisiae* (Lisowsky *et al.*, 1992) (Fig. 1.4), which is part of the mitochondrial respiratory chain (Grivell *et al.*, 1989) and plays an essential role in the control of mitochondrial gene expression (Lisowsky *et al.*, 1994). Moreover, the ALR can replace the yeast gene in the heterologous situation by placing ALR gene in an expression plasmid and introducing inactivated scERV1 gene into the yeast (Lisowsky *et al.*, 1995). This suggests that the ALR is not only structural, but also functional homologous to the scERV1 gene. Thus, ALR is thought to be

the mammalian equivalent of ERV1 (Hagiya *et al.*, 1994).

ALR belongs to Erv1p/ALR protein family. The respective genes are found in eukaryotes from yeast to human and even on the genome of some double-stranded DNA viruses (Lee *et al.*, 2000). They have essential functions in the biogenesis of mitochondria, the cell division cycle and development of organ like liver and testis in mammal. This ALR has been shown to control mitochondrial gene expression and the lytic activity of liver-resident natural killer cells through the levels of interferon- γ . Both *in vitro* and *in vivo* studies showed that ALR can stimulate proliferation of hepatocytes and hepatoma cells and can promote regeneration and recovery of damaged hepatocytes (Yang *et al.*, 1997). An *in vivo* model study by Gandhi *et al.* (1999) found that ALR could increase the proliferative response induced by 40 % partial hepatectomy (PH) or porta-cava shunt (PCS) (Polimeno *et al.*, 1999). ALR could directly stimulate DNA synthesis of hepatocytes in primary culture in a dose-dependent manner (Yang *et al.*, 1998).

ALR was also identified as FAD-linked sulphhydryl oxidases. These enzymes exist as homodimers, using FAD (flavin adenine dinucleotide) as a cofactor,

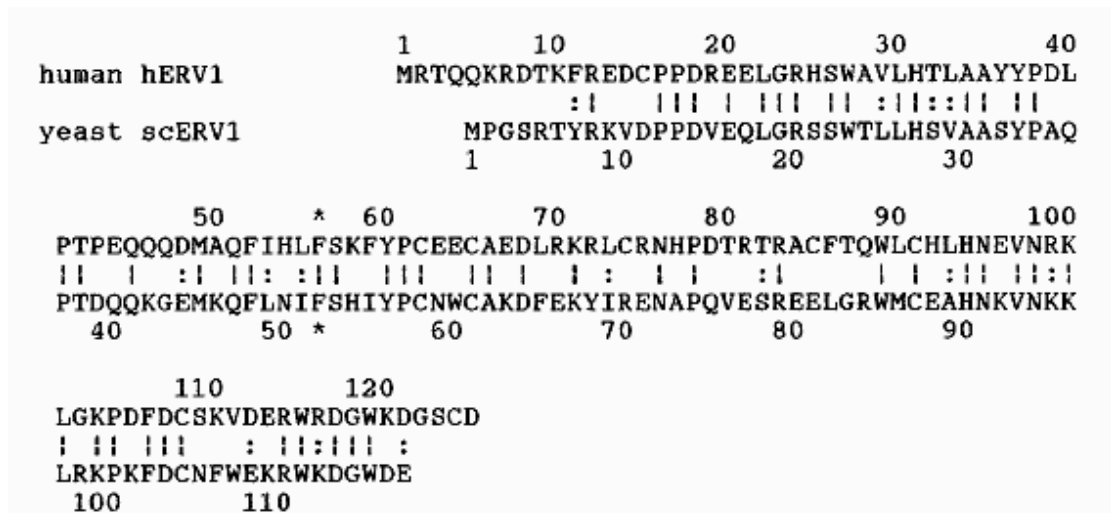


Fig. 1.4 Sequence alignment of yeast (sc) and the putative human (h) ERV1 (ALR protein). The sequences can be aligned without any gap. Identical amino acids at identical positions are marked by vertical bars; conservative amino acid substitutions are indicated by two dots. Using the 125 residues of the human protein as reference, the sequence identity is 42 % (52/125) and the similarity is 53 % (66/125), based on grouping conserved amino acids as follows: (P, G), (S, T), (Q, N), (E, D), (K, R), (M, C), (V, L, I, A), (F, Y, W, H). For the yeast polypeptide the amino acid phenylalanine at position 52 (*) was found to be of functional importance (Lisowsky, 1994). This residue is also conserved in the human protein (*). The sequence of the yeast scERV1 protein was taken from Lisowsky (1992) (GenBank GI: 6136037 for hERV1 and GI: 172377 for scERV1).

and O₂ as final electron acceptor. An internal redox-active cysteine pair was used to generate disulphide bridges.

1.3.1.1 Proposed working mechanism of ALR

ALR was found to be liver and testis specific. It stimulates proliferation of hepatocytes as well as hepatoma cells *in vitro*, promotes liver regeneration and recovery of damaged hepatocytes, and rescues acute hepatic failure *in vivo*.

ALR displays no effect on non-hepatocytes or tumor cell lines derived from tissue other than liver. These unique characteristics distinguish ALR from various well known hepatic stimulators, such as insulin, epidermal growth factor (EGF), hepatocyte growth factor (HGF), insulin-like growth factor-1 (IGF-1) and transformation growth factor (TGF- α), which can stimulate proliferation of a wide variety of cell types (Li *et al.*, 2000). He *et al.* identified the existence of ALR-specific receptor on the surface of liver cells (Wang *et al.*, 1999, Chen *et al.*, 2003). Thus, they propose that the extracellular ALR stimulates proliferation of hepatocytes and enhances liver regeneration by activating the MAPK signaling pathway under the mediation of ALR-specific receptor. However, ALR cannot induce the phosphorylation of STAT3 (signal

transducer and activator of transcription 3) in HepG2 cells that EGF does. This further indicates the difference of signaling pathways between ALR and EGF. After binding to the specific receptor, ALR stimulates tyrosine phosphorylation of epidermal growth factor receptor (EGFR). The Grb2/Sos complex binds to the activated EGFR, then recruiting Sos to the Ras protein on the plasma membrane. This translocation makes the exchange of GDP to GTP and activates the Ras. The activated Ras induces a kinase cascade, including Raf, MEK and MAPK, resulting in cell proliferation (Fig. 1.7). The ALR specific receptor has high affinity ($K_d = 0.7$ pM) and abundance in cells (55,000 sites/cell) (Wang *et al.*, 1999).

On the other hand, the intracellular ALR can specifically modulate the AP-1 (activating protein 1) pathway through JAB1 (Jun activation domain-binding protein 1) via MAPK-independent pathways and can enhance the phosphorylation level of c-Jun through JAB1 (Wang *et al.*, 2004, Pawlowski *et al.*, 2006). ALR interacts with JAB1, the fifth subunit of mammalian COP9 signalosome (CSN). COP9 have kinase activities that phosphorylate the c-Jun (Seeger *et al.*, 1998) leading to the activation of AP-1 activity, which promotes cell division. So it is also known as a co-activator of c-Jun/AP-1 transcription

factor (Lu *et al.*, 2001). In addition, the cysteine residues in the CXXC motif were necessary for the intracellular potentiation of AP-1 activity whereas the extracellular cytokine effect, stimulation of MAPK pathway via specific receptor, did not associate with the sulfhydryl oxidase activity (Chen *et al.*, 2003).

ALR also inhibits liver natural killer (NK) cell activity in rat and human (Polimeno *et al.*, 1999). The ALR in rat appears to have two effects. The first one is reduction of IFN- γ in liver-resident NK cells, which is responsible for the inhibition of NK cell lytic activity in liver. The second effect is increase of hepatic mt-TFA, which causes an up-regulation of mt-DNA expression (Polimeno *et al.*, 2000). However, the ALR effect on human is still unknown; we can just look the effect of native ALR inside the body. The mRNA of ALR and activity of NK cells were measured in patients with different liver diseases such as acute hepatitis and fulminant hepatitis. It was found that the hepatic ALR mRNA expression was higher in liver disease patients than in non-liver disease control group. Also the ALR showed inhibition of hepatic NK cells activity, which is specific against regenerating hepatocytes. Therefore, liver regeneration can be promoted by agents such as ALR, which cause immunosuppression to the liver only.

ALR is a FAD-linked sulfhydryl oxidase and the CXXC motif is essential for its enzymatic activity. The FAD binding gives the yellow colour to the protein. There are eight cysteines in ALR, in which 2 internal disulfides are formed between C62-C65 and C85-C91. He *et al.* found that C62 and C65 comprise the invariant C-X-X-C motif. All members of Erv1p/ALR family have this specific motif, which is known as the thiol active site (Senkevich *et al.*, 2000). Therefore, the mutant at this site will lose the enzyme activity completely and the yellow colour as well (Li *et al.*, 2002).

As the ALR has the ability to stimulate hepatocytes proliferation, and to protect specifically the liver, it is a potential drug for liver disease. Li *et al.* (2005) suggested that it may be potentially useful for the treatment of patients with liver cirrhosis. ALR increases the degradating capacity of collagen I, III, decrease the deposition of ECM and the expression of TIMP-1 in pathologic liver tissue and thus reverse the hepatic fibrosis. ALR may also relieve acute hepatic injury and hepatic failure by promoting hepatic cell proliferation (Zhang *et al.*, 2005).

1.3.2 HPO-205

Like rALR, the hALR also contains another isoform. Li *et al.* (2002) screened a human fetal liver cDNA library using the yeast two hybrid system with ALR as the bait. They found not only the ALR, but also an alternatively spliced form of ALR (named HPO-205) (Li *et al.*, 2002). HPO-205 encodes a peptide of 205 amino acids with 23 kDa. It is a protein with 80 additional amino acids at the N-terminal of the ALR. The amino acid sequence alignment of HPO-205 and ALR was shown in Fig. 1.5. It is also a heat stable protein, which can retain stability up to 70 °C. It is resistant to neuraminidase, SDS and reducing agents. It can be found in almost all organs and is not species specific. The ALR and HPO-205 are probably synthesized from the same messenger RNA by using different initiation codons (Giorda *et al.*, 1996, Rose *et al.*, 1997). In addition, ALR exists only in the nuclear fractions of the liver tissue but HPO-205 mainly in the cytosol fraction (Li *et al.*, 2002). Lu *et al.* (2002) proved that the HPO-205 also had similar biological activity as ALR *in vitro*. HPO-205 could stimulate the DNA synthesis of HepG2 cells and increase the activation of MAPK phosphorylation. The level of MAPK phosphorylation in HPO-205 transfected cells was significantly higher than that of ALR transfected cells.

However, papers reporting the HPO-205 are very limited, so whether the mechanism and activity of HPO-205 are similar to ALR remain to be investigated. The ALR can functionally substitute the yeast Erv1p *in vivo*, whereas the HPO-205 cannot (Hofhaus *et al.*, 1999). This suggested that the ALR performs similar enzymatic activity as Erv1p and the amino-terminal of the HPO-205 is species specific, which cannot be functionally substituted in other species such as yeast.

```

1  MAAPGERGRF HGGNLFFLPG GARSEMDDL ATDARGRGAG RRDAASAST
51 PAQAPTSDSP VAEDASRRRP CRACVDFKTW MRTQQRDTK FREDCPPDRE
    MRTQQRDTK FREDCPPDRE
101 ELGRHSWAVL HTLAAYYDDL PTPEQQRDMA QFIHLFSKFY PCEECAEDLR
    ELGRHSWAVL HTLAAYYDDL PTPEQQRDMA QFIHLFSKFY PCEECAEDLR
151 KRLCRNHPDT RTRACFTQWL CHLHNEVNRE LGKPDFDCSK VDERWRDGWK
    KRLCRNHPDT RTRACFTQWL CHLHNEVNRE LGKPDFDCSK VDERWRDGWK
201 DGSCD*
    DGSCD*

```

Fig. 1.5 Amino acid sequence alignment of HPO-205 and ALR (GenBank GI: 54112432 for HPO-205 and GI:7576256 for ALR). The upper one is the amino acid sequence of HPO-205 and the lower one is ALR.

1.3.3 Hepatocyte growth-promoting factor (pHGF)

Since the production technology of HSS developed by LaBrecque is comparatively complex and the molecular weight of HSS is heavier (around 12,000 to 18,000 Dalton), it can easily lead to allergic effect (Zhang *et al.*, 1995). Zhang *et al.* of Guangzhou Hospital of Air Force used a new technology of hyperfiltration for purifying a polypeptide substance with small molecular weight and biological activity from selected infant pig liver. The substance is called hepatocyte growth-promoting factor (pHGF). The pHGF like HSS can promote hepatocyte DNA synthesis and regeneration (Xie *et al.*, 1993). The pHGF also reinforces the function of phagocytes, T cells and NK cells (Zhu *et al.*, 1993), inhibits the activity of TNF (tumor necrosis factor) (Kong *et al.*, 1989), stabilizes cell membrane and prevents fibrogenesis in the case of CCl₄-induced liver injury (Sato *et al.*, 1999). Moreover, the pHGF has been used clinically in patients with hepatitis in China. The pHGF combined with general comprehensive therapy can obviously reduce the mortality of fulminant hepatitis by decreasing the serum bilirubin (SB) as well as alanine transferase (ALT) (Zhong *et al.*, 2003) and improving liver function (Gu *et al.*, 2003) and little side effect was observed such as rash, low fever and mild headache.

However, the pHGF like HSS is mixture of substances; six component peaks were observed in high performance liquid chromatography (HPLC). The complex ingredients may lead to some side effects in patients, thus Yang *et al.*, the City University of Hong Kong, further purified the pHGF and discovered the protein, Fi-brocorin. They claimed that this is the active ingredient and they will modify the protein to become the second generation of drug.

1.4 Epidermal Growth factor (EGF)

Epidermal growth factor (EGF) is a common mitogenic factor that stimulates the proliferation of different types of cells, especially fibroblast and epithelial cells. EGF was discovered by Cohen in 1962 (Cohen *et al.*, 1962). EGF is a single polypeptide consisting of 53 amino acid residues, of which 6 are cysteine (Carpenter *et al.*, 1979). Fig. 1.6 shows that there are 6 cysteines, which form three intramolecular disulfide bonds (Savage *et al.*, 1973) that are important for maintaining the biological activity of EGF (Wong *et al.*, 2004). The interactions between EGF and EGF receptor generate localized biological effect. Interestingly, other growth factors such as TGF- β and amphiregulin with structures similar to EGF can also activate EGF receptors. All the growth factors are recognized by having six spatially conserved cysteine residues that form three intramolecular disulfide bonds, which are critical for the function of the EGFR tyrosine kinase (Harris *et al.*, 2003).

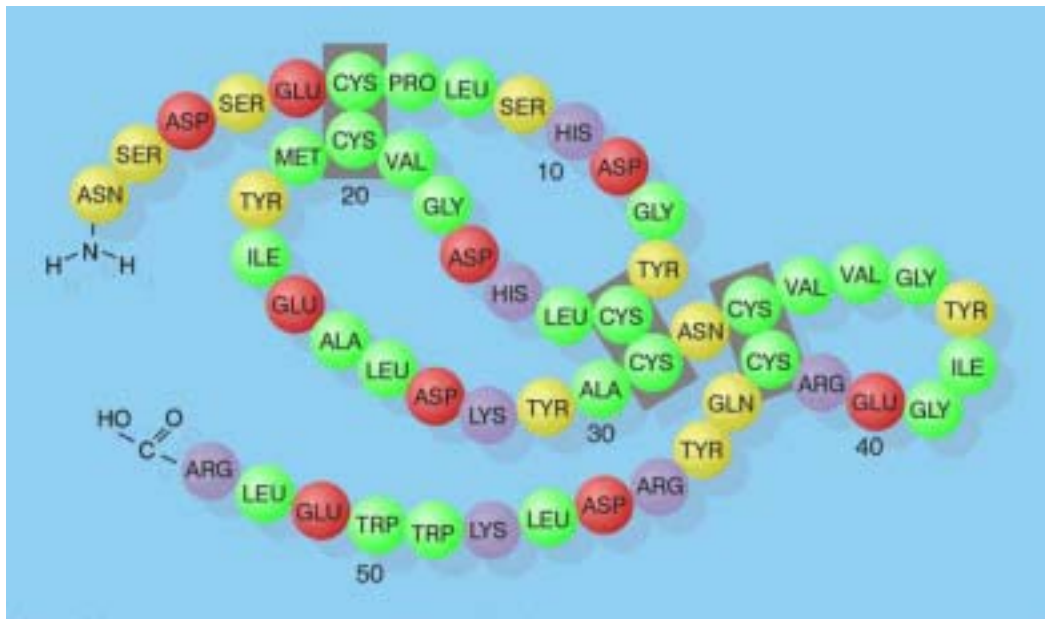


Fig. 1.6 The protein sequence of human epidermal growth factor. There are 6 cysteines, which form three intramolecular disulfide bonds. The grey box represents the disulfide bonds. (http://www.ust.hk/roundtable/hi-tech.series/1_b1.jpg)

The EGFR, a receptor tyrosine kinase, is dimerized, activated, then autophosphorylated on its tyrosine residues, after the binding of EGF (Schlessinger *et al.*, 1992). The activated EGFR facilitates the efficient tyrosine phosphorylation of phospholipase C (PLC), which generates diacylglycerol (DG) and inositol 1,4,5-trisphosphate (IP-3) (Yamada *et al.*, 1997). DG is a physiological activator of protein kinase C (PKC), which is a family of ubiquitous serine/threonine protein kinases involved in growth control (Nishizuka *et al.*, 1992). IP-3 induces Ca^{2+} release from intracellular stores, affecting Ca^{2+} -regulated processes in the cell. On the other hand, Grb2 links the activated EGFR to the Ras signaling pathway (Pawson *et al.*, 1995). The Grb2/Sos complex binds to the activated EGFR through the SH2 domain of Grb2, recruiting Sos to the plasma membrane where the Ras protein is located. This translocation makes the exchange of GDP to GTP on Ras, resulting in its activation. The activated Ras induces a kinase cascade including Raf (a serine/threonine kinase), MEK (mitogen-activated, ERK-activated kinase) and MAPK (mitogen-activated protein kinase). MAPK can phosphorylate and activate several transcription factors such as Elk-1 and c-Myc, which can promote cell division (Yamada *et al.*, 1997). EGF also activates another pathway, which involves activation of the non-receptor

tyrosine kinases called Jak and the cytoplasmic transcription factors called Stat (signal transducer and activator of transcription). Stat is tyrosine-phosphorylated by activated Jak, which associates with the ligand–receptor complex, and then Stat moves into the nucleus where it stimulates the transcription of the targeted genes. EGF induces the tyrosine phosphorylation and activation of Stat1 and Stat3. EGF also activates Jak1, therefore, the EGF-induced activation of Stat(s) may be controlled by activated Jak1 (Fig. 1.7).

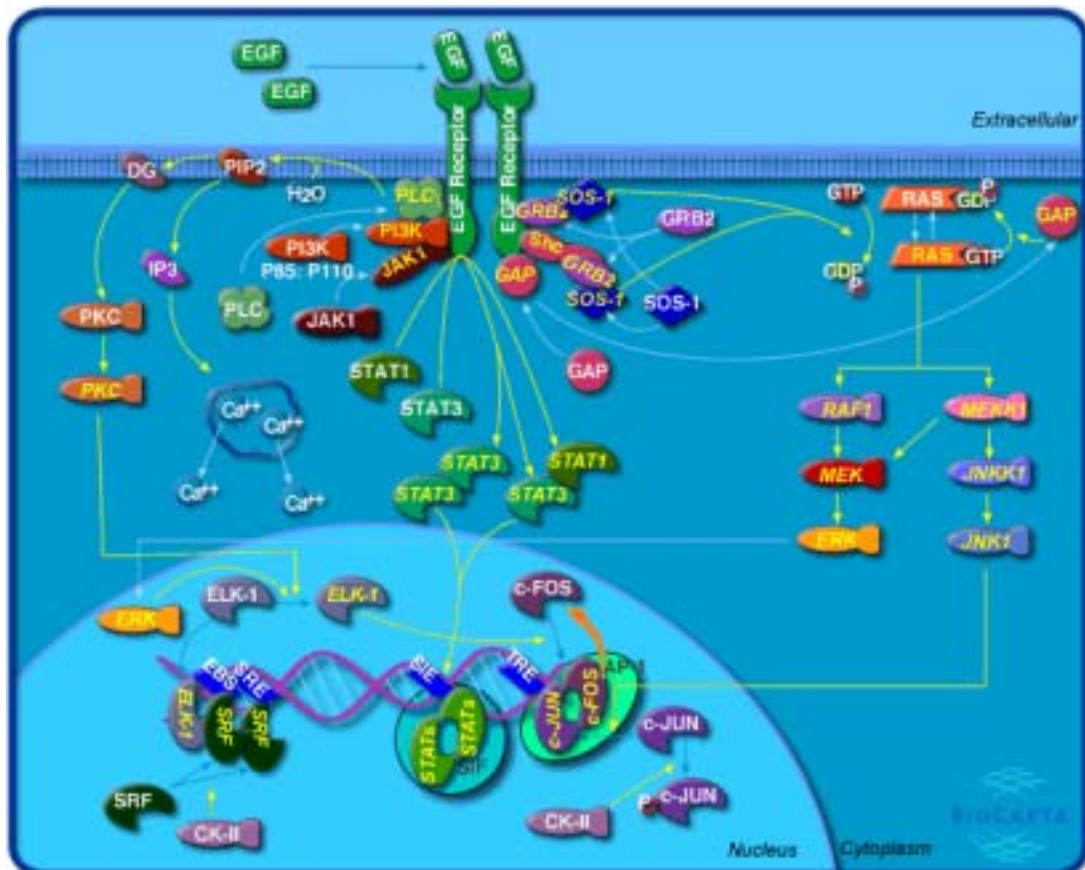


Fig. 1.7 The EGFR signaling mechanism

(http://www.biocarta.com/pathfiles/h_egfPathway.asp#description)

1.5 ERV/ALR protein family

1.5.1 *Saccharomyces cerevisiae* ERV1 protein

The yeast ERV1 (essential for respiration and vegetative growth) protein ortholog can be found in a large number of lower eukaryotes and some double stranded DNA viruses. The yeast *ERV1* gene encodes a small polypeptide of 189 amino acids with a mass of 22 kDa. ERV1 is essential for mitochondrial function, cell viability, respiratory function, and the cell-division cycle (Lisowsky, 1992, 1994). It is located in the intermembrane space of mitochondria (Lee *et al.*, 2000). This protein has a complex influence on different aspects of mitochondrial biogenesis and is essential for the survival of the yeast cell. Some groups identified the Erv1p as a novel component that is specifically required for the maturation of Fe/S proteins in the cytosol and is important for cellular iron homeostasis (Lange *et al.*, 2001). They consist of about ten proteins, and this complex apparatus was termed ISC (iron-sulfur cluster) assembly machinery. The ISC components of the mitochondrial matrix pre-assemble and pack the Fe/S cluster, which may then be exported into cytosol. This process involves the ABC (ATP-binding cassette) transporter Atm1p/ABC7. Since Erv1p is located in the intermembrane space, the proteins may be exported subsequently through

Atm1p/ABC7. However, the exact mechanism is still unknown.

Like ALR, Erv1p is also a FAD-linked sulfhydryl oxidase. It is a yellow coloured protein and the yellow colour is also due to the bound FAD. Hofhaus *et al.* found that the FAD was bound on the carboxy-terminus of the Erv1p. Moreover, the C130-C133 pair is part of the primary redox-active centre (Hofhaus *et al.*, 2003).

1.6 Polyhistidine tag

The polyhistidine tag is a very useful tool for purifying recombinant proteins (Bang *et al.*, 2005), which would also be useful for diagnostic applications especially in Western blot immunoassays (Khoo *et al.*, 2004). Poly-histidine tag has high affinity for divalent metal ions (such as Ni^{2+}), as electron donor groups on the histidine imidazole ring readily form coordination bonds with the immobilized transition metal (Terpe *et al.*, 2003). The advantages of using polyhistidine tag as carrier peptide are that the His tag is far smaller than most other affinity tags (such as S-tag, calmodulin-binding peptide, chitin-binding domain and SBP-tag), is poorly immunogenic in most species, rarely interferes with protein structure or function, and does not require removal by protease cleavage (Terpe *et al.*, 2003).

1.7 Protein pegylation technology

The increasing use of recombinant therapeutic proteins in the pharmaceutical industry has highlighted several issues such as stability during long-term storage and means of efficacious delivery that avoid adverse immunogenic side effects, which are reflected in poor biopharmaceutical properties (Kompella *et al.*, 1991). In particular, peptides and proteins undergo rapid clearance from the body by a combination of events including proteolysis, renal ultrafiltration, liver clearance and starvation by the immune system. Interaction and accumulation within tissues represent an additional pathway for removal of peptides and proteins from blood.

Controlled chemical modification, PEGylation, is a solution to these problems (Veronese *et al.*, 2002). Pegylation is a technique that links polypeptide drugs to soluble polymers such as poly(ethylene glycol) (PEG), which protects them and improves their pharmacodynamic and pharmacokinetic profiles (Harris *et al.*, 2003). Poly(ethylene glycol) is a linear or branched neutral polyether with the chemical formula $\text{HO}-(\text{CH}_2\text{CH}_2\text{O})_n\text{-H}$. PEG is highly soluble in water and in many organic solvents such as ethanol, acetone and chloroform (Hinds *et al.*,

2002). PEG conjugation masks the protein's surface and increases the molecular size of the polypeptide. The PEG molecules are hydrophilic, and the long chains can create a protective shield around the pegylated protein in aqueous media, thus the pegylated protein can have greater solubility, a longer elimination half-life, more stable plasma concentration, greater physical and thermal stability, greater protection against enzymatic degradation and less immunogenicity and antigenicity (Reddy *et al.*, 2000, Bowen *et al.*, 1999). In addition, PEG has been found to be nontoxic and is approved by the FDA for use in drugs, foods and cosmetics (Fuertges *et al.*, 1990). There are already some pegylated proteins reported such as IFN-mPEG (Diwan *et al.*, 2003), mPEG-PLA-haloperidol (Hans *et al.*, 2005) and PEG-insulin (Hinds *et al.*, 2005).

In our experiment, the mPEG derivatives, monomethoxy-PEG, were used. The monomethoxylated form of PEG is generally used in protein conjugation, since its monofunctionality yields cleaner chemistry (Veronese *et al.*, 2001). Since ALR is developed for pharmaceutical use, the low solubility will cause unstable activity and difficulty in storage. Therefore, the ALR was modified with PEG molecules in this project.

1.8 Objectives

Augmenter of liver regeneration (ALR) belongs to Erv1p/ALR protein family.

ALR can stimulate proliferation of hepatocytes and hepatoma cells and can

promote regeneration and recovery of damaged hepatocytes. Since liver disease

is a major problem in Asia, especially in China, this project aims to develop a

drug using ALR for treating patients suffered from liver failure. The ALR was

over-expressed in *E. coli*. In this project, we added poly-histidine tags to the C-

terminus of the protein in order to improve its purification and the properties.

The recombinant ALR was further characterized by gel electrophoresis, activity

assay and circular dichroism. In addition, the ALR was chemically modified by

pegylation to improve its stability. In order to screen the best PEG molecules to

use, different PEG derivatives were used for the pegylation of ALR such as

mPEG-N-hydroxysuccinimide, MW= 10,000 (mPEG-NHS); mPEG-maleimide,

MW= 5,000 (mPEG-MAL); mPEG-succinimidy propionate, MW= 5,000

(mPEG-SPA) and mPEG-propionaldehyde, MW= 5,000 (mPEG-ALD).

Chapter Two: Methodology

2.1 Construction of recombinant human augmenter of liver regeneration (hALR)

The construction of hALR was carried out by Dr. H. B. Liu and Miss Kareena Tsang. Augmenter of liver regeneration (ALR) was obtained from cDNA library. In order to obtain the human ALR (named as 0ALR0), forward (Arg1: 5'-AATTACATATGCGGACGCAGCAG-3') and reverse (Arg2: 5'-AATTAAAGCTTCTAGTCACAGGAGCC-3') primers were designed and applied to amplify transcripts using the *Taq* polymerase kit (Roche, U.S.A). Primer Arg1 contains NdeI restriction enzyme recognition site and primer Arg2 contains a HindIII site. These two primers were added to the human liver 5'-stretch plus cDNA library (Clontech, U.S.A.) in a 0.2 ml micro-tube. DNA polymerase (2.0 units), the four deoxyribonucleotides (final concentration 200 μ M of each), reaction buffer and distilled-deionized water (ddH₂O) were also added. PCR was performed and a band of PCR product was observed between 250 bp and 500 bp by the use of gel electrophoresis. The human ALR PCR product was inserted into the NdeI / HindIII sites of pAED4 using Rapid Ligation Kit (Roche, U.S.A.). The recombinant plasmid containing human ALR was named as pAEDALR and confirmed by DNA sequencing.

Besides the 0ALR0, hexa-histidine tagged (0ALR6), dodeca-histidine tagged (0ALR12) and octa-deca-histidine tagged (0ALR18) ALR proteins were also constructed for simplifying the purification step. All the polyhistidine molecules were added to the C-terminus of the ALR. The primers used for polyhistidine ALR preparation were listed in Table 2.1. All the 5' terminus primers contain NdeI restriction enzyme recognition site and the 3' terminus primers contain HindIII recognition site. With the aid of these recognition sites, the polyhistidine ALR derivatives could be cloned into the corresponding restriction sites of the expression vector. The native human ALR was used as a template for the polyhistidine ALR derivatives preparation. PCR was performed by High Fidelity *Taq* Polymerase Kit (Roche, U.S.A.). The human ALR PCR product was inserted into the multiple cloning sites (NdeI / HindIII) of pAED4 using Rapid Ligation Kit (Roche, U.S.A.). The recombinant plasmids containing human ALR with different number of histidine molecule were named as pAEDALR-6His, pAEDALR-12His and pAEDALR-18His and their sequences were confirmed by DNA sequencing.

2.2 Small scale production of recombinant ALR proteins

2.2.1 Shake flask culture

The plasmids pAEDALR, pAEDALR-6His, pAEDALR-12His and pAEDALR-18His constructed by Miss Kareena Tsang were transformed into *E. coli* strain BL21(DE3)pLysS by the standard CaCl₂-phosphate transformation method, as described by Cohen *et al.* (1972). Each transformant was inoculated in 5 ml 2xYT (yeast tryptone) medium (16 g tryptone, 10 g Yeast extract and 5 g sodium chloride for 1 L culture) and incubated for 12 h at 37 °C with shaking at 280 rpm. One percent volume of the culture was transferred to 200 ml 2xYT medium with 10 µM riboflavin (Sigma, U.S.A.), 0.1 mg/ml ampicillin (Sigma, U.S.A.) and 0.2 % glucose and incubated at 37 °C with shaking at 280 rpm. At cell density OD₆₀₀ 0.8, protein expression induction was performed by adding 0.2 mM isopropyl β-D-thiogalactoside (IPTG) (USB, U.S.A.). The cells were harvested after 4 h induction by centrifugation at 6,000 x g for 20 min and the cell pellet was stored at -80 °C until use.

2.2.2 Purification of recombinant human ALR

2.2.2.1 Purification of 0ALR0

The harvested cells were resuspended in lysis buffer (50 mM Tris-Cl, 1 mM EDTA, pH 8.0) at a concentration of 10 ml buffer per 100 ml of cells and 15 µg/ml lysozyme (Sigma) was added. The suspension was incubated at 30°C for 1 h and then sonicate the cell suspension with 6 short burst of 30 s followed by intervals of 30 s for cooling by Vibra-Cell VCX130 (Sonics & Materials, Inc., U.S.A.). After sonication, the lysate was centrifuged at 9,000 x g for 1 h at 4 °C. The supernatant (soluble protein) was collected for protein purification by gel filtration column (HiPrep 26/60 Sephacryl S-100 High Resolution, Amersham Pharmacia, Sweden) using a FPLC (Amersham Pharmacia, Sweden). Before the column purification, the protein was clarified by filtration through a 0.22 µm filter (Millipore) and the column was first equilibrated with start buffer (0.05 M sodium phosphate, 0.15 M NaCl, pH 7.2). The protein was eluted by 1 column volume of start buffer. All the eluants were analyzed by 12% SDS-PAGE to estimate the yield and purity, and the fractions containing the required protein were pooled for further studies.

2.2.2.2 Purification of 0ALR6, 0ALR12 and 0ALR18

For the purification, the presence of the histidyl-tag on the proteins allowed rapid purification with nickel agarose column (Amersham Pharmacia, Sweden). The harvested cells were resuspended in 10 ml of solubilization buffer (50 mM Tris, 0.1 M NaCl) and 15 µg/ml lysozyme (Sigma, U.S.A.). The suspension was incubated at 30 °C for 1 h and then sonicated on ice for about 8 min. After sonication, the supernatant was collected by centrifugation at 9,000 x g for 1 h at 4 °C. The supernatant was collected and subjected to affinity chromatography (Hitrap Chelating 5 ml column) (Amersham Pharmacia, Sweden) after filtration through a 0.45 µm filter (Millipore, U.S.A.). The nickel column was prepared and loaded with nickel sulphate ions (1 mM NiSO₄) and equilibrated with binding buffer (0.5 M NaCl, 0.02 M sodium phosphate, pH 7.4). Two gradients of two segments (0-0.15 M imidazole and 0.15–0.5 M imidazole) were established for the protein elution and ALR protein was eluted out from the column in the second segment. All eluates were analyzed by 12 % SDS-PAGE to estimate the yield and purity, and the fractions containing the required protein were pooled for further studies.

2.2.3 Buffer exchange

After running the SDS-PAGE, fractions with the targeted protein were concentrated and buffer exchanged by Tangential Flow Filtration system (TFF) (Millipore, U.S.A.). Membrane PXB00850 (Millipore, U.S.A.) with nominal cutoff of 8 kDa was used for the buffer exchange of ALR. The TFF system was first flushed with 500 ml MilliQ water. Then the system was pre-equilibrated with 100 mM histidine solution. The feed pressure and the retentate pressure for the TFF system were adjusted to about 30 psi and 10 psi, respectively, and the rate of permeate collected was about 5 ml/min. The dilution factor of the ALR sample was about 20000 for the removal of the imidazole. The protein concentration can be up to 1 mg/ml.

2.2.4 Freeze-drying

The buffer-exchanged ALR was freeze-dried in fractions of 5 ml with 1mg/ml protein in centrifuge tubes. All samples were frozen by liquid nitrogen and then inserted into the valve of the freeze-dryer (Flexi-Dry MP™ Freeze-Dryer, U.S.A.) and allowed for vacuum drying overnight. After freeze-drying, the samples were stored at $-20\text{ }^{\circ}\text{C}$.

2.3 Characterizations of recombinant ALR

2.3.1 Solubility test

2.3.1.1 Sodium Dodecyl Sulfate Polyacrylamide Gel Electrophoresis (SDS/PAGE)

According to Laemmli (1970), proteins could be separated according to their molecular weights. Proteins were separated in non-reducing SDS/polyacrylamide gel by electrophoresis (Bio-rad Mini Protein III, U.S.A.). The SDS-polyacrylamide gel was composed of a 12 % separating gel. Electrophoresis was performed in 1X Laemmli running buffer (62.5 mM Tris-HCl, pH 6.8, 25 % glycerol, 2 % SDS and 0.01 % Bromophenol Blue) at 200 V for 1 h.

The stacking gel was cut and the separating gel was soaked in Coomassie blue R-250 staining solution (Sigma, U.S.A.) for 30 min with gentle shaking. The gel was then destained in destaining solution (20 % methanol and 10 % acetic acid solution). The solution was replaced several times until the background of the gel was clear. The gel was subsequently dried by Bio-rad drying kit.

The solubility test is to measure the percentage of target protein within total proteins. It was measured by comparing the band intensity of target protein against the total proteins. The band intensity was measured by Kodak 1D Image Analysis Software ver. 3.5.4.

The formula for the percentage of ALR of total protein expressed and percentage of soluble fraction were shown as below:

Percentage of ALRs of total proteins expressed

$$\% = \frac{\text{sum intensity of ALRs}}{\text{sum intensity of total proteins}} \times 100 \%$$

Percentage of soluble fraction

$$\% = \frac{\text{sum intensity of soluble proteins}}{\text{sum intensity of soluble proteins} + \text{sum intensity of insoluble proteins}} \times 100 \%$$

2.3.1.2 Western blotting

Proteins separated by SDS-PAGE were transblotted onto PVDF membrane (Millipore) for immunological assay. After gel electrophoresis, the gels were equilibrated in transfer buffer (39 mM glycine, 48 mM Tris base, 0.02 % SDS, 20 % methanol) for 5 min to remove salts and detergents. The PVDF membrane was immersed in methanol for 15 s for activation, and then in transfer buffer for 1 min. The transfer assembly (Bio-Rad, U.S.A.) was set up according to the manufacture's instruction and the samples were transferred at 100 V for 1 h 30 min at 4 °C with stirring.

The transblotted membrane was blocked in 5 % skimmed milk for 120 min. After rinsing in 1 X TTBS washing buffer (20 mM Tris base, 500 mM NaCl, 0.05 % Tween) for 10 min for 3 times. The primary antibody, polyclonal rabbit anti-His IgG (1: 1,000 dilution) (Santa Cruz, U.S.A.) was applied for 2 h at room temperature. The membrane was then washed 3 times in 1 X TTBS. Secondary antibody, anti-rabbit goat IgG: HRP (1: 10,000 dilution) (Santa Cruz, U.S.A.), was applied and incubated for 90 min at room temperature. The membrane was then washed in 1 X TTBS again for 3 times to remove the excess antibodies.

Finally, the ALR was detected by SuperSignal® West Pico Chemiluminescent Substrate (Pierce) and visualized by Lumicap 3.1 software.

2.3.2 Protein assay

The protein concentrations were determined by the Bradford assay (Bradford *et al.*, 1976). Using a micro-protein assay, 800 μ l of the diluted samples was incubated with 200 μ l Bradford Reagent (Bio-rad, U.S.A.) for 10 min at room temperature. The absorbance was measured at 595 nm. Bovine serum albumin (BSA) (Sigma, U.S.A.) was used as a standard protein and a standard curve was plotted in the range of 0-20 μ g/ml.

2.3.3 Far-UV circular dichroism (CD) analysis

Far-UV CD analysis (Jasco J-810 spectrophotometer) was used to estimate the secondary structure of proteins. Before CD measurement, recombinant ALR proteins were dissolved in 10 mM potassium phosphate buffer at pH 7.0. ALR protein (200 μ l) was added into a cuvette (0.1 cm path-length) and diluted with potassium phosphate until the end of signal is below 800. The CD was scanned over the far-UV range of 190 to 250 nm under constant nitrogen flush with a path length of 0.1 cm. Each CD spectrum represented the average of three scans. The CD signals were expressed in term of mdeg.

2.3.4 Mass spectrometry analysis

Mass spectrometry analysis was carried out by Mr. So Pui Kin. This technique was used to identify the molecular mass of the ALR. Prior to mass analysis, the samples were desalted by Amicon Ultra-4 centrifugal filter devices (cut-off = 10,000 Da; Millipore, USA) in Milli-Q water. Over 10,000 dilution was performed at 4,000 x g in a swing out bucket rotor.

ESI-MS measurements were performed on an ESI-Q-TOF (electrospray ionization-tandem quadrupole/orthogonal-acceleration time-of-flight) (Q-TOF II, Micromass, Altrincham, UK) mass spectrometer, which is equipped with a Masslynx 3.5 version software. Prior to mass spectrometric analysis, equal amounts of acetonitrile containing 0.2 % formic acid were added to the protein solutions to produce final solutions containing acetonitrile:buffer 50:50 (v/v) and 0.1 % formic acid. The final protein solutions were injected into the mass spectrometer using a syringe pump (Cole Parmer, series 74900, U.S.A.) at a flow rate of 300 ul/h. For all experiments, the capillary voltage was set to 2.5 KV and the cone voltage was maintained at 30 V. The mass axis was calibrated externally by Horse Heart Myoglobin (MW = 16950.5). Multiply charged

spectra were obtained by scanning over a mass range of 600-2000 m/z and the multiply charged spectra were deconvoluted by the Maximum Entropy program included in the MassLynx 3.5 package.

2.3.5 Isoelectric focusing

Isoelectric focusing (IEF) of ALR was performed in polyacrylamide gels containing ampholytes (Pharmalyte, broad range pH 3-10, Amersham Pharmacia, Sweden) by using a Model 111 Mini-IEF Cell (Bio-Rad, U.S.A.) with broad range marker (Broad pI kit, pH 3.5-9.3, Amersham Pharmacia, Sweden). The procedure was adopted from Bio-Rad Manual 9108. BSA with known isoelectric points (pI) was used as control. The IEF gel was ran in 3 steps

	Voltage	Current	Time
Step 1:	100 V	6 mA	15 min
Step 2:	200 V	6 mA	15 min
Step 3	450 V	4 mA	75 min

After the running, the gel was stained in Coomassie Blue G-250 “Quick Stain” for 1 h without shaking and destained in 7 % (v/v) acetic acid for 1 h for intensification and preservation.

2.3.6 FAD content measurement

2.3.6.1 Spectroscopy of recombinant ALR

The visible spectra of different ALR derivatives were directly recorded by a Lambda 35 UV/VIS Spectrometer (Perkin Elmer) and analyzed by UV WinLab version 2.85.04. Absorbance range from 350 nm to 550 nm was measured. Under identical conditions a reference of 7.5 μM pure FAD (Sigma, U.S.A.) was also measured. The FAD content of the proteins was calculated from the OD_{460} values using an extinction coefficient of $10 \text{ mM}^{-1}\text{cm}^{-1}$.

2.3.6.2 Release of protein-bound FAD by heat and acid treatment

After determining the concentration, the protein was heated in 5 % trichloroacetic acid to detach the FAD molecule from the protein. Denatured protein was pelleted by centrifugation. Detached FAD was then measured by Lambda 35 UV/VIS Spectrometer (Perkin Elmer). The FAD content was then calculated from the OD value of maximum peak with the aid of free FAD standard. FAD content of proteins can be calculated by protein denaturation.

2.3.7 Solubility of 0ALR12 in various buffers

In this part, the purified 0ALR12 was buffer exchanged with different common buffers to test the solubility of the protein by dialysis tubing (Sigma, U.S.A.).

The different buffers used are shown in Table 2.2.

Table 2.2 The list of different buffer used in buffer test

Buffer	Tested concentration
H ₂ O	
PBS	With 0.8 % - 3 % NaCl
MgCl ₂	20 mM
Glucose	5 %, 10 %, 15 %
Sorbitol	5 %, 10 %, 15 %
Glycerol	5 %, 10 %, 15 %
Glycine	0.1 %, 0.2 %, 0.3 %
Histidine	20 mM, 50 mM, 0.2 M

2.3.8 Activity assay

2.3.8.1 Enzyme assay for sulfhydryl oxidase activity

Different forms of ALR protein were adjusted to 10 pmol and 20 pmol per reaction. The enzyme reaction was started in enzyme assay buffer (2 M urea in 100 mM potassium phosphate, 1 mM EDTA, pH 7.5) together with dithiothreitol (DTT) substrate that corresponded to 50 nmol reduced thiol groups. Aliquots of 200 μ l of this reaction mixture were used for each time point. The thiol content was determined by diluting 200 μ l sample with 790 μ l of enzyme assay buffer and then 10 μ l DTNB (Ellman's reagent) (Riddles *et al.*, 1979) were added to give a final concentration of 10 μ M. After 2 min, the extinction at 412 nm was measured and the enzyme activity was calculated. The initial thiol content was determined from a 200 μ l aliquot collected at time zero.

2.3.8.2 Cell proliferation activity test of recombinant ALR

Liver cancer cell line (HepG2), breast cancer cell line (MCF-7), colorectal cancer cell line (Ht29) and lung cancer cell line (A549) (ATCC, U.S.A.) were used to test the biological activity and specificity of the recombinant ALR. Three thousand cells were plated on a 96-well plastic culture plate (IWAKI, Japan) per well and cultured with Dulbecco's modified Eagle's medium (DMEM) (Gibco, U.S.A.) or RPMI 1640 medium (Gibco, U.S.A.) containing 10 % fetal bovine serum (Gibco, U.S.A.) under 5 % CO₂ and 21 % O₂ in air at 37 °C. After 24 h, the medium was changed to serum free DMEM to starve the cell for another 24 h. Various concentrations of recombinant human ALR were added with pHGF as the positive control. After incubation for 48 h, MTS assay was performed with a CellTiter⁹⁶ Aqueous MTS Reagent Powder Kit (Promega, Madison, WI, U.S.A.) according to the manufacturer's manual (Bio-gene).

2.4 Pegylation of recombinant ALR

Purified ALR was pegylated with mPEG-maleimide, MW= 5,000 (mPEG-MAL) to generate ALR-MAL5K. A 0.34 g of mPEG-MAL (in 1:25 mole ratio) was first dissolved in 10 ml elution buffer (0.5 M NaCl, 0.02 M sodium phosphate, 0.5 M imidazole, pH 7.4) and added to 0.1 g ALR in elution buffer and the mixture was mixed gently. Pegylation was allowed to take place at room temperature for overnight. Free PEG molecules were removed by Tangential Flow Filtration system (TFF) (Millipore, U.S.A.). Membrane PXB00850 (Millipore, U.S.A.) with nominal cutoff of 8 kDa was used for the buffer exchange of pegylated ALR-MAL5K.

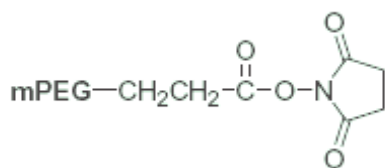
The effect of pegylation was monitored with 12 % SDS-PAGE by Coomassie blue stain as well as iodine stain (Kurfurst *et al.*, 1992). In addition, the ALR-MAL5K was subjected to western blotting with the anti-his antibody to identify the 0ALR12. The dialyzed ALR-MAL5K was freeze-dried and stored at -20 °C.

The enzymatic activity of ALR-MAL5K was also measured.

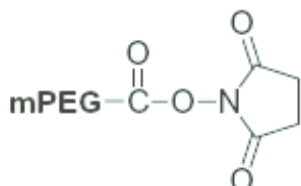
2.4.1 Pegylation of ALR with different PEG molecules

ALR was pegylated with four different PEG molecules; they are: mPEG-N-hydroxysuccinimide, MW= 10,000 (mPEG-NHS); mPEG-maleimide, MW= 5,000 (mPEG-MAL); mPEG-succinimidy propionate, MW= 5,000 (mPEG-SPA) and mPEG-propionaldehyde, MW= 5,000 (mPEG-ALD).

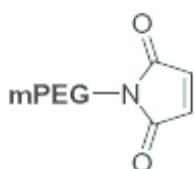
Each type of PEG molecules was added to ALR in mole ratio of 1:50. Samples were then stirred overnight to allow reaction between PEG and ALR. The effect of ALR Pegylation was monitored with 12 % SDS-PAGE.



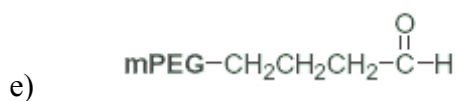
b)



c)



d)



e)

Fig. 2.1 Structure of polyethylene glycol (PEG) molecules with different derivatives. a) mPEG, monomethoxy-PEG; b) mPEG-SPA, mPEG-succinimidy propionate; c) mPEG-NHS , mPEG-N-hydroxysuccinimide; d) mPEG-MAL, mPEG-maleimide and e) mPEG-ALD, mPEG-propionaldehyde.

2.4.2 Pegylation of ALR with mPEG-MAL in different mole ratios

ALR was pegylated with mPEG-MAL, which was added to ALR in different mole ratios (1:10, 1:25, 1:50 and 1:100). Samples were stirred overnight to allow attachment of PEG molecules to ALR. The effect of the ALR pegylation was monitored with 12 % SDS-PAGE.

2.5 Pilot scale production of recombinant ALR

2.5.1 Fed-batch fermentation

The fed-batch fermentation was carried out by Mr. Johnson Choi. *E. coli* strain BL21(DE3)pLysS was incubated in 1-L shake flask with 200 ml fermentation medium (2xYT medium with 10 μ M riboflavin and 0.2 % glucose) with 0.1 mg/ml ampicillin at pH 7.0 on an orbital shaker rotating at 280 rpm and 37 °C overnight. After cultivation for 10-12 h, the OD₆₀₀ reached around 3-4. Then the 200 ml culture was transferred into 2-L stirred tank bioreactor (B. Braun, Biostat B, Germany), equipped with on-line monitoring of temperature, agitation rate, pH and oxygen concentration..

Aeration was set to 11 L/min; temperature at 37 °C; pH was controlled to 6.95 – 7.04 by addition of 2.5 M sodium hydroxide. Agitation was set to 400 rpm and was automatically adjusted if the dissolved oxygen dropped to less than 70 % (with a minimum limit of 20 % of air saturation). When OD₆₀₀ reached about 13, 0.5 mM IPTG (USB, U.S.A.) and glucose were supplied. The culture was harvested after 4 h. The cells were then centrifuged at 6,000 x g for 20 min and stored at -80 °C until use.

2.5.2 Purification of ALR

The cells were resuspended in 400 ml solubilization buffer and loaded into a cell homogenizer (APV-1000). The sample was digested with 5,000 units of DNase I (Sigma, U.S.A.) for 15 min at 37 °C. After DNase I digestion, the cells were centrifuged at 8,000 x g at 4 °C for 60 min. The supernatant was clarified by filtration through a 0.22 µm filter and subjected to affinity chromatography (Chelating Sepharose Fast Flow 30 ml) (Amersham Pharmacia, Sweden). The column was prepared by mixing the packing buffer (20 % ethanol) with the medium (Chelating Sepharose Fast Flow) by shaking to form 50 % - 70 % slurry. Then the slurry was poured into the column (XK 26/20 column) in a single continuous motion. The gel medium was packed by compressing it with MilliQ water. The column was prepared and loaded with nickel sulphate ions (1 mM NiSO₄) and equilibrated with binding buffer (0.5 M NaCl, 0.02 M sodium phosphate, pH 7.4). Two gradients of two segments (0-0.15 M imidazole and 0.15-0.5 M imidazole) were established for the protein elution and ALR protein was eluted out from the column in the second segment. All elutes were analyzed by 12 % SDS-PAGE to estimate the yield and purity, and the fractions containing the required protein were pooled together for further use.

Chapter Three: Results

3.1 Small scale production of recombinant ALR in *Escherichia coli* and their purification

3.1.1 Expression of recombinant ALR

E. coli BL21(DE3)pLysS based strains carrying plasmids pAEDALR, pAEDALR-6His, pAEDALR-12His and pAEDALR-18His were constructed as described in chapter 2.1. The proteins 0ALR0, 0ALR6, 0ALR12 and 0ALR18 were successfully expressed in *E. coli* BL21(DE3)pLysS. The recombinant ALR expression in *E. coli* system was initiated by IPTG-induction at OD₆₀₀ of 0.8-1.0. The induction condition was based on the standard protocol. After 20mM IPTG-induction, the culture was grown for 4 more hours and harvested. The growth curves of different ALR producing strains are shown in Fig. 3.1. The crude proteins isolated from the cultures were analyzed by SDS-PAGE.

The SDS-PAGE data in Figs. 3.2-3.5 show the soluble proteins in the supernatant after cell breaking and centrifugation. The amount of soluble ALR was slightly increased from 0ALR0 to 0ALR6 and dropped when more histidine molecules were added to the C-terminus. However, after adding more histidine molecules, the protein formed inclusion body or aggregated inside the

cells. The 0ALR18 was totally insoluble and more complex steps such as unfolding and refolding have to be done in order to purify it. Interestingly, the percentage of ALR in the total protein was increased (Table 3.2) while the number of histidine molecules was increased. Among these 4 proteins, the most soluble one is 0ALR6, which has ~ 60 % soluble protein, while the 0ALR0 protein is ~ 55 % soluble, 0ALR12 is ~ 40 % soluble and 0ALR18 is not soluble. The measurements were described in chapter 2.3.1.

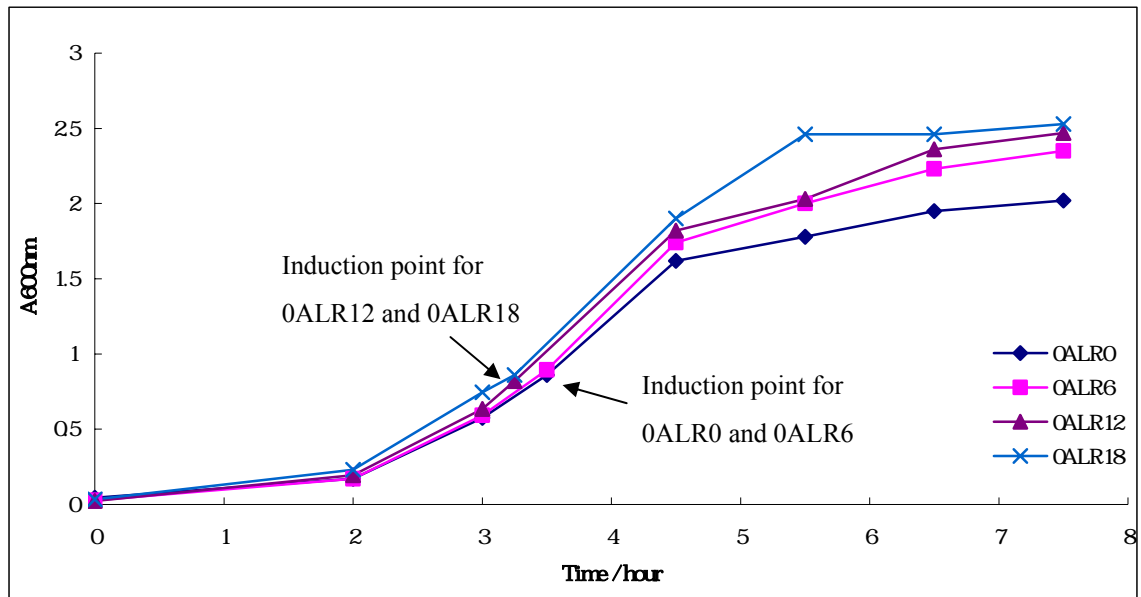


Fig. 3.1 Growth of *E. coli* BL21(DE3)pLysS carrying various plasmids.

Bacterial growth was monitored by measuring the absorbance at 600 nm.

0ALR0, cells carrying pAEDALR; 0ALR6, cells carrying pAEDALR-6His;

0ALR12, cells carrying pAEDALR-12His; 0ALR18, cells carrying

pAEDALR-18His. The induction points were the time point when IPTG was

added.

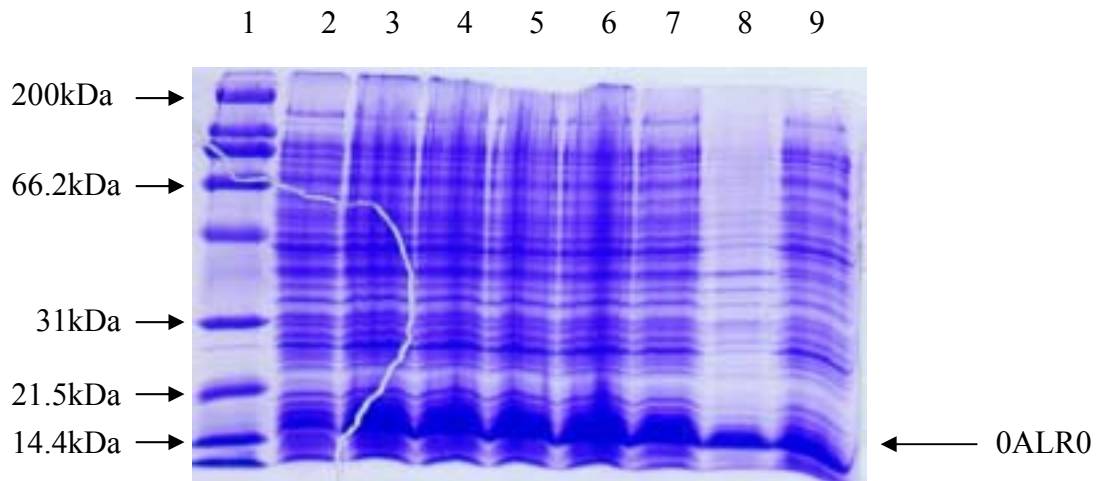


Fig. 3.2 12 % SDS-PAGE analysis showing the protein (0ALR0) expression at different time points. The molecular weights of 0ALR0 were about 15 kDa for monomer and 30 kDa for dimer. Lane 1: broad range molecular weight marker; Lanes 2-6: crude extract obtained at 0 h, 1 h, 2 h, 3 h and 4 h after IPTG induction, respectively; Lane 7: total protein; Lane 8: insoluble protein; Lane 9: soluble protein.

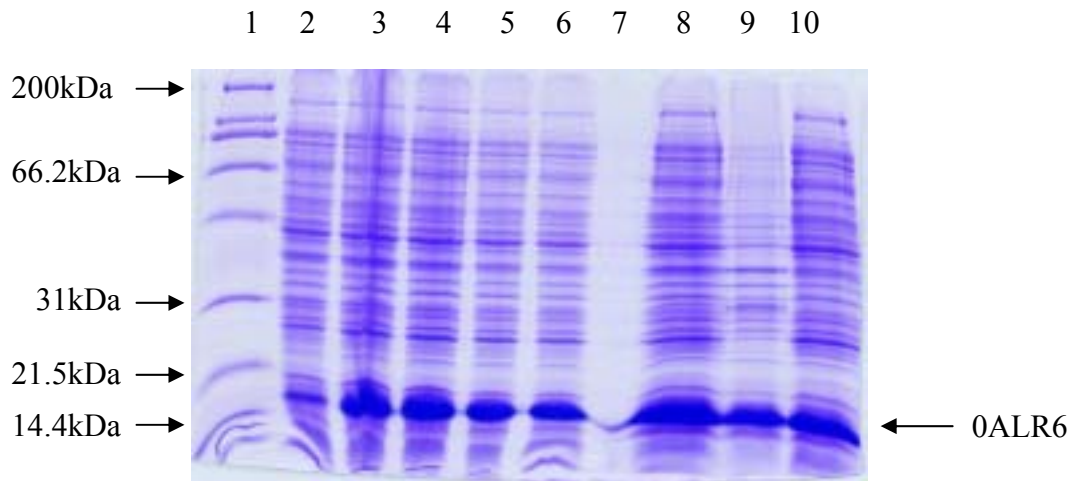


Fig. 3.3 12 % SDS-PAGE analysis showing the protein (OALR6) expression at different time points. The molecular weights of OALR6 were about 15.8 kDa for monomer and 31.7 kDa for dimer. Lane 1: broad range molecular weight marker; Lanes 2-6: crude extract obtained at 0 h, 1 h, 2 h, 3 h and 4 h after IPTG induction, respectively; Lane 7: empty; Lane 8: total protein; Lane 9: insoluble protein; Lane 10: soluble protein.

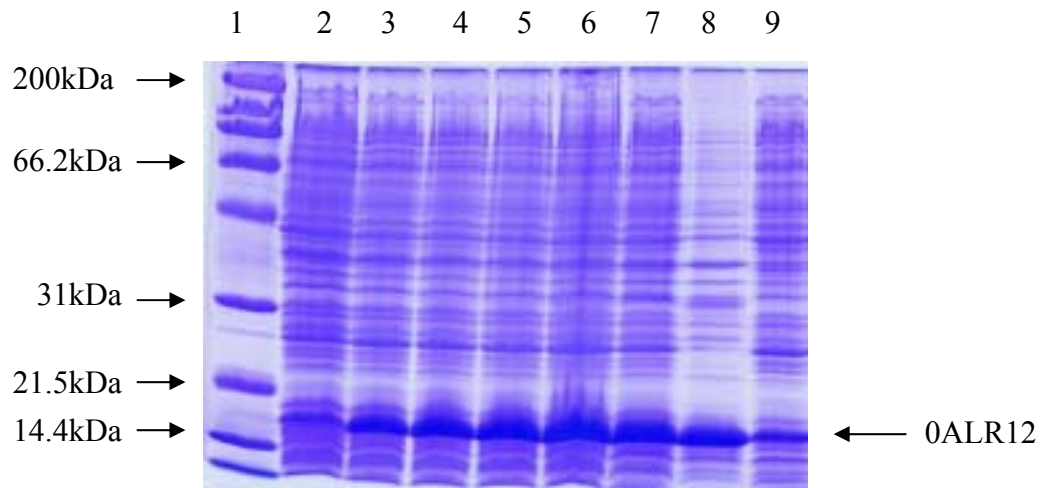


Fig. 3.4 12 % SDS-PAGE analysis showing the protein (0ALR12) expression at different time point. The molecular sizes of 0ALR12 were about 16.6 kDa for monomer and 33.3 kDa for dimer. Lane 1: broad range molecular weight marker; Lanes 2-6: crude extract obtained at 0h, 1h, 2h, 3h and 4h after the induction, respectively; Lane 7: total protein; Lane 8: insoluble protein; Lane 9: soluble protein.

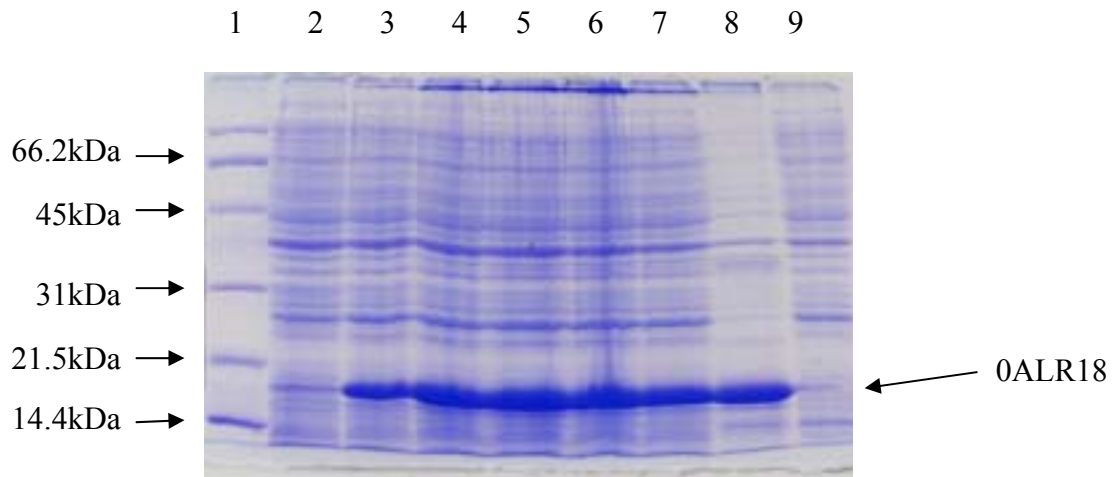


Fig. 3.5 12% SDS-PAGE analysis showing the protein (0ALR18) expression at different time point. The molecular sizes of 0ALR18 were about 17.5 kDa for monomer and 35 kDa for dimer. Lane 1: low range molecular weight marker; Lane 2-6: crude extract obtained at 0h, 1h, 2h, 3h and 4h after the induction, respectively; Lane 7: total protein; Lane 8: insoluble protein; Lane 9: soluble protein.

3.1.2 Purification of recombinant ALR

3.1.2.1 Purification of 0ALR0

The recombinant ALR was produced in *E.coli* strain BL21(DE3)pLysS with plasmid pAEDALR. Gel filtration column was used to purify the protein 0ALR0. The 0ALR0 was eluted depending on the size difference. The molecule with higher molecular weight was eluted out first, and the lighter one came out later.

Fig. 3.6 shows the elution profile of the 0ALR0. The fraction eluted from the HiPrep 26/60 Sephacryl S-100 High Resolution column were analyzed by SDS-PAGE and the Bradford assay. Fig. 3.7 shows the result of the 12 % SDS-PAGE analysis of different fractions eluted from the gel filtration column. Fractions containing 0ALR0 were pooled together for buffer exchange and characterization.

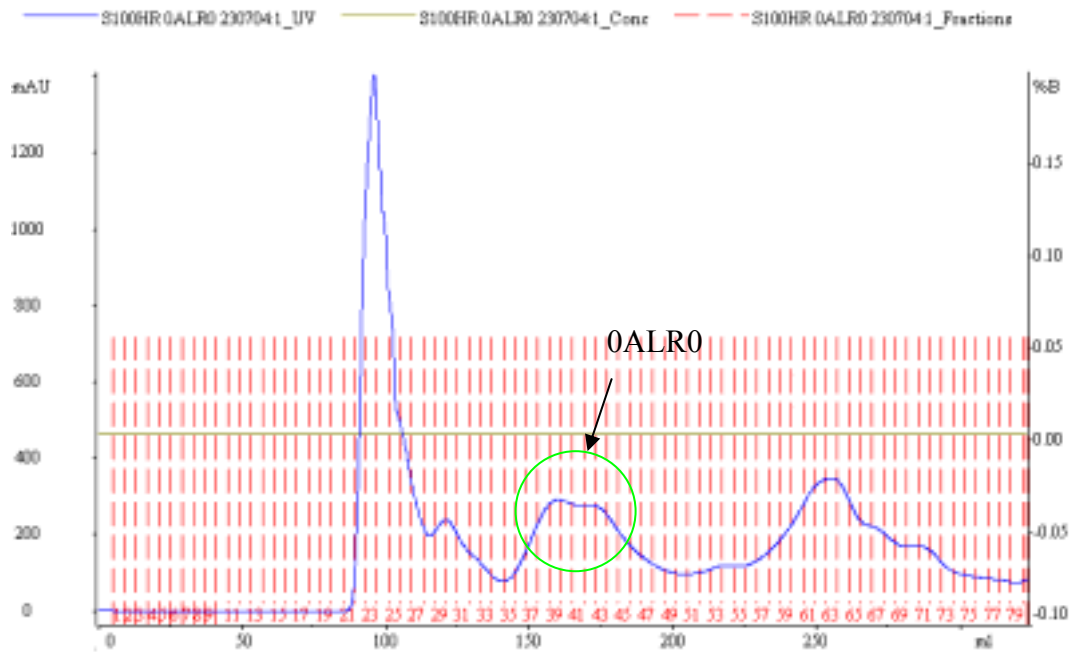


Fig. 3.6 Elution profile of 0ALR0 from HiPrep 26/60 Sephacryl S-100 column.

The protein concentration of the sample was measured by absorbance at 280 nm. The y-axis represents the amount of absorbance (mAU, absorbance units) and the x-axis represents the percentage of buffer B (%B). All the measurement was performed by a Pharmacia AKTA_{FPLC}.

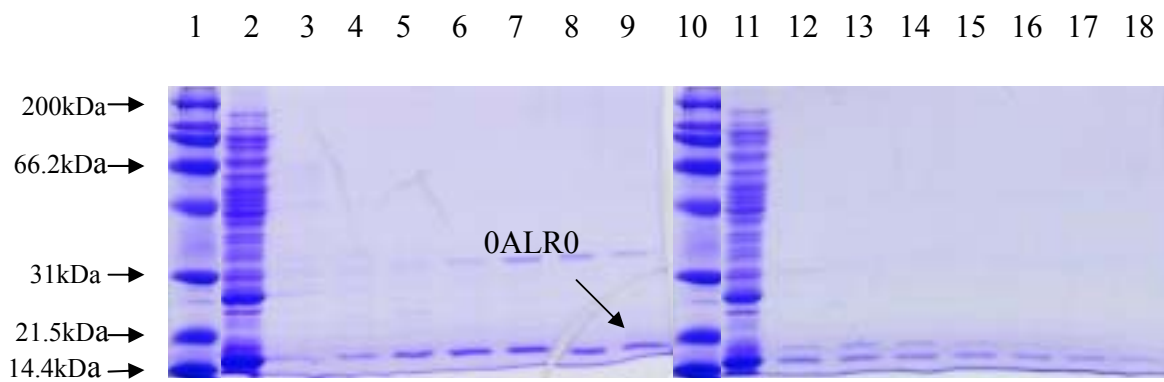


Fig. 3.7 12 % SDS-PAGE analysis showing fractions eluted from the gel filtration column. The molecular size of 0ALR0 was about 15 kDa for monomer. Lanes 1 and 10: broad range molecular weight markers; Lanes 2 and 11: soluble protein; Lanes 3 - 9 and 12 - 18: fractions 35 – 41 and 42 – 48, respectively.

3.1.2.2 Purification of 0ALR6

The recombinant 0ALR6 was produced in *E.coli* strain BL21(DE3)pLysS with plasmid pAEDALR6His. HiTrap chelating chromatography column was used to purify the protein 0ALR6. The presence of the hexahistidyl-tag at the C-terminus of the protein allowed rapid purification with the nickel agarose column (Amersham Pharmacia, Sweden). The 0ALR6 will bind to the nickel agarose with the binding buffer (0.5 M NaCl, 0.02 M sodium phosphate, pH 7.4) and eluted with elution buffer (0.5 M NaCl, 0.02 M sodium phosphate, 0.5 M imidazole, pH 7.4)

Fig. 3.8 shows the elution profile of the 0ALR6. The fractions eluted from the HiTrap chelating chromatography column were analyzed by SDS-PAGE and the Bradford assay. Fig. 3.9 shows the result of the 12 % SDS-PAGE analysis of the different fractions eluted from affinity column. Fractions containing 0ALR6 were pooled together for buffer exchange and characterization.

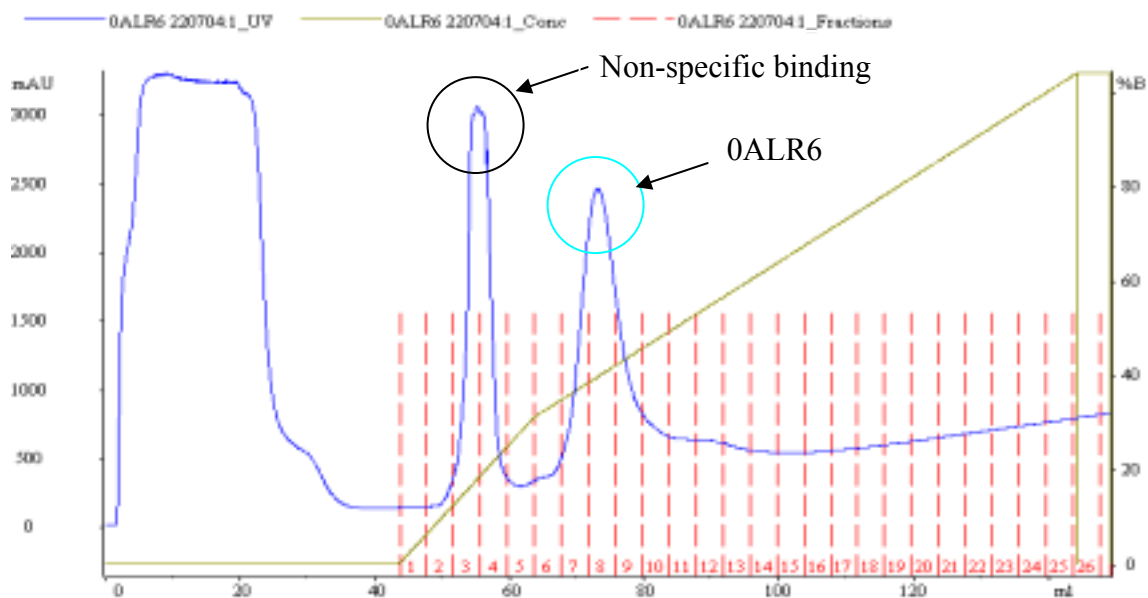


Fig. 3.8 Elution profile of 0ALR6 from the HiTrap chelating chromatography column. The protein concentration of the sample was measured by absorbance at 280 nm. All the measurement was performed by using the Pharmacia AKTA_{FPLC}. The elution concentration was detected by the conductivity flow cell, and it was represented by conductivity, i.e. 100 % = 0.5 M imidazole. The y-axis represents the amount of absorbance (mAU, absorbance units).

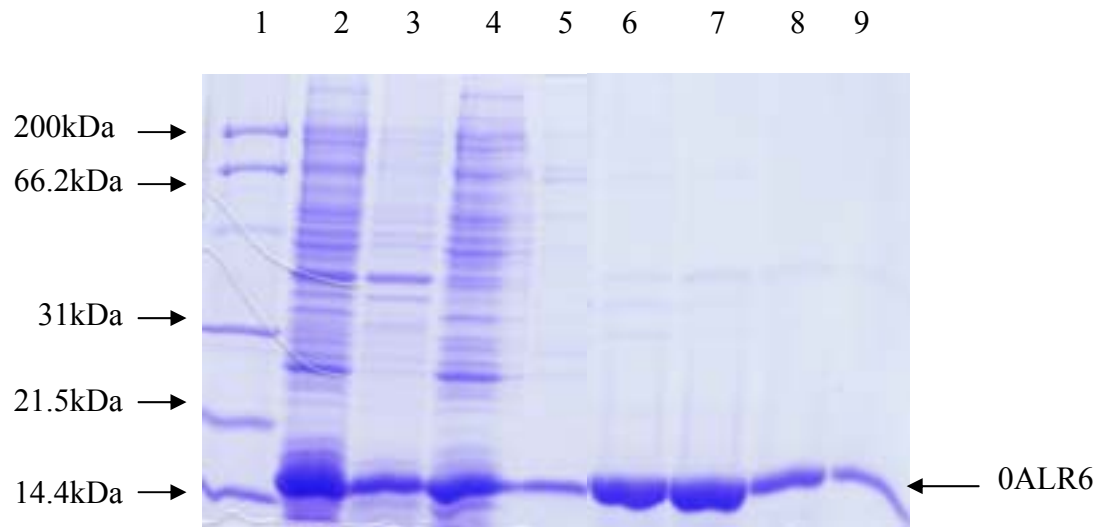


Fig. 3.9 12 % SDS-PAGE analysis showing fractions eluted from the HiTrap chelating chromatography column. The molecular size of 0ALR6 was about 15.8 kDa for monomer. Lane 1: broad range molecular weight markers; Lane 2: soluble protein; Lane 3: flow through; Lane 4: fraction 3; Lanes 5 – 9: fractions 6 - 10 respectively.

3.1.2.3 Purification of 0ALR12

The recombinant 0ALR12 was produced in *E.coli* strain BL21(DE3)pLysS with plasmid pAEDALR-12His. HiTrap chelating chromatography column was used to purify the protein 0ALR12. The presence of the dodeca-histidyl-tag at the C-terminus of the protein allowed rapid purification with the nickel agarose column (Amersham Pharmacia, Sweden). The 0ALR12 will bind to the nickel agarose with the binding buffer (0.5 M NaCl, 0.02 M sodium phosphate, pH 7.4) and eluted with elution buffer (0.5 M NaCl, 0.02 M sodium phosphate, 0.5 M Imidazole, pH 7.4)

Fig. 3.10 shows the elution profile of the 0ALR12. The fractions eluted from the HiTrap chelating chromatography column were analyzed by SDS-PAGE and the Bradford assay. Fig. 3.11 shows the result of the 12 % SDS-PAGE analysis of the different fractions eluted from affinity column. Fractions containing 0ALR12 were pooled together for buffer exchange and characterization.

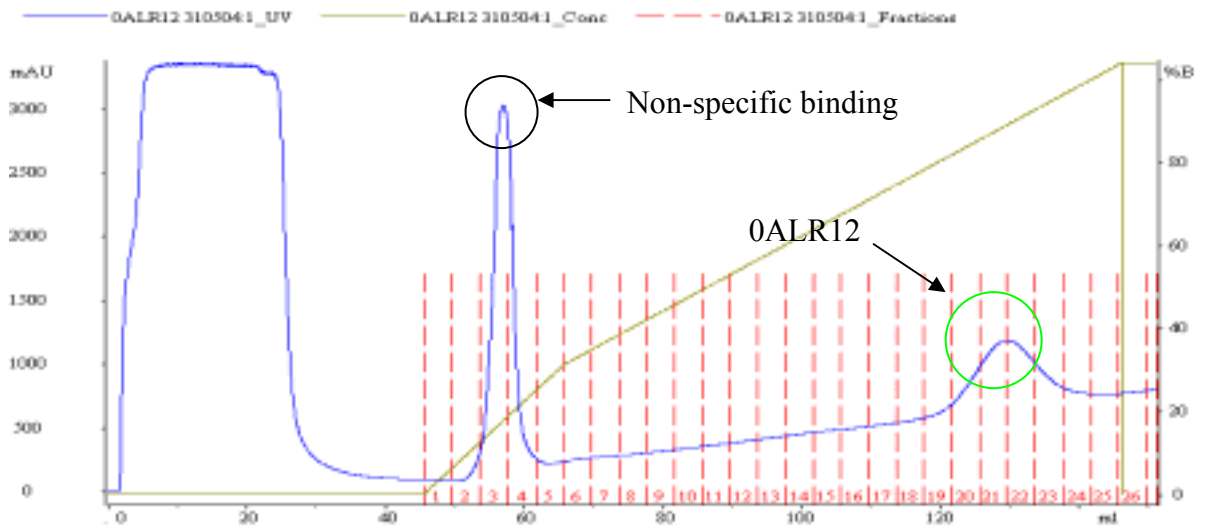


Fig. 3.10 Elution profile of 0ALR12 from the HiTrap chelating chromatography column. The protein concentration of the sample was measured by absorbance at 280 nm. All the measurements were performed by using the Pharmacia AKTA_{FPLC}. The elution concentration was detected by the conductivity flow cell, and it was represented by conductivity, i.e. 100 % = 0.5 M imidazole. The y-axis represents the amount of absorbance (mAU, absorbance units).



Fig. 3.11 12 % SDS-PAGE analysis showing fractions eluted from the HiTrap chelating chromatography column. The molecular size of 0ALR12 was about 16.6 kDa for monomer. Lane 1: broad range molecular weight markers; Lane 2: soluble protein; Lane 3: flow through; Lane 4: fraction 3; Lanes 5 – 10: fractions 19 – 24, respectively.

3.1.2.4 Purification of 0ALR18

The recombinant 0ALR18 was produced in *E. coli* strain BL21(DE3)pLysS with plasmid pAEDALR-18His. HiTrap chelating chromatography column was used to purify the protein 0ALR18. The presence of the dodeca-histidyl-tag at the C-terminus of the protein allowed rapid purification with the nickel agarose column (Amersham Pharmacia, Sweden). The soluble 0ALR18 will bind to the nickel agarose with the binding buffer (0.5 M NaCl, 0.02 M sodium phosphate, pH 7.4) and eluted with elution buffer (0.5 M NaCl, 0.02 M sodium phosphate, 0.5 M imidazole, pH 7.4)

Fig. 3.12 shows the elution profile of the 0ALR18. The fractions eluted from the HiTrap chelating chromatography column were analyzed by SDS-PAGE and the Bradford assay. Fig. 3.13 shows the result of the 12 % SDS-PAGE analysis of the different fractions eluted from affinity column.

The yield of different purified soluble ALR proteins was showed in Table 3.1. 0ALR6 and 0ALR12 have the higher yield than 0ALR0. 0ALR18 also has been expressed, but all are insoluble protein.

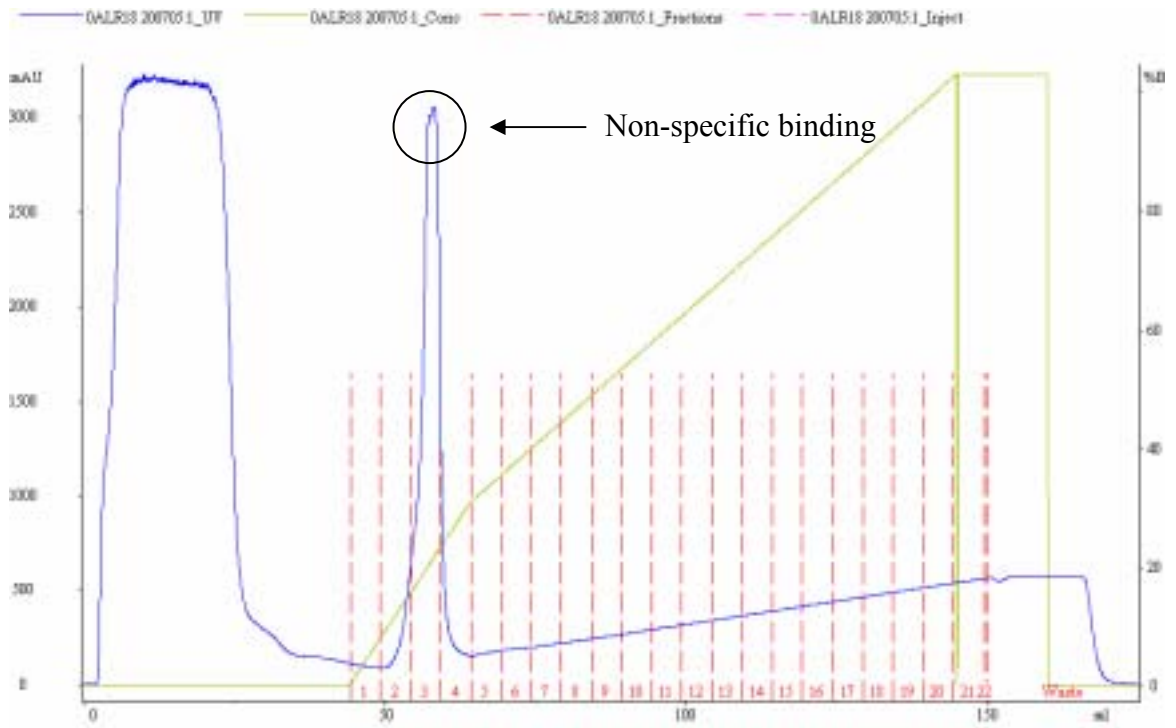


Fig. 3.12 Elution profile of 0ALR18 from the HiTrap chelating chromatography column. The protein concentration of the sample was measured by absorbance at 280 nm. All the measurements were performed by using the Pharmacia AKTA_{FPLC}. The elution concentration was detected by the conductivity flow cell, and it was represented by conductivity, i.e. 100 % = 0.5 M imidazole. The y-axis represents the amount of absorbance (mAU, absorbance units).

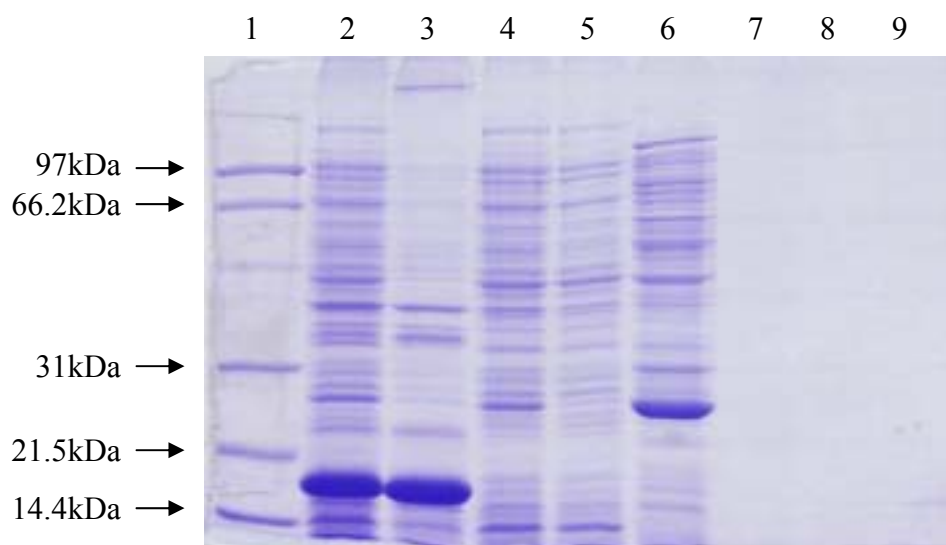


Fig. 3.13 12 % SDS-PAGE analysis showing fractions eluted from the HiTrap chelating chromatography column. The molecular size of 0ALR18 was about 17.4 kDa for monomer. Lane 1: low range molecular weight markers; Lane 2: total protein; Lane 3: insoluble protein; Lane 4: soluble protein; Lane 5: flow through; Lane 6: fraction 3; Lane 7: fraction 5; Lane 8: fraction 7; Lane 9: fraction 9.

Table 3.1 The yield of purified soluble ALR proteins with different length of polyhistidine tag.

Proteins	0ALR0	0ALR6	0ALR12	0ALR18
Yield mg/L	30	150	120	0

3.2 Characterizations of recombinant human ALR

3.2.1 Solubility test

Sodium Dodecyl Sulfate Polyacrylamide Gel Electrophoresis (SDS/PAGE)

From the result shown in Fig. 3.14, the percentage of ALR presented in the *E. coli* was increasing from 0ALR0 to 0ALR18. On the contrary, the percentage of soluble ALR was decreasing from 0ALR6 to 0ALR18. When 6 histidines were added to the 0ALR0, there was no significant change in protein solubility. However, when 12 and 18 histidines were added to the 0ALR0, the protein solubility was decreased 23 % and 60 % respectively.

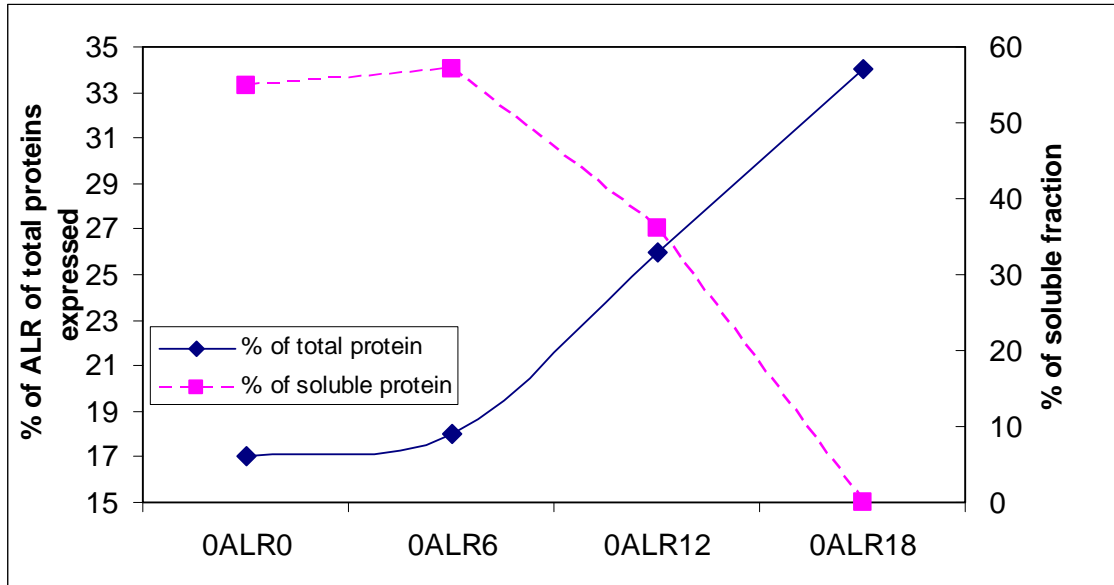


Fig. 3.14 The relationship between number of histidine in C-terminus and the percentage of solubility. The percentage of ALR presented in the *E. coli* was increasing from 0ALR0 to 0ALR18. But contrarily, the percentage of soluble ALR was decreasing from 0ALR6 to 0ALR18. Each data point represents the data from one single experiment.

3.2.2 Dimer formation

The purified ALR was isolated as monomer and homodimer from *E. coli*. Fig. 3.15 shows the presence of monomer and dimer of 0ALR12 mainly in 20 mM Tris-HCl buffer as well as a small amount of trimer and tetramer. However, after buffer exchange to 5 mM histidine solution, only monomer and dimer can be observed.

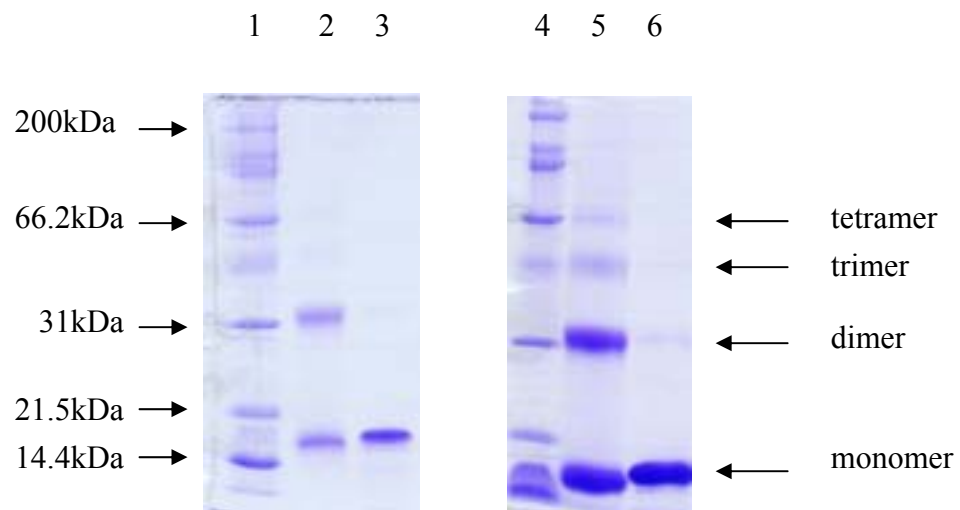


Fig. 3.15 SDS-PAGE (denaturing gel) analysis showing dimer formation of 0ALR12 by Coomassie blue stain. Lanes 1 and 4: broad range molecular marker; Lane 2: 0ALR12 in 5 mM histidine solution without 30 mM DTT in sample buffer; Lane 3: 0ALR12 in 5 mM histidine solution with 30 mM DTT in sample buffer; Lane 5: 0ALR12 in 20 mM Tris-HCl buffer without 30 mM DTT in sample buffer; Lane 6: 0ALR12 in 20 mM Tris-HCl buffer with 30 mM DTT in sample buffer. A single chain is shown in reducing condition (Lane 3), while the dimer is shown in non-reducing condition (Lane 2).

3.2.3 Far-UV circular dichroism (CD) analysis

Circular dichroism provides a direct method for determining the gross conformational properties of protein. CD spectra of 0ALR0, 0ALR6 and 0ALR12 were measured from 190 to 250 nm by using Jasco 810 spectrophotometer (JASCO) (Fig. 3.16) (Table 3.2). The secondary structure was estimated by the Jasco secondary structure estimation using Yang's reference provided by the JASCO. All 3 proteins showed very similar profiles, this means that 0ALR6 and 0ALR12 retain the native conformation of the native protein (0ALR0).

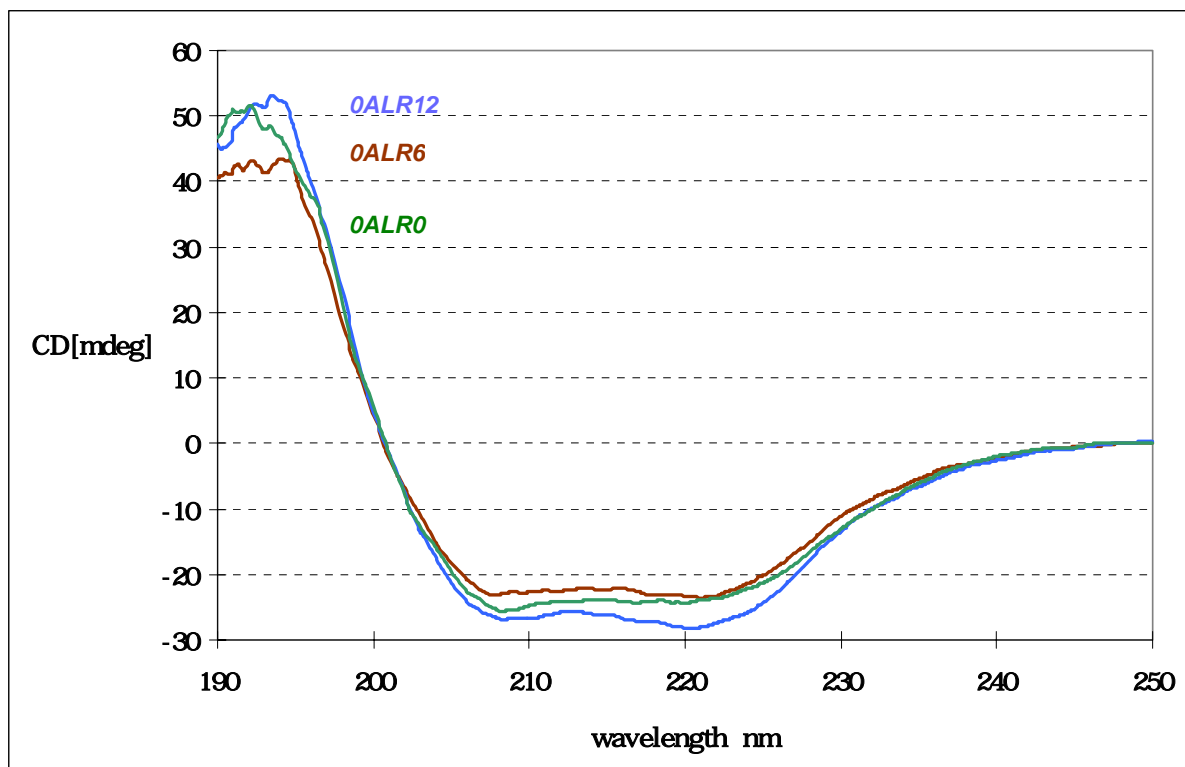


Fig. 3.16 Far-UV CD analysis showing the CD spectra of 0ALR0, 0ALR6 and 0ALR12.

Table 3.2 The result of Jasco secondary structure estimation.

	0ALR0	0ALR6	0LAR12
Helix	38.1%	33%	32.7%
Beta	34.4%	40.8%	41.4%
Turn	0	0	0
Random	27.5%	26.3%	25.9%
Total	100%	100%	100%

3.2.4 Isoelectric focusing

The isoelectric points of the purified proteins were calculated from standard curve. Table 3.3 shows the calculated isoelectric points of polyhistidine-tagged ALR. The 0ALR0 (pI 7.17), 0ALR6 (pI 7.16) and 0ALR12 (pI 7.093) have similar isoelectric points. This indicated that the presence of histidine-tag did not affect the isoelectric point of protein. Fig. 3.18 shows the calibration curve of pI calibration kit (pH3-10).

Table 3.3 Calculated isoelectric points of polyhistidine-tagged ALR.

Protein	0ALR0	0ALR6	0ALR12
PI	7.17	7.16	7.09

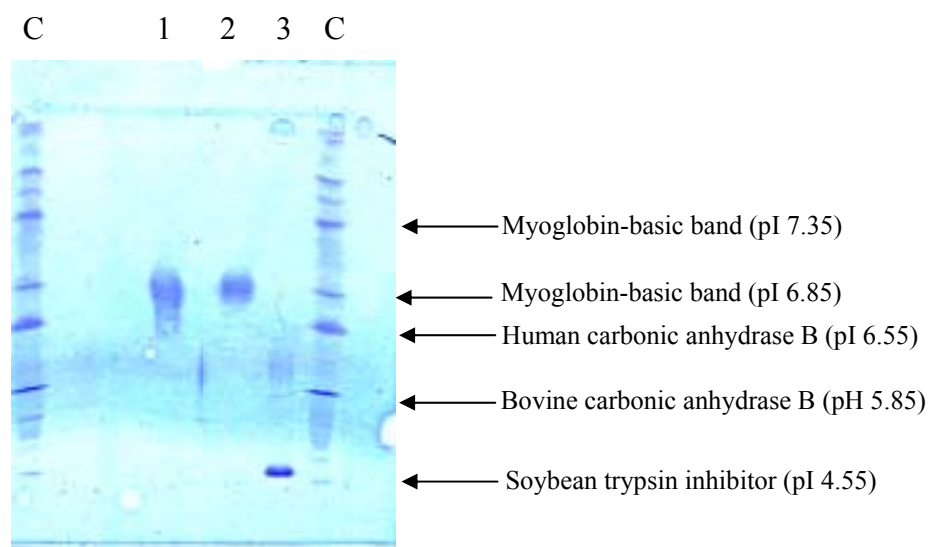


Fig. 3.17 The results of the isoelectric focusing of purified ALR. Lane C, broad range calibrator, some of the calibrated proteins and their pI are listed in the figure; Lane 1, 0ALR0; Lane 2, 0ALR6; Lane 3, bovine serum albumin (BSA).

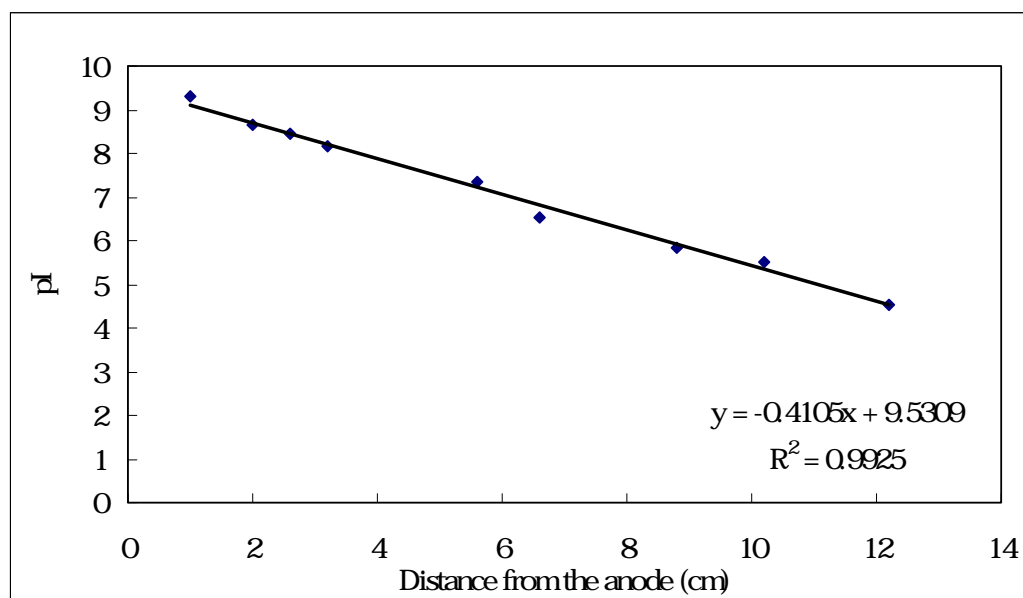


Fig. 3.18 The calibration curve of pI calibration kit (pH3-10)

3.2.5 FAD content measurement

3.2.5.1 Spectroscopy of recombinant ALR

The visible spectroscopy of 0ALR0, 0ALR6, 0ALR12 and pure FAD are shown in Fig. 3.19. The absorbance in the range from 350 nm to 550 nm was measured. These spectra of the 0ALR0, 0ALR6 and 0ALR12 are characteristic for an FAD moiety, but exhibit the distinct difference from pure FAD (Lee *et al.*, 2000). The absorbance maximum of pure FAD at 449 nm is shifted by about 5 nm in the protein. The shoulder at 480 nm is also shifted and appears more pronounced for protein-bound FAD.

The FAD content of the proteins was calculated from the OD₄₆₀ values using and extinction coefficient of 10 mM⁻¹cm⁻¹. After determination of the protein concentration it was calculated that about 0.6 FAD molecules per monomer unit of protein are found. This suggests the presence of one FAD molecule per monomer unit.

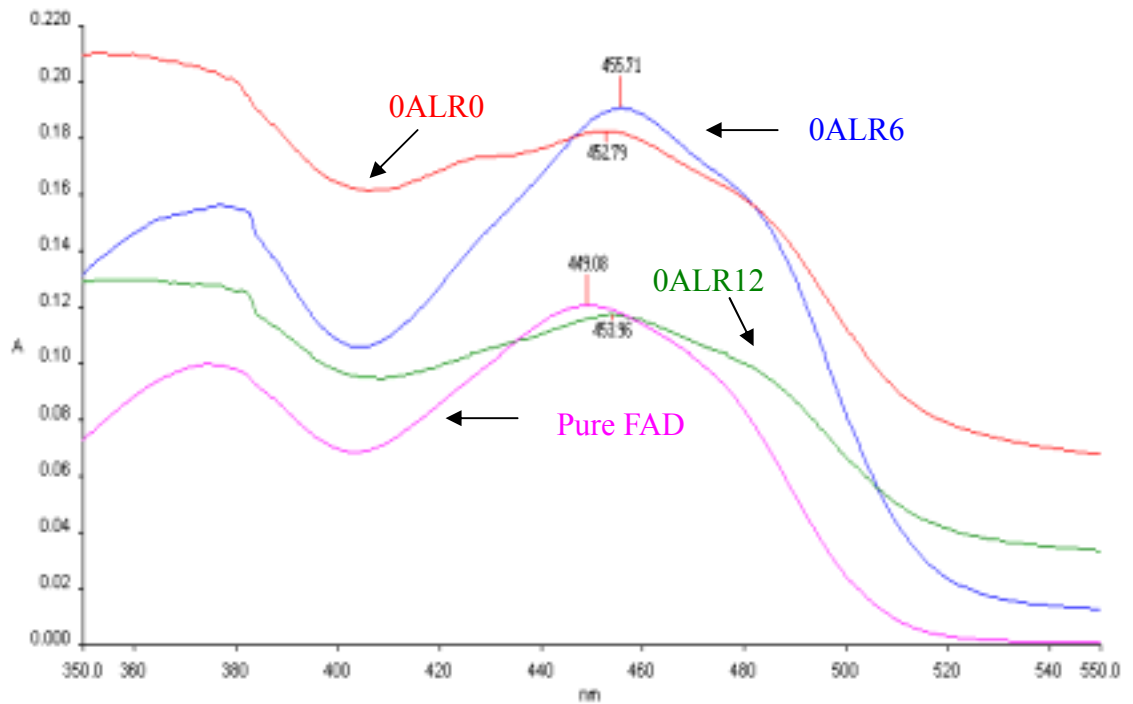


Fig. 3.19 Spectroscopy of the purified 0ALR0, 0ALR6, 0ALR12 and pure FAD.

The absorbance in the range from 350 nm to 550 nm was measured. Red line represents the spectrum for the 0ALR0, blue line represents the spectrum for the 0ALR6, green line represents the spectrum for the 0ALR12 and the purple line is a reference sample with 10 μ M pure FAD. The ALR spectra are characteristic for an FAD moiety, but show distinct differences from pure FAD.

3.2.5.2 Release of protein-bound FAD by heat and acid treatment

After boiling the protein for one hour and 5 % trichloroacetic acid (TCA) treatment, the bound FAD was released and the protein was precipitated out at the same time. Fig. 3.20 shows the visible spectra of 0ALR12 after heat and acid treatment. The spectrum of the released FAD is similar to that of the pure FAD, suggesting the FAD is released out. It demonstrates FAD is firmly attached, but not covalently linked, to the protein. However, the absorbance maximum of the free FAD at 445 nm is shifted by about 5 nm in the released FAD, it is because the TCA might cause some changes to the FAD. Fig. 3.21 shows the standard curve of the pure FAD.

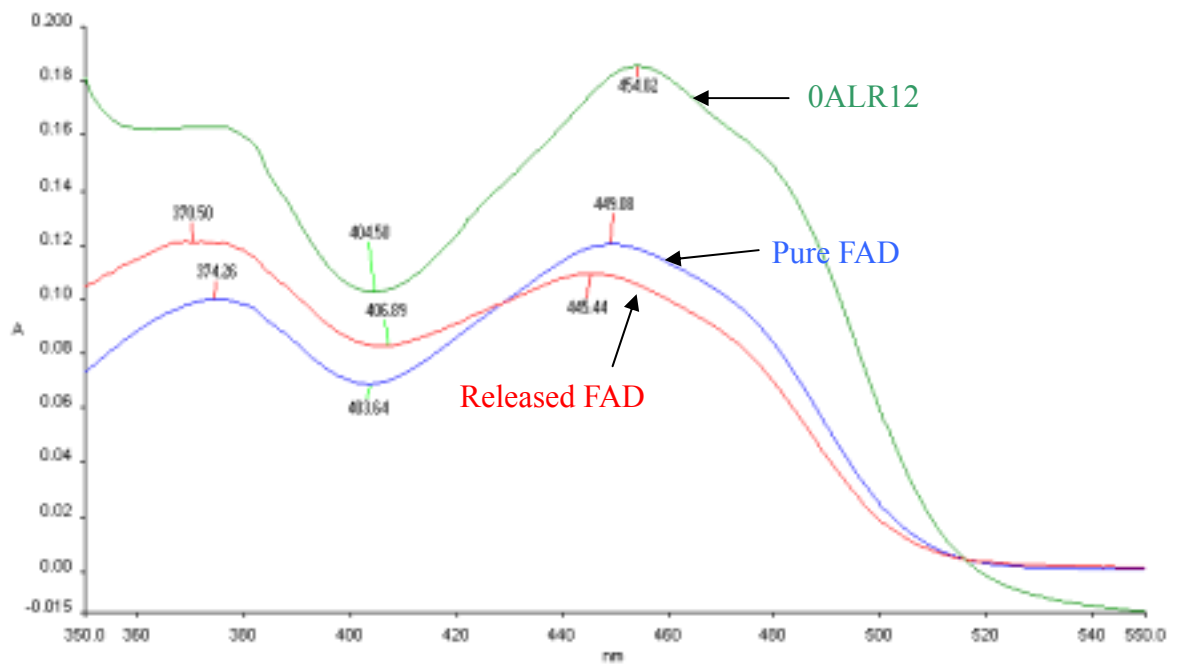


Fig. 3.20 The visible spectra of non-covalently bound FAD after heat and acid treatment. The absorbance in the range from 350 nm to 550 nm was measured. Green line represents the spectrum for the 0ALR12, red line represents the spectrum of released FAD and blue line is a reference sample with 10 μ M pure FAD.

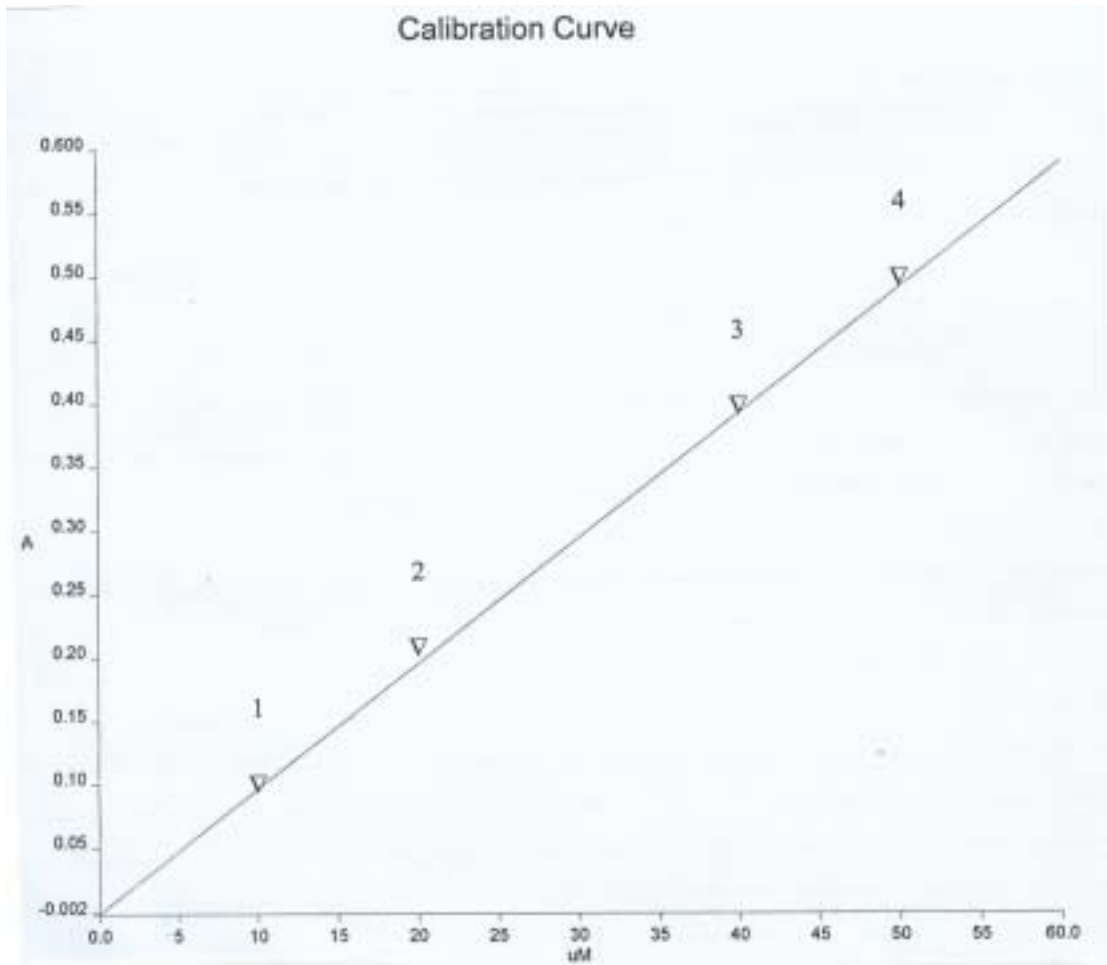
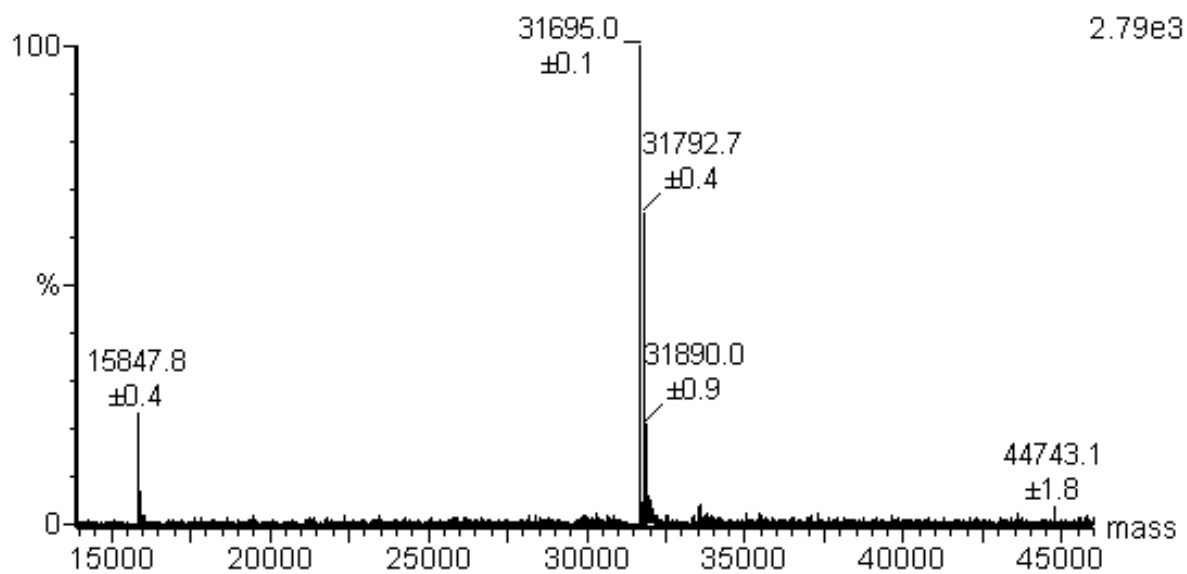


Fig. 3.21 Standard curve of the free FAD at A_{450} . Good linearity was observed in the concentrations from 0 μM to 50 μM of FAD with correlation coefficient of 0.9998, indicating that the concentration used was optimal.

3.2.8 Mass-spectrometric analysis

To identify ALR molecular mass by mass spectrometry, the samples were buffer exchanged with Milli-Q water in order to remove the salt before injecting into the ESI-Q-TOF mass spectrometer. The ESI-Q-TOF-MS analysis show that the molecular masses were 15847.8 Da for monomer and 31695 Da for dimer of 0ALR6 and 33436.6 Da for dimer of 0ALR12.

(a)



(b)

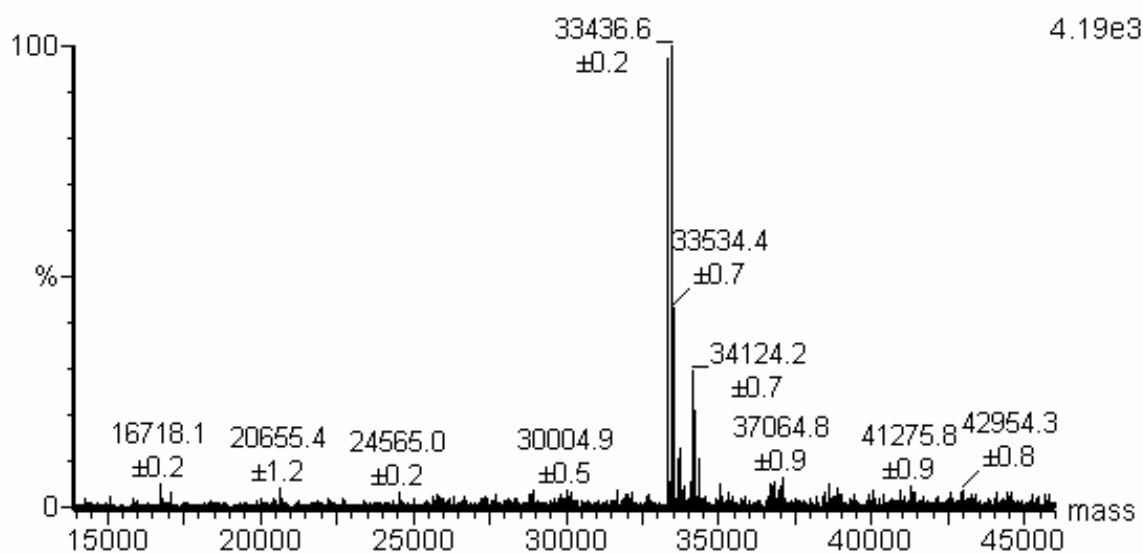


Fig. 3.22 Mass spectra (ESI-MS) of polyhistidine-tagged (a) 0ALR6 and (b)

0ALR12. (a) Two peaks were detected in 0ALR6, corresponding to the

monomer and dimer of the 0ALR6. The first peak represents the monomer of 0ALR6. Since the theoretical value is 15849.8 Da, the value is very close and the error is only 0.012 %. The second peak represents the dimer of 0ALR6. Since the theoretical value is 31699.6 Da, the error is only 0.014 %. The minor peaks close to the second peak may be due to some phosphate molecules on the protein because the molecular weight different is 98 Da, which is equal to the molecular weight of PO_4^- . (b) One major peak for 0ALR12. The peak represents the dimer of the 0ALR12. Since the theoretical value is 33345.4 Da, there is a 91 Da difference. This might be due to one PO_4^- molecule that was bound to the protein and causing the weight increase. Two more minor peaks were observed with the same pattern as (a).

3.2.8 Solubility of 0ALR12 in various buffers

In order to find a suitable buffer to keep the ALR protein soluble, different buffers were tested and 100 mM histidine solution was found to be the best for the ALR. Most of the buffer could not support protein concentration higher than 10 µg/ml such as PBS, MgCl₂, glycerol and glucose buffers. Sorbitol and glycine buffers showed better solubility, however the protein concentration still cannot reach 50 µg/ml. Only the histidine buffer could support the high protein concentration (up to 1000 µg/ml) (Table 3.4).

Table 3.4 Results of buffer test. Nearly all buffers gave poor solubility of 0ALR12 (less than 10 µg/ml) except histidine solution. Up to 2000 µg/ml of soluble ALR was obtained in high histidine concentration solution (0.2 M).

Buffer	Tested concentration	Soluble protein concentration
H ₂ O		Less than 10 µg/ml
PBS	With 0.8 % - 3 % NaCl	Less than 10 µg/ml
MgCl ₂	20 mM	Less than 10 µg/ml
Glucose	5 %, 10 %, 15 %	Less than 10 µg/ml
Sorbitol	5 %, 10 % 15 %	Less than 10 µg/ml Less than 20 µg/ml
Glycerol	5 %, 10 %, 15 %	Less than 10 µg/ml
Glycine	0.1 %, 0.2 %, 0.3 %	Less than 50 µg/ml
Histidine	100 mM 0.2 M	Up to 1000 µg/ml Up to 2000 µg/ml

3.2.8 Activity assays

3.2.8.1 Sulphydryl oxidase activity

To investigate the *in vitro* activity of the enzyme, dithiothreitol (DTT) was used as a substrate. Due to the sulphydryl oxidase activity, the DTT was oxidized. At difference time points, the remaining free thiol groups of the substrate were quantified with the Ellman's reagent. Fig. 3.23 shows that 0ALR0 and 0ALR12 have the highest sulphydryl oxidase activities whereas 0ALR6 shows nearly half of the sulphydryl oxidase activity of the 0ALR12. In this experiment, pure FAD was used as a negative control. Pure FAD and without protein sample show no sulphydryl oxidase activity. Fig. 3.24 shows that the pegylated ALR gave even more sulphydryl oxidase activity than the native protein.

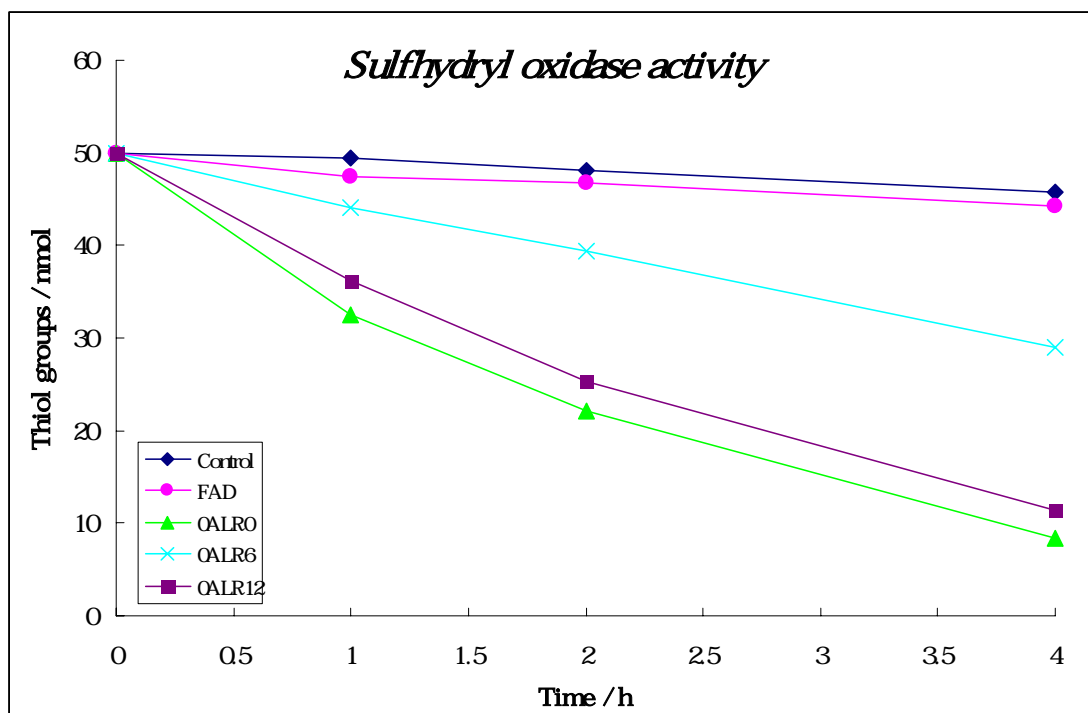


Fig. 3.23 Sulphydryl oxidase activity assay of different ALR. DTT corresponding to 50 nmol thiol groups was incubated with 10 pmol 0ALR0 (▲), 0ALR6 (×), 0ALR12 (■), pure FAD (●) or without protein () at 25 for different timepoint. The oxidation of the thiol groups was detected spectrophotometrically at 412 nm after the addition of DTNB. The time-dependent decrease of extinction indicates the oxidation of the thiol groups.

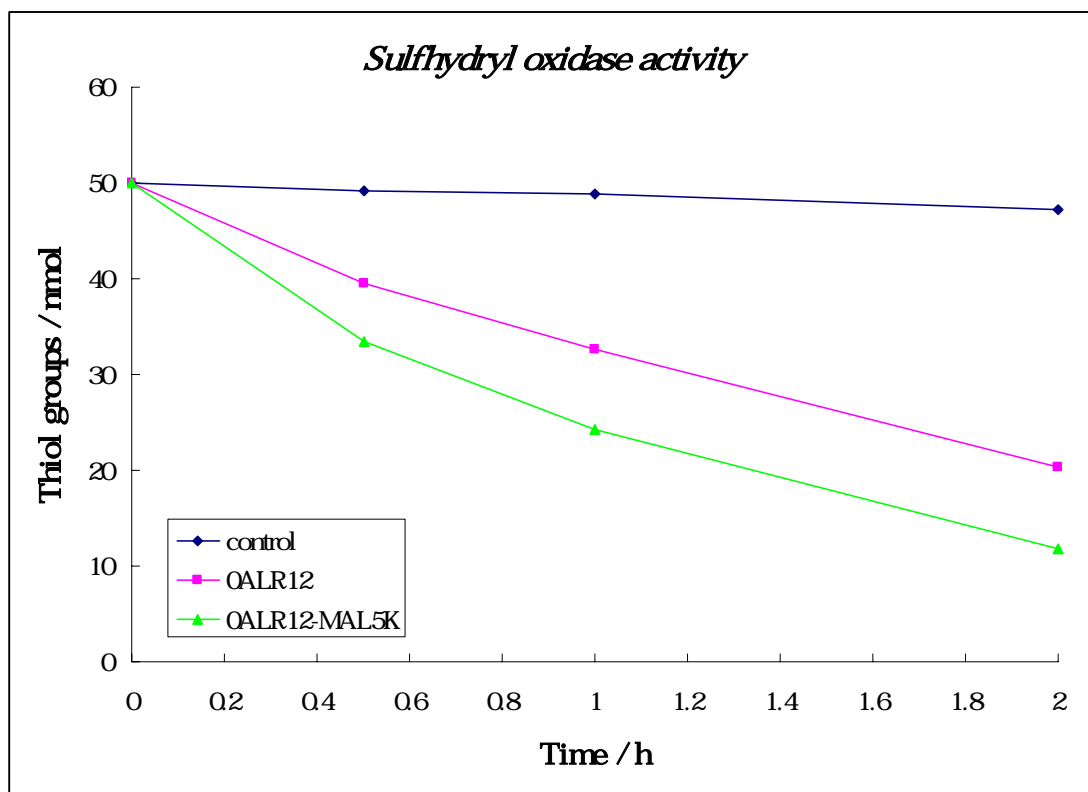


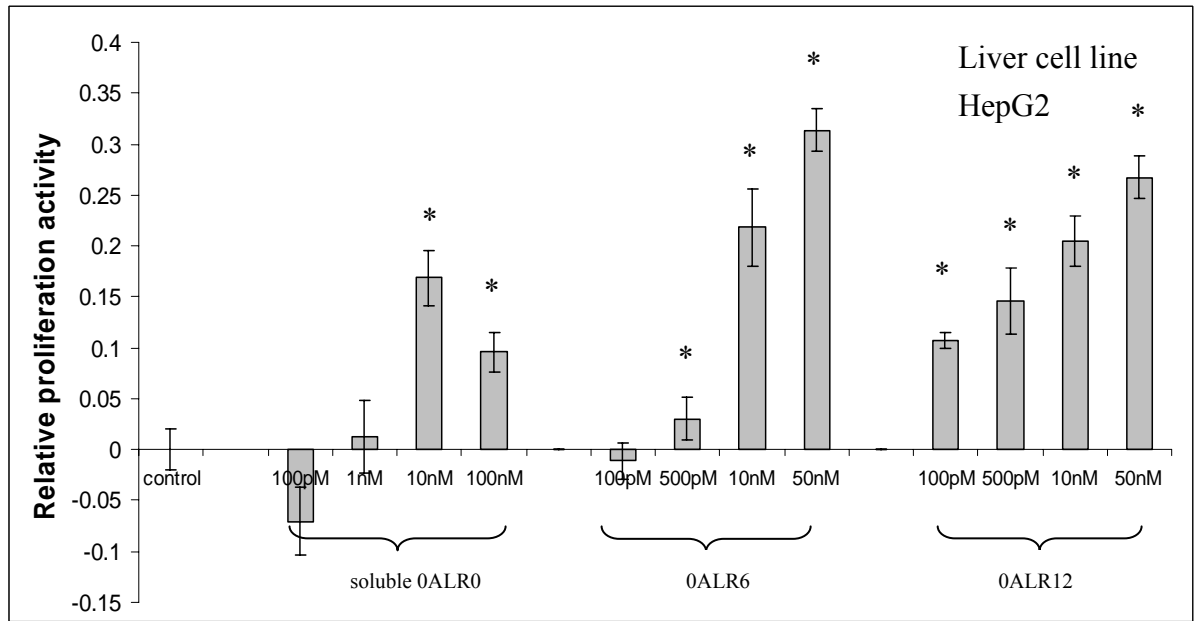
Fig. 3.24 Sulphydryl oxidase activity assay of pegylated ALR (0ALR12-MAL5K) and native ALR. DTT corresponding to 50 nmol thiol groups was incubated with 10 pmol 0ALR12 (■), 0ALR12-MAL5K (▲) or without protein (○) at 25 °C for different timepoint. The oxidation of thiol groups was detected spectrophotometrically at 412 nm after the addition of DTNB. The time-dependent decrease of extinction indicates the oxidation of the thiol groups.

3.2.8.2 Cell proliferation activity test

To investigate the cell proliferation ability of the protein, different cell lines were used in this experiment. Three ALRs (0ALR0, 0ALR6 and 0ALR12) were added to 4 different cell lines (Liver cell line, breast cell line, colorectal cell and lung cell line) to test the cell proliferation ability by the MTS assay. Fig. 3.25 shows the effect of polyhistidine-tagged ALR on proliferation of different cell lines. Fig. 3.25a shows that ALR promoted the proliferation of liver cell line (HepG2). After 24 h of starvation, 0ALR0, 0ALR6 and 0ALR12 all showed stimulatory effect on cell proliferation when incubated for 72 h. In addition, the stimulatory effect for 50 nM of 0ALR6 and 0ALR12 is significantly higher than 100 pM. There was a significant difference in the relative cell number between the control and ALRs-treated cell ($*_{\text{HepG2}} p < 0.05$). In addition, different concentrations of pHGF were added to another set of HepG2 culture ($^{\#}_{\text{pHGF}} p < 0.05$). Fig. 3.26 shows the result of the proliferation assay of pHGF. It also showed the cell proliferation effect towards HepG2. Cell lines other than liver cells did not show any significant growth effect between the control and ALR-treated cell (Figs. 3.25b, c and d) ($^{\text{A549}} p > 0.05$, $^{\text{Ht29}} p > 0.05$ and $^{\text{MCF7}} p > 0.05$).

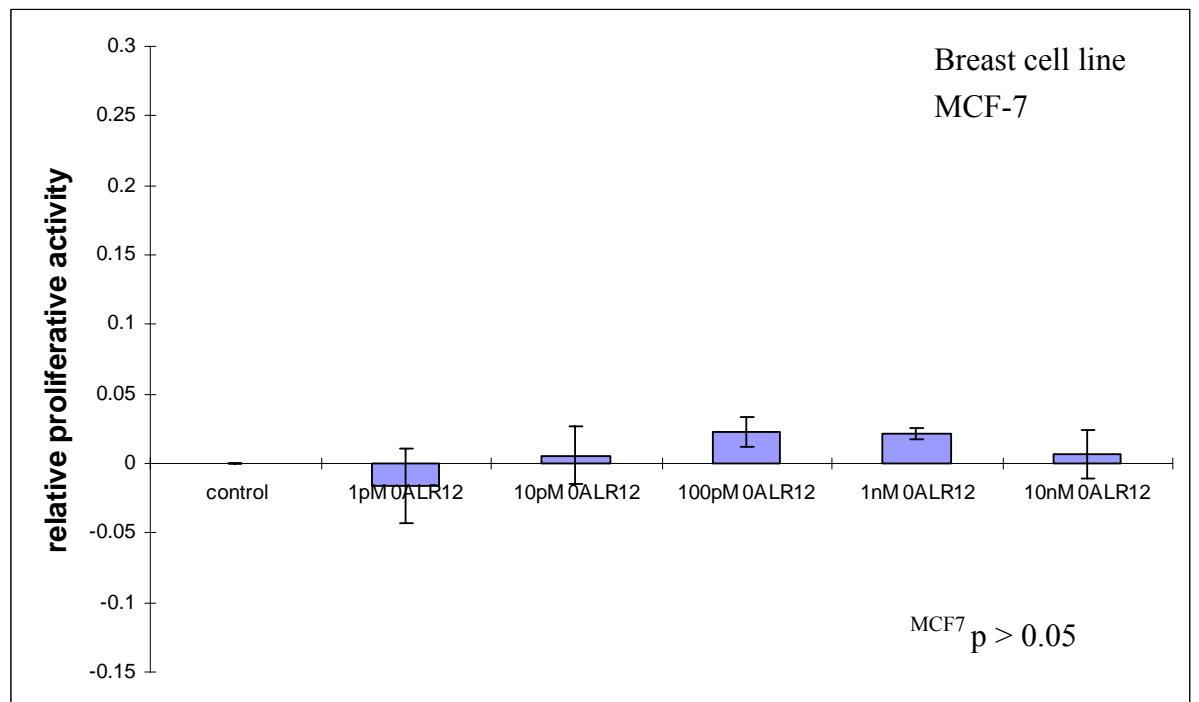
In addition, after 0ALR12 was chosen as our target protein. It was pegylated by mPEG-MAL and tested for the cell proliferation ability. The pegylated ALR (0ALR12-MAL5K) was tested with the liver cell line and the results in Fig 3.26 show that 0ALR12-MAL5K also promoted proliferation on the liver cell line and the effect was significantly greater than the native one ($p < 0.05$ vs native 0ALR12) (Fig. 3.27).

a)

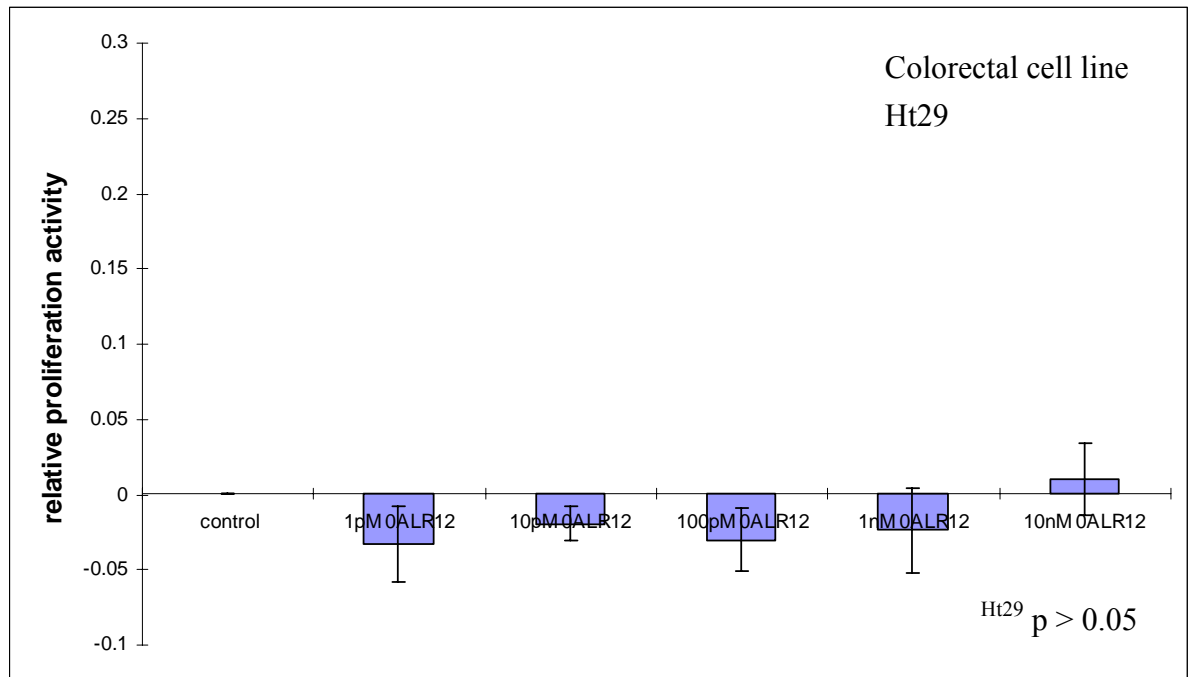


*HepG2 $p < 0.05$

b)



c)



d)

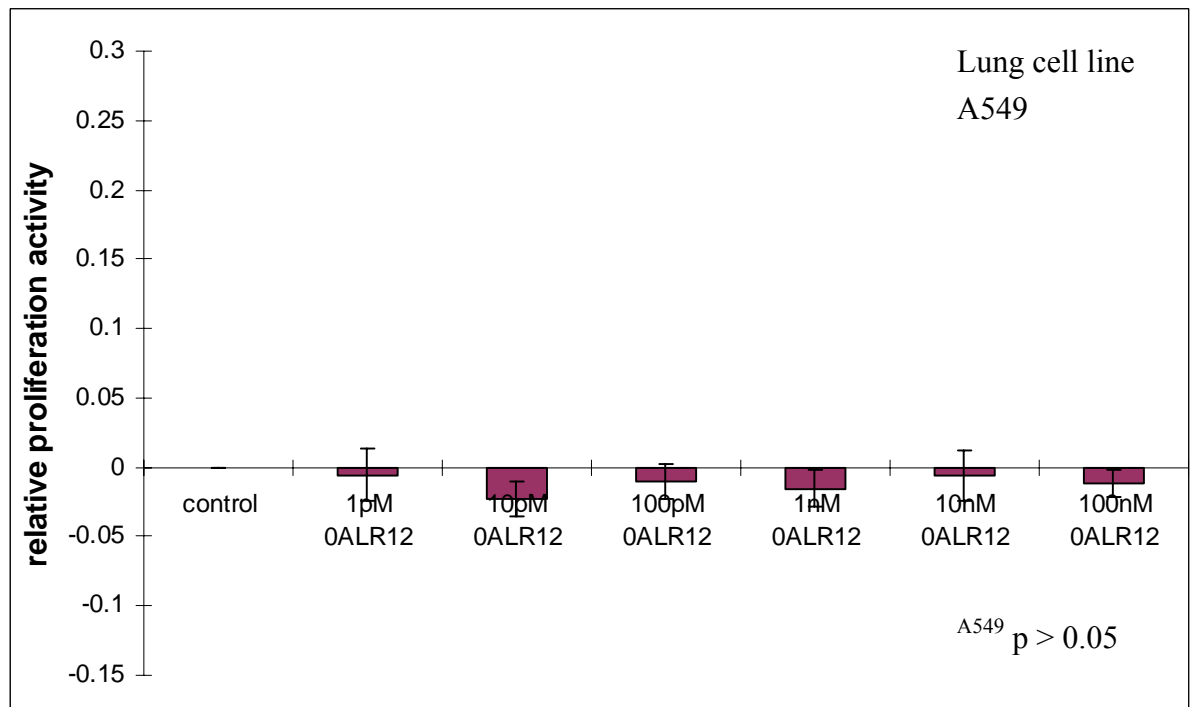


Fig. 3.25 Effect of polyhistidine-tagged ALR on proliferation of different cell

lines. a) Liver cell line, HepG2, b) Breast cell line, MCF-7, c) Colorectal cell line, Ht29, d) Lung cell line, A549. Cells (3000 cells/well) were seeded in 96-well culture plates in DMEM and allowed to adhere for 24 h, and then the cells were starved for another 24 h. Cells were treated with different concentrations of ALR for 3 days. Cell viability was determined by using the MTS assay. Results are expressed as percentages of cell growth normalized to cell number of viable cells in controls. (*^{HepG2} p < 0.05 vs control, ^{MCF7} p > 0.05 vs control, ^{Ht29} p > 0.05 vs control, ^{A549} p > 0.05 vs control)

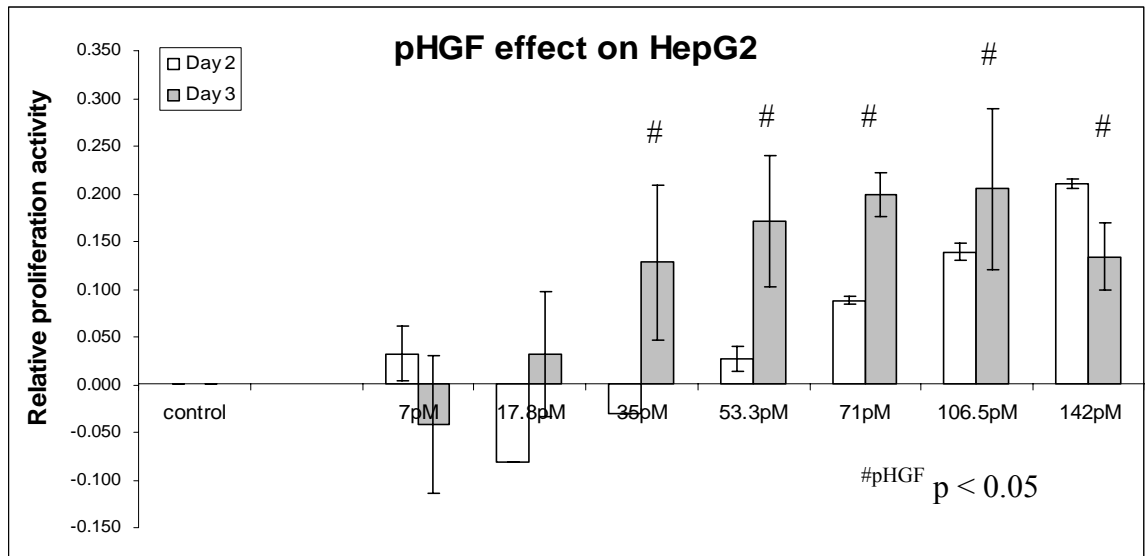


Fig. 3.26 Effect of pHGF on proliferation of HepG2. Cells (3000 cells/well) were seeded in 96-well culture plates in DMEM and allowed to adhere for 24 h, and then the cells were starved for another 24 h. Cells were treated with different concentrations of pHGF for 2 or 3 days. Cell viability was determined by using the MTS assay. Results are expressed as percentages of cell growth normalized to cell number of viable cells in controls. (^{#pHGF} p < 0.05 vs control)

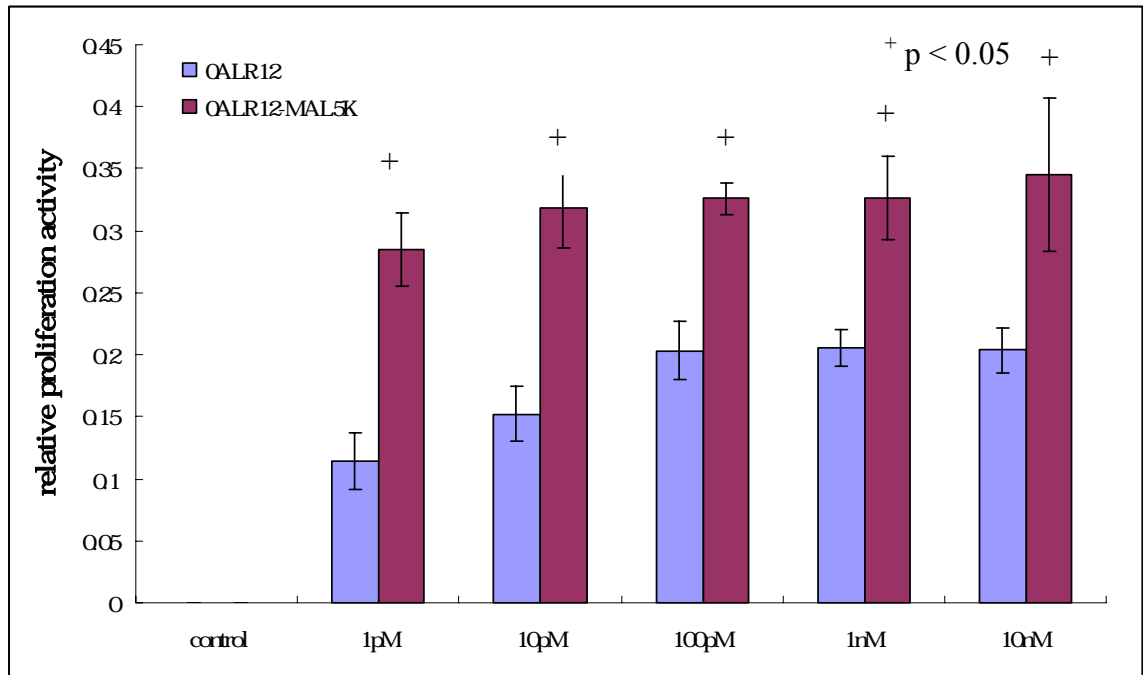


Fig. 3.27 Effect of the pegylated ALR and native ALR on proliferation of HepG2 cells. Cells (3000 cells/well) were seeded in 96-well culture plates in DMEM and allowed to adhere for 24 h, and then the cells were starved for another 24 h. Cells were treated with different concentrations of 0ALR12 and 0ALR12-Mal5K for 3 days. Cell viability was determined by using the MTS assay. Results are expressed as percentages of cell growth normalized to cell number of viable cells in controls. (⁺ $p < 0.05$ vs native 0ALR12)

3.3 Pegylation of recombinant ALR

3.3.1 Pegylation of ALR with different PEG molecules

ALR has a poor solubility and needs large amount of histidine to stabilize it. Modification of ALR with polyethylene glycol (PEG) would overcome these problems. Four PEG molecules were used for ALR pegylation; they are: mPEG-NHS, mPEG-MAL, mPEG-SPA and mPEG-ALD.

A 12 % SDS-PAGE was used to analyze the modification of ALR with various PEGs. 0.1 g of purified 0ALR12 was used in each reaction. The results are presented in Figs. 3.28-3.31. For the mPEG-NHS and mPEG-ALD, the protein was remained in native form after 24 h reaction. For the mPEG-SPA, the pegylation reaction occurred within 1 h, but only a small degree of protein was pegylated. For the mPEG-MAL, the 0ALR12 was pegylated within 1 h and over 70 % of protein is pegylated. From the result, it indicated that mPEG-MAL pegylated 0ALR12 more efficiently, followed by mPEG-SPA. Both mPEG-ALD and mPEG-NHS showed no observable amount of pegylated protein. In Figs. 3.24 and 3.27, it was observed that pegylation of ALR using mPEG-MAL5K did not significantly affect the sulphhydryl oxidase activity and

the ability to stimulate the cell proliferation of the ALR. Therefore, mPEG-MAL (MW= 5000) was selected for the pegylation of ALR in future experiments.

In order to identify the pegylated protein, western blot analysis was used. In Fig. 3.32, anti-His primary antibody was used to analyze the pegylated ALR. In lane 2, the lowest band was the native OALR12 and the 3 upper bands indicated the 3 form of pegylated OALR12.

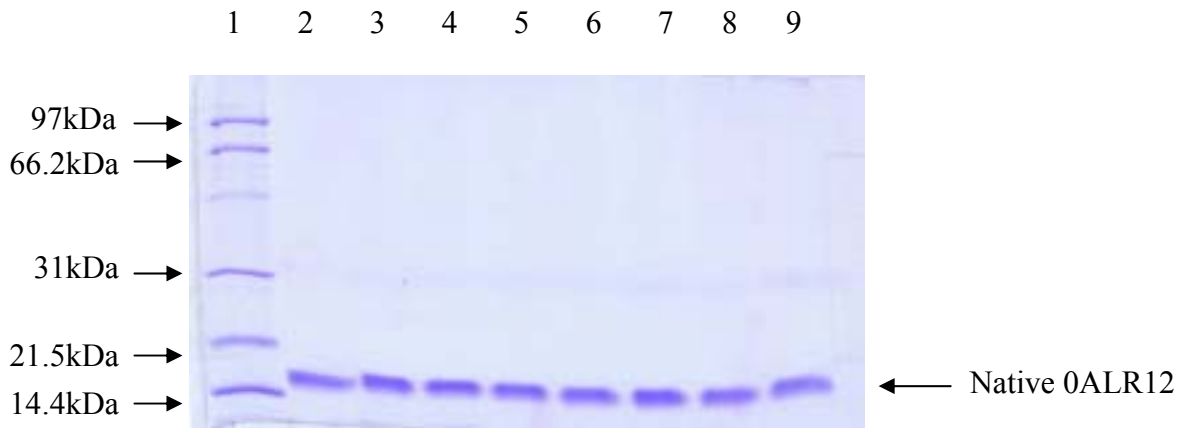


Fig. 3.28 Pegylation of purified 0ALR12 with mPEG-NHS. 12 % of SDS-PAGE was used to analyze the pegylation products at different time points. Lane 1: low-range protein marker; Lane 2: native 0ALR12. Lanes 3, 4, 5, 6, 7, 8, 9 are 1 h, 2 h, 3 h, 4 h, 5 h, 6 h, overnight, respectively. 0.1 g of purified 0ALR12 was used in each reaction.

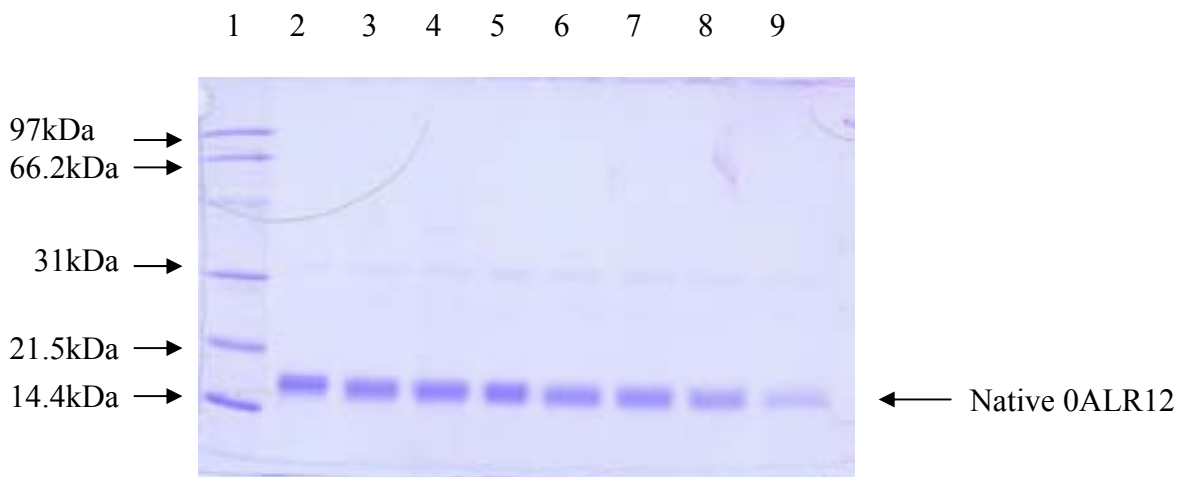


Fig. 3.29 Pegylation of 0ALR12 with mPEG-ALD. 12 % of SDS-PAGE was used to analyze the reaction products at different time points. Lane 1: low-range protein marker; Lane 2: native 0ALR12. Lanes 3, 4, 5, 6, 7, 8, 9 are 1 h, 2 h, 3 h, 4 h, 5 h, 6 h, overnight, respectively.



Fig. 3.30 Purified 0ALR12 was modified with mPEG-SPA. 12 % of SDS-PAGE was used to analyze the reaction products at different time points. Lane 1: low-range protein marker; Lane 2: native 0ALR12. Lanes 3, 4, 5, 6, 7, 8, 9 are 1 h, 2 h, 3 h, 4 h, 5 h, 6 h, overnight, respectively.

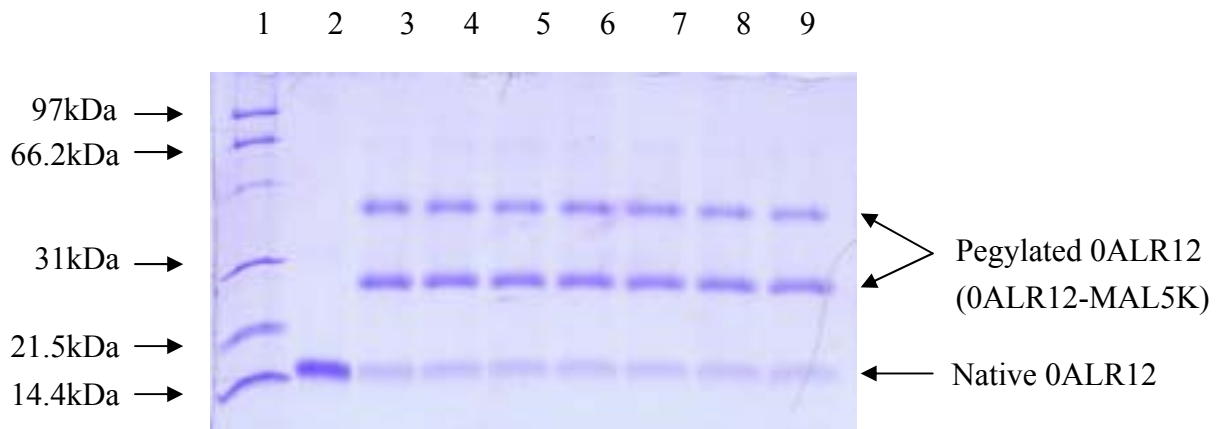


Fig. 3.31 Purified 0ALR12 was modified with mPEG-MAL. 12 % of SDS-PAGE was used to analyze the reaction products at different time points. Lane 1: low-range protein marker; Lane 2: native 0ALR12. Lanes 3, 4, 5, 6, 7, 8, 9 are 1 h, 2 h, 3 h, 4 h, 5 h, 6 h, overnight, respectively.

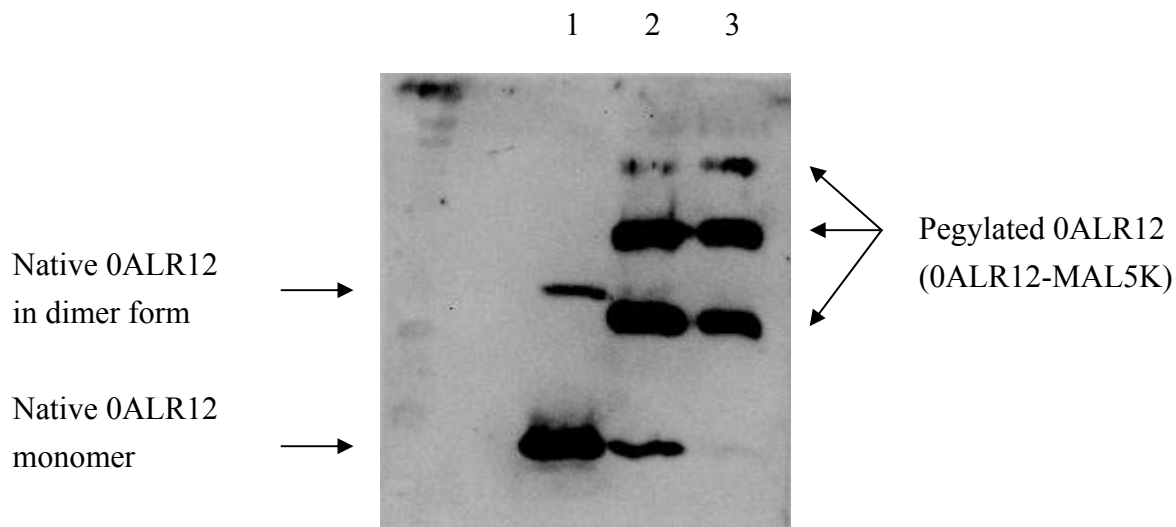
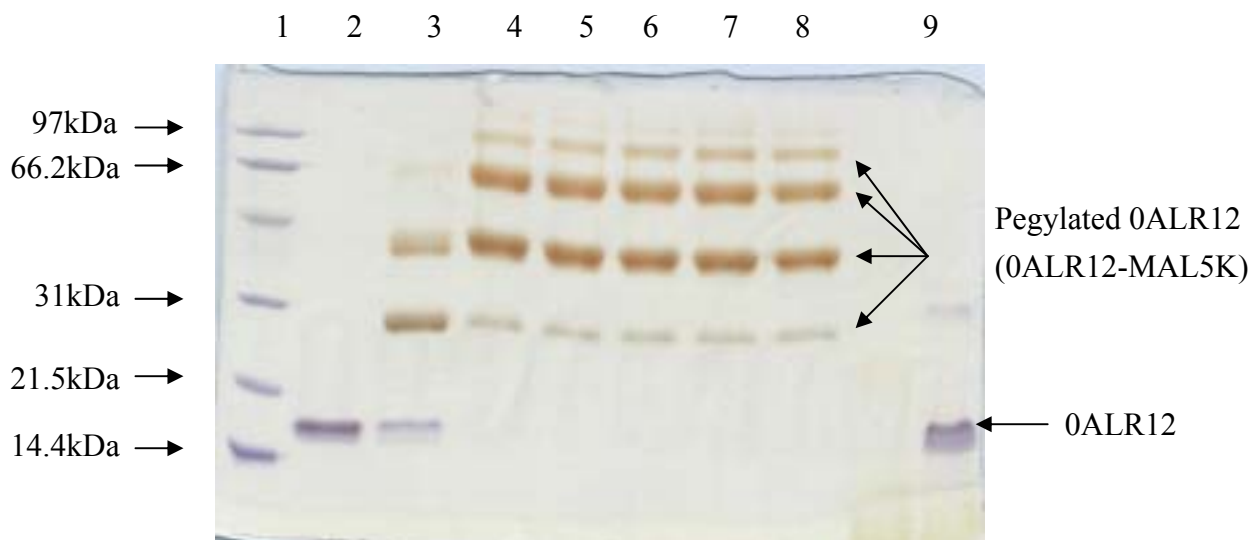


Fig. 3.32 Western blot analysis of purified 0ALR12 and its pegylated products (0ALR12-MAL5K). Anti-His primary antibody was used to analyze the pegylated ALR. Lane 1: native 0ALR12; Lane 2: 0ALR12 was pegylated overnight; Lane 3: pegylated 0ALR12 after buffer exchange with distilled water.

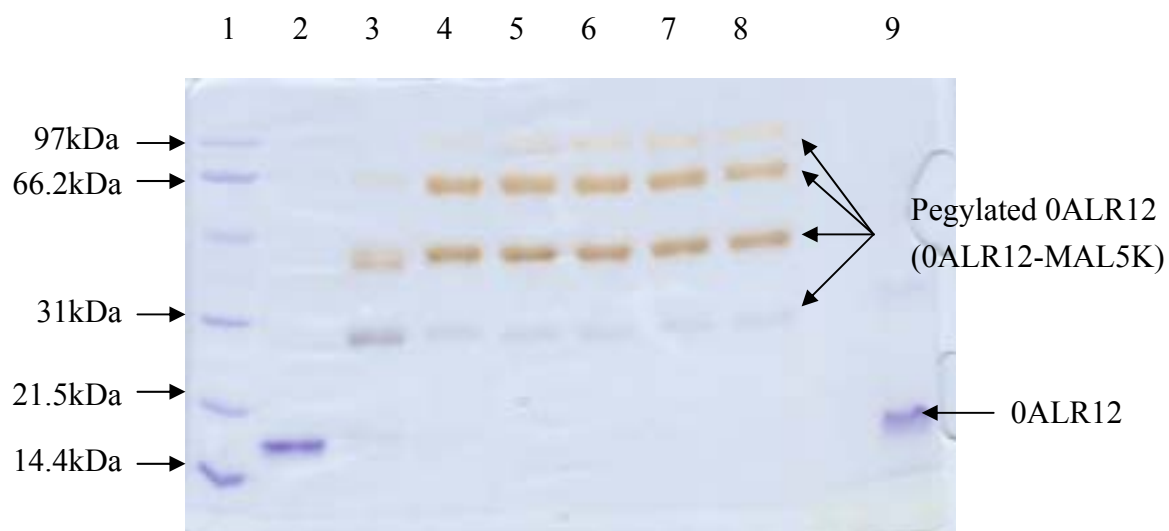
3.3.2 Pegylation of ALR with mPEG-MAL at different mole ratios

mPEG-MAL (MW= 5000) was selected for ALR pegylation. The effect of PEG-to-ALR mole ratio on pegylation was studied. Different mole ratio of mPEG-MAL (1:10, 1:25, 1:50 and 1:100) was allowed to react with 0ALR12. As the PEG-to-ALR mole ratio increased, the amount of native ALR remained was decreased. The time course profile of pegylation products using different (mPEG-MAL)-to-ALR mole ratios were analyzed by 12 % SDS-PAGE and Coomassie blue stain as well as iodine stain as shown in Fig. 3.33. In protein to PEG ratio 1:5 and 1:25, the native protein can still be observed after 1 h stirring while 1:50 has no unpegylated protein in after 1 h mixing. For the protein to PEG ratio 1:10, due to the intensity of dye was too light, the native protein in lane 3 was not obvious. The results suggested that the optimum PEG-to-ALR ratio for the pegylation of ALR was 50:1 and the optimum time used for pegylation was 1 h.

a)



b)



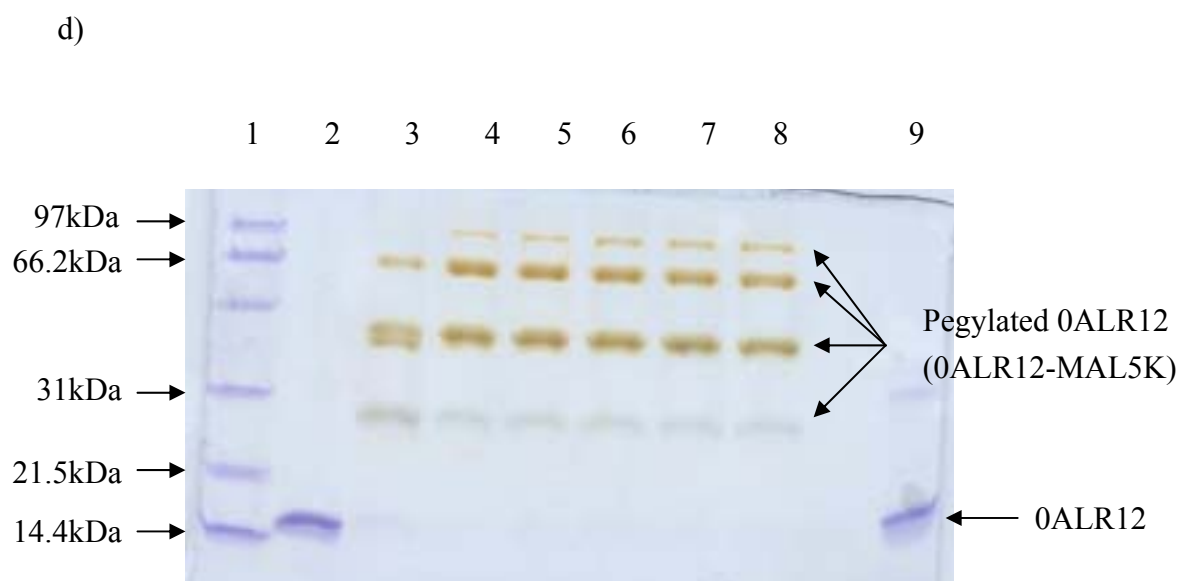
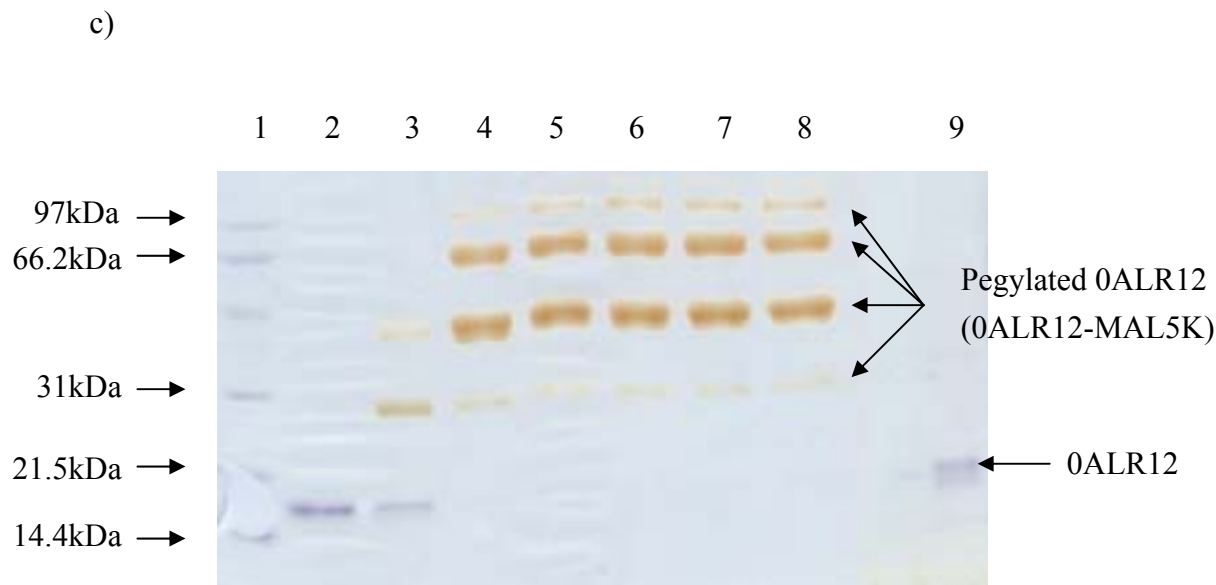


Fig. 3.33 Time course profile of pegylation products of 0ALR12 using different mole ratio of mPEG-MAL were analyzed by Coomassie blue stain and iodine stain. a) protein to PEG ratio 1:5 b) protein to PEG ratio 1:10 c) protein to PEG ratio 1:25 d) protein to PEG ratio 1:50. Lane 1: low-range protein marker; Lane

2: native 0ALR12; Lane 3: 1 min pegylation time; Lane 4: 30 min pegylation time; Lane 5: 1 h pegylation time; Lane 6: 2 h pegylation time; Lane 7: 3 h pegylation time; Lane 8: 0ALR12 was pegylated overnight; Lane 9: 0ALR12 was stirred overnight. The protein was stained blue by Coomassie blue and the pegylated proteins are stained brown by the iodine solution.

3.4 Pilot scale production of recombinant ALR

When ALR was successfully produced and purified from shake flask fermentation, the scale of fermentation was increased from 200 ml to 2-L s in order to scale up the process from small scale to larger scale. Fermentation was carried out in a 2-L Fermentor.

3.4.1 Fed-batch fermentation

The growth curve of the *E. coli* is shown in Fig. 3.34. After cell breaking, the cell debris was centrifuged down and supernatant was collected for affinity chromatography. The elution profile is shown in Fig. 3.35. 0ALR12 was come out form the fourth peak. In general, about 660 mg of purified 0ALR12 was obtained from 2-L of *E. coli* culture. Thus, about 330 mg of 0ALR12 was obtained from one liter of bacterial culture. The yield of the fed-batch fermentation (330 mg/L) was around 3 times higher than the batch culture (120 mg/L).

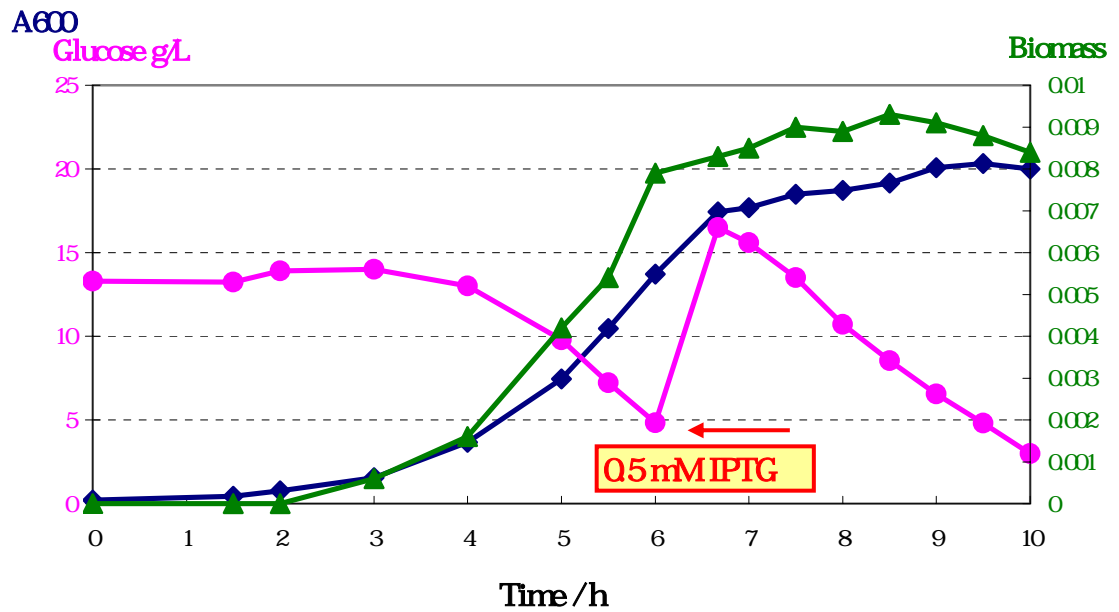


Fig. 3.34 Growth of the *E.coli* strain BL21(DE3)pLysS carrying the ALR gene in a 2-L fermentor. The bacterial growth was monitored by measuring the absorbance at 600 nm (A_{600}). The biomass was measured by weighing the oven-dried mass. The red line is the induction point and glucose feeding point. The scale of absorbance (A_{600}) is the same as the glucose (g/L).

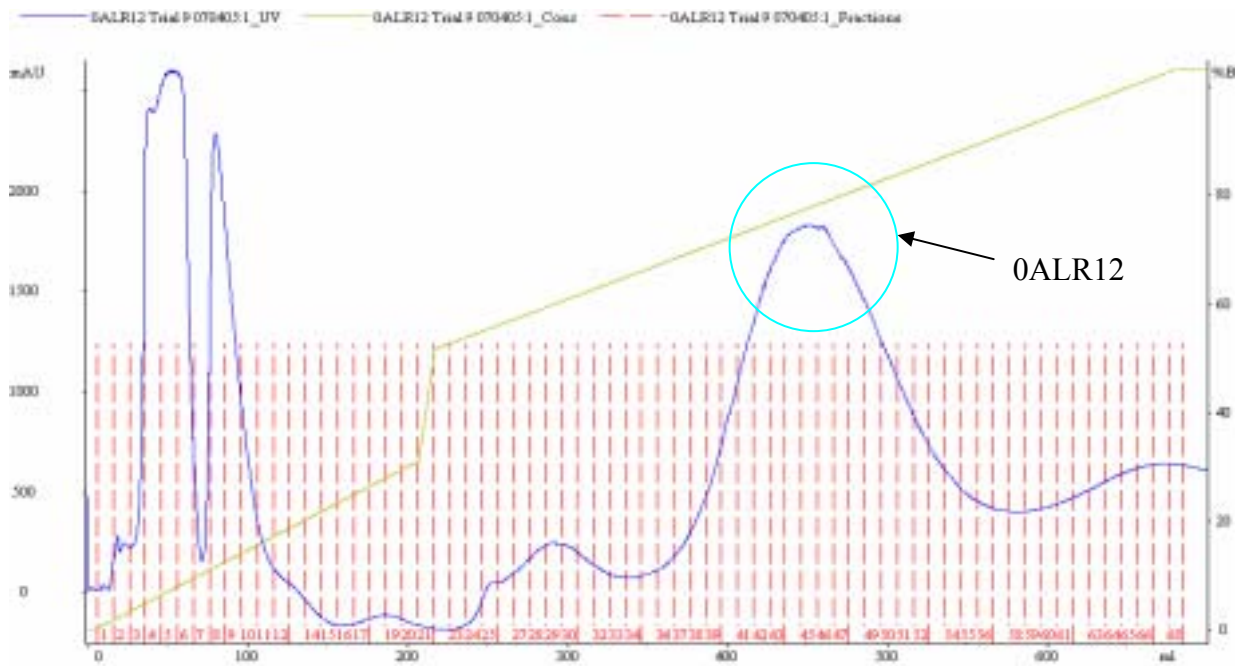


Fig. 3.35 Elution profile of 0ALR12 from a Chelating Sepharose FF column.

The protein concentration of the sample was measured by absorbance at 280 nm. All the measurements were performed by using the Pharmacia AKTA_{FPLC}.

The elution concentration was detected by the conductivity flow cell, and it was represented by conductivity, i.e. 100 % = 0.5 M imidazole.

Chapter Four:

Discussion

ALR plays a very important role in regulation of liver regeneration. It enhances the survival rate of liver failure animals (Zhang *et al.*, 2005), stimulates hepatic cell proliferation (Zhang *et al.*, 2001) and is able to promote hepatic cell regeneration by inhibiting hepatic natural killer cells (Tanigawa *et al.*, 2000) and liver-resident mononuclear leukocytes (Rose *et al.*, 1997) in acute liver injury. The application of ALR as a pharmaceutical agent is getting more attention nowadays. In order to produce sufficient amount of ALR for studies, recombinant DNA technology was used.

Recombinant DNA technology has been used for the production of medical proteins over twenty years. In 1985, the US Company Genentech produced hGH (human growth factor) and human insulin by introducing vectors with hGH and human insulin to *E. coli*. In 1986, Chiron Corp. succeeded in producing vaccines against hepatitis B virus surface antigen with yeast. The recombination of DNA is a technique that artificially alters DNA. First, the target gene (DNA) is fished out from a cDNA library and then sub-cloned to an appropriate expression vector. After the sub-cloning, it is called “recombinant DNA”. The recombinant DNA is then introduced into a bacterium, and the DNA sequence can undergo replication, transcription and translation to

synthesize protein. Bacteria reproduce rapidly and hence the selected gene and its gene product (protein) can be intensively produced.

In this project, the recombinant hALR was expressed in a Gram-negative bacterium *E. coli*. The advantages of using *E. coli* system for protein expression are easy to grow and can achieve high expression level, which increase the yield of hALR. In addition, the genetics are well-understood and the culture media are relatively cheap. The recombinant hALR gene was put under the control of T7 promoter in the pAED4 plasmid. The C-terminus coding sequence of the hALR gene was fused with different numbers of histidines to facilitate purification of the gene products (Valdez-Ortiz *et al.*, 2005, Schmidbauer *et al.*, 1997)

4.1 Small scale production and purification of ALR

Shake flask culture is a convenient method to grow microorganism in a submerged culture especially in a research and development level. Also it is an essential step to find out the optimal conditions before scaling up to production level.

For the native ALR (0ALR0), the purification steps were more complex and time consuming after breaking the cells. In the gel filtration chromatography, 0ALR0 was eluted in the second peak and the purity was about 85 %. The purity was lower than the His-tagged ones (see Figs. 3.7 and 3.9). Moreover, the efficiency was low especially for the gel filtration step. It took over a day to prepare, run and clean the column, and also, only a small volume of samples (about 10 ml) could be applied to the column each time. Therefore, another method has been tested to replace the gel filtration chromatography. As the pI value of 0ALR0 is 7.14, the anion exchanger (Q XL) was used to purify the protein when the protein was in 20 mM Tris-HCl (pH 8.0). The protein could successfully bind to this column. However, when 0.5 M NaCl in 20 mM Tris-HCl (pH 8.0) was used to elute the protein, 0ALR0 as well as a large amount of

other specific proteins were eluted together. So this step could only remove about 5 % of the non-specific proteins.

For 0ALR6 and 0ALR12, purification was done by making use of the polyhistidyl-tag at the C-terminus of the protein. The purity of 0ALR12 can be up to 95 % whereas that of 0ALR6 can only be up to 85 %. This may be due to the presence of 6 more His residues in 0ALR12 which make the protein to bind more strongly to the column. Therefore, the protein would be eluted out at a higher concentration of imidazole, increasing the purity of the protein. Therefore it is essential to add a suitable His-tag to ALR for the ease of the purification both in research scale and production scale.

4.2 Optimization of ALR production

Our results showed that all 4 proteins have a substantial amount of insoluble proteins. We tried to increase the soluble protein amount by lowering the incubation temperature (Weickert *et al.*, 1997). The temperature of 30 °C was tested; however, the amount of soluble protein was not increased at this temperature. The yield of FAD-binding proteins can be increased by adding riboflavin to the culture medium (Yoshikane *et al.*, 2004). Since ALR is a FAD-binding protein (Wu *et al.*, 2003), addition of riboflavin is expected to increase the expression level and increase the active form of ALR. As riboflavin is the pre-cursor of FAD, riboflavin enters the *E. coli* cells and be changed to FAD by certain pathways and therefore FAD-binding proteins can have sufficient FAD for their synthesis. In addition, *E. coli* cells can only transport riboflavin but not FAD and change riboflavin to FAD in the cells, and so far, there are no reports that the cells can transport FAD into the cells. We reported here that when 50 mM riboflavin was added to the culture medium, the yield of 0ALR12 was increased up to 120 mg/L.

4.3 ALR solubility

Although the ALR proteins were successfully purified, they precipitated easily during buffer exchange. The 0ALR6 and 0LAR12 precipitated easily when changing from elution buffer to phosphate buffer saline (PBS) or distilled water; the protein concentration could not be set higher than 0.02 mg/ml. The decrease in solubility may be due to the length of polyhistidine tag, as 12 histidine tags was added to the native protein, the solubility was decreased by 23 % and 0ALR18 was not soluble at all. However, in some other proteins, the length of polyhistidine tag was significant effect on solubilization such as *E. coli* water channel protein aquaporin Z (AqpZ) (Arun *et al.*, 2004). As the proteins are quite stable in imidazole buffer, this buffer might contribute to stabilize the proteins. Therefore, several commonly used stabilizers were tried such as sorbitol, glycerol, NaCl, glucose and MgCl₂ (Barbour *et al.*, 2002). However, all these stabilizers did not improve the solubility. Intriguingly, amino acid histidine was tried and it worked well to keep ALR soluble. Protein concentrations could be set at up to 1 mg/ml in 100 mM histidine solution. As the common functional group between imidazole and histidine is the imidazole ring, so imidazole ring seems to stabilize ALR. Golovanov *et al* (2004) also

reported that using Arg and Glu can improve protein solubility and long-term stability. It has also been observed that when ALR was freeze-dried in Tris buffer and PBS, the yellowish powder could not be re-suspended and dissolved in any buffer. The freeze-drying process could have destroyed the native structure of the protein. However, when the protein was freeze-dried in histidine buffer, the yellowish powder could be re-suspended in PBS and even distilled water. It has been reported that histidine functions as a buffer (Osterberg *et al.*, 1997). In addition, the histidine molecules may protect ALR from surface adsorption and may preserve the structural integrity of the molecules during freeze-drying and buffer exchange. Histidine also reduces solution viscosity (Chen *et al.*, 2003). The important point is that we have shown for the first time that histidine has protective and stabilizing properties towards ALR.

4.4 Dimer formation

After purification, several forms of ALR were found in elution buffer. In Fig 3.15, the SDS-PAGE analysis shows that there were four bands after purification of 0ALR12. After adding reducing agent DTT to the loading dye, only one band was left, which means that all the different forms were reduced and only monomer was left, indicating that those bands might be due to monomer, dimer, trimer and tetramer of 0ALR12. It is interesting that after buffer exchange to histidine solution, only monomer and dimer were left and other bands were gone. In addition, mass spectroscopy (ESI-MS) detected the dimer form of the protein. Fig. 3.21 shows the peak at 33436.3 Da, which was due to the dimer of 0ALR12. Since there was 91 Da difference from the theoretical value, it could be due to the attachment of phosphate ion (PO_4) to the ALR. This suggested that the native form of the ALR should be in dimer and monomer forms but they might also interact with each other to form trimer and tetramer. However, histidine solution stabilizes the protein and so the protein cannot form trimer and tetramer. This might be the reason for the dramatic increase in solubility of ALR in histidine solution.

4.5 Pegylation of ALR

The disadvantages of using 0ALR12 or wild-type ALR as a pharmaceutical agent include the poor solubility of ALR and the presence of histidine in the buffer. Although histidine is safe to human, the adverse effect of prolonged injection of excessive amino acid is hard to determine. On the other hand, pegylation is a well developed process for pharmaceutical agents with several potential clinical advantages such as the lack of immunogenicity, the increase in half life and FDA has approved it for the use in pharmaceuticals (Harris *et al.*, 2003).

In this project, 0ALR12 was pegylated with four different PEGs. They are: mPEG-NHS, mPEG-MAL, mPEG-SPA and mPEG-ALD. For these four PEGs, mPEG-MAL is a cysteine-active PEG whereas mPEG-ALD, mPEG-NHS and mPEG-SPA are lysine-active. They are commercially available from Shearwater Corp. of Huntsville, AL, now known as Nektar Therapeutics, AL.

From our results, mPEG-NHS and mPEG-ALD were not suitable for the pegylation of ALR. One possible reason is the pegylation reaction condition is

not good enough for ALR. In Figs. 3.28-29, more than 90 % of 0ALR12 remained unpegylated. In Fig. 3.30, although mPEG-SPA showed signs of pegylation, only less than 5 % of ALR was pegylated. The results indicated that mPEG-NHS, mPEG-ALD and mPEG-SPA were not suitable for the coupling of ALR in elution buffer (0.5 M NaCl, 0.02 M sodium phosphate, 0.5 M imidazole, pH 7.4) at room temperature. mPEG-NHS and mPEG-SPA are both specific for primary amine (lysine specific). hALR has seven lysine residues and the lack of coupling might be due to the structure of hALR that all lysine residues might be located at the inside of the protein and not on the surface, and so the PEGs could not react with them. Another possible reason could be the presence of imidazole (Fig 4.1b). The NH in imidazole ring with lone pair of electrons acts as a nucleophile and it will attack the carbonyl group of the PEGs just like the amine does. Although the nucleophilicity of primary amine is stronger than that of the imidazole, the concentration of the imidazole in elution buffer is much higher than the concentration of the protein. Thus, most of the PEGs may couple with the imidazole instead of the hALR. In addition, although mPEG-ALD has higher affinity for N-terminal amine than the lysine, it still could not be attached to hALR.

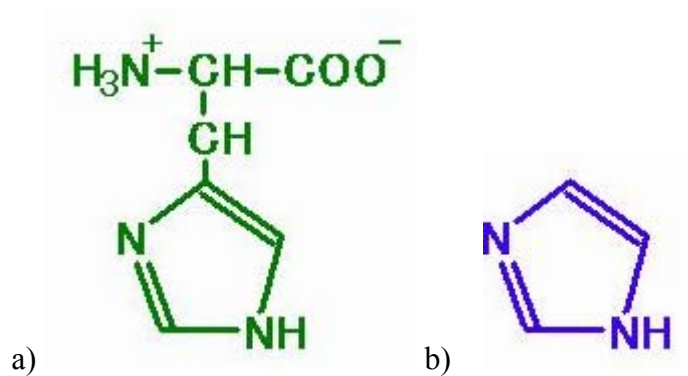


Fig. 4.1 The chemical structure of a) histidine and b) imidazole.

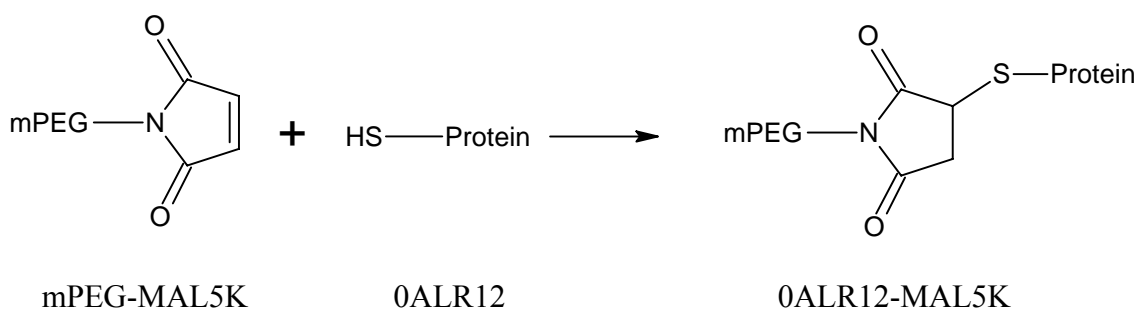


Fig. 4.2 The coupling reaction between 0ALR12 and mPEG-MAL.

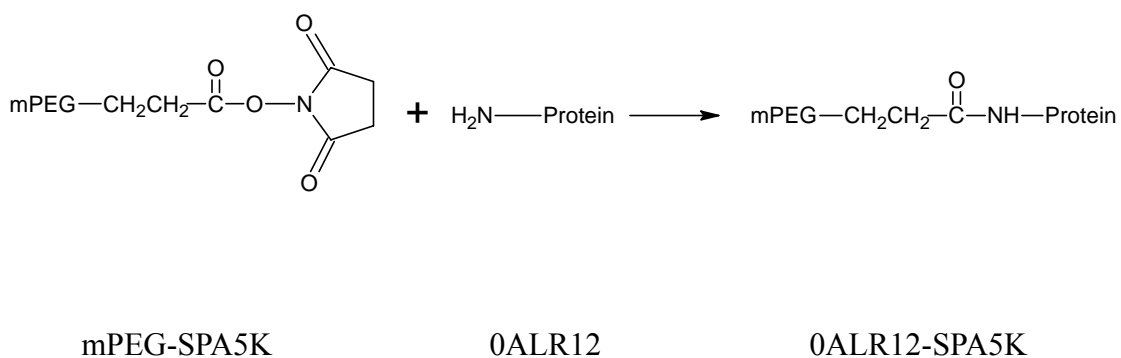


Fig. 4.3 The coupling reaction between 0ALR12 and mPEG-SPA.

One possible solution was to do buffer exchange in order to remove the imidazole. However, any buffer exchange would result in precipitation and histidine (Fig. 4.1a) would affect the pegylation by reacting with the PEG itself. As histidine also contains the imidazole ring, so it also has similar effect as imidazole. Therefore, mPEG-NHS, mPEG-ALD and mPEG-SPA were not used in this experiment.

Finally, mPEG-MAL was selected for ALR pegylation because mPEG-MAL could be reacted with ALR (Fig. 4.2) without any buffer exchange and at room temperature (Fig. 3.31). The optimal mole ratio of ALR to mPEG-MAL molecules was 1: 50 for 1 h pegylation time. However, in order to make it more cost effective, longer time for coupling at lower mole ratio would be preferred, such as using overnight coupling at 1: 25 mole ratio. With the addition of such a mole ratio of protein to mPEG-MAL, over 90 % of the 0ALR12 was pegylated resulting in an increased molecular size (Fig 3.32). After buffer exchange with distilled water, only the pegylated protein was isolated and the native ALR was precipitated and filtered out. Thus, pegylation increases the solubility of ALR and the protein concentration can go up to 1 mg/ml in distilled water. Moreover, the pegylated protein even showed enhanced

sulfhydryl oxidase activity (Fig 3.24) and cell proliferation activity towards the liver cells HepG2 (Fig 3.27). This suggested that the coupling of the mPEG-MAL with the cysteine residues did not affect or block the active site of ALR. The enhancement of activity might be due to the increase in stability of the protein and the absence of histidine in the buffer. The result of western blot showed that there are three bands of pegylated ALR. One possible reason is that at least three of the seven cysteines could couple with mPEG-MAL and therefore three different sizes of the pegylated protein molecules were observed. In addition, the pegylated protein can be freeze-dried and re-suspended in PBS as well as distilled water without loss of activity.

4.6 Characterization of the recombinant human ALR

4.6.1 Far-UV circular dichroism (CD) analysis

Far UV-CD was used to estimate the secondary structure of the proteins. The Jasco software was used and the results showed that the secondary structures of 0ALR6 and 0ALR12 are similar, whereas 0ALR0 has some differences in the proportion of alpha helix and beta sheet. These differences may be due to the presence of the polyhistidine-tag at the C-terminus of the protein. Table 3.3 shows that the pegylated protein 0ALR12-MAL5K also has similar secondary structure as 0ALR12. Pegylation does not affect the secondary and tertiary structures of many proteins (Hinds *et al.*, 2002), since the PEG coupling only occurs on the surface of the protein; and hence suggesting that pegylation only affects the size but not the structure.

4.6.2 Spectroscopy of recombinant ALR

Visible spectra show that FAD molecules are bound to 0ALR0, 0ALR6 and 0ALR12. The FAD spectrum shifted by 4-5 nm as FAD was bound, and the yellowish colour of the protein can also suggest the presence of FAD in the protein. When the protein undergoes heat treatment (boiling at 100 °C for 1 h) and 5 % TCA treatment, the protein precipitated out and only the free FAD was left and, so the FAD spectrum is shifted backward. By comparing the FAD concentration with the ALR concentration, we found that the ratio is about 0.8 which means that there is only 80 % of the protein contains FAD. This ratio is quite consistent in 0ALR0, 0ALR6 and 0ALR12.

4.6.3 Sulphydryl oxidase activity

Yeast Erv1p and human Q6 protein have been reported to have sulphydryl oxidase activity. Our results showed that 0ALR0, 0ALR6, 0ALR12 also have the sulphydryl oxidase activity. Among these three proteins, 0ALR0 has the highest activity followed by 0ALR12. The 0ALR6 protein only has half of this activity.

In addition, the pegylated protein 0ALR12-MAL5K also has the sulphydryl oxidase activity, which is about 90 % of the native 0ALR12. One of the considerations of using cysteine-active mPEG-MAL is that if the PEG could bind to the redox active disulfide pairs, the sulphydryl oxidase activity of ALR could much be affected. Fig. 3.24 shows the presence of activity, which proved that the pegylation did not alter the internal disulfide pairs in C62 and C65, and also the coupling reaction only occurred on the surface of the protein under native conditions. Moreover, the enhancement of the activity may be due to the increase in the protein stability, which may stabilize the substrate binding, and so the reaction rate would be increased.

4.6.4 Cell proliferation activity test

In the biological activity test, all native proteins (0ALR0, 0ALR6, 0ALR12) show stimulating effect on the cell proliferation of the HepG2 liver cells. The stimulatory effect for 50 nM of 0ALR6 and 0ALR12 is also significantly higher than 100 pM. We used the pHGF as a positive control which is a commercial drug in China to treat liver failure. In this experiment, 71 pM of pHGF was used. When comparing with ALR, their effects were similar. The results of the sulfhydryl oxidase activity assay showed that 0ALR6 was less active than 0ALR0 and 0ALR12. But in this cell proliferation assay, these proteins showed similar activity. Thus, it seems that the mechanisms of these two assays are different and the results are not correlated. In addition, the pegylated protein, 0ALR12-MAL5K, also showed stimulating effect towards HepG2 and the effect was even more significant than the native one. This suggests that the attachment of PEG does not affect the protein binding towards the specific receptor on the HepG2 cells. Moreover, the increase in activity may be due to the improved stability of the protein, and so the protein can bind to the receptor for a longer time without precipitation.

ALR was reported as cell specific (Wang *et al.*, 1999) and so different cell lines were used to test the cell specificity in our studies. Cell specificity is very important for a drug to be both effective and safe. If the protein is not cell specific, such as epidermal growth factor (EGF), it will accelerate the growth of ectoderm, blood capillary and can promote the growth of epidermis (Wong *et al.*, 2004). The effect is so wide spread that it may cause side effects other than to promote the cell regeneration of the liver. In Fig. 3.25, 0ALR12 seems to have no stimulating effect on the cell lines from other organs such as breast, colorectal and lung. One possible reason for that was the lack of ALR receptors in these cell lines. All these data suggest that the effect of ALR is specific to liver cells.

Furthermore, it will be important to perform animal tests to see if the ALR proteins can enhance the regeneration and protective effect towards liver in an animal model such as mouse.

4.7 Summary of the properties of ALR proteins

Table 4.1 summarizes the properties of different polyhistidyl-tagged ALR proteins. The wild-type protein, 0ALR0, is the most soluble and has high sulfhydryl oxidase activity. However, the purification is complicated and efficiency is low, and so it is not suitable for large scale production. For 0ALR6, although it has the highest yield and a simple purification step, the sulfhydryl oxidase activity is very poor and the biological activity is not as good as 0ALR12 and so it is not a good choice. The 0ALR12, protein is the preferred choice, as it has a reasonable yield, the highest purity and a simple purification step, and the sulfhydryl oxidase activity as well as biological activity are both the highest.

Table 4.1 Summary of the properties of 0ALR0, 0ALR6 and 0ALR12.

	0ALR0	0ALR6	0ALR12
Ease of purification	+	+++	+++
Purity	~ 70 %	~ 85 %	~ 95 %
Yield	30 mg/L	150 mg/L	120 mg/L
Solubility in elution buffer	High	Medium	Medium
Sulphydryl oxidase activity	+++	+	+++
Biological activity	+	++	+++

4.8 Pilot scale production of ALR in fed-batch fermentation

As a potential pharmaceutical agent, it would be important to ensure that the production could be scaled up in order to get large quantities of the ALR protein. Therefore, ALR was produced in a 2-L fermentor containing 1.6 L of culture under fed-batch conditions.

In batch fermentation (such as shake flask culture), the *E. coli* was inoculated in the sterile medium without monitoring the growth conditions and without adding more nutrient to the culture. Fed-batch fermentation is a production technique in between batch and continuous fermentation (Longobardi *et al.*, 1994). In fed-batch culture, glucose was added after induction to provide sufficient carbon source for supporting high cell density (Shiloach *et al.*, 2005), thus, resulted in increased biomass and protein production. Although the fed-batch fermentation requires more equipment for monitoring and feeding, it is more common for handling large amount of culture. Therefore, it is essential for the development of the expression system for the production of 0ALR12 by *E. coli* to achieve large amount of products.

The results from batch (shake flask) and fed-batch fermentations are summarized in Table 4.2. The optical density of the cultures was increased from 3.6 to 20 whereas the yield of purified protein was increased from 120 mg/L to 330 mg/L. The cell density was increased more than 5 times but the yield has only improved by less than 3 times. This might be due to insufficient nutrient supply for the cell production as we have limited information about the protein production at high cell density. Another possible reason is that the protein was lost during the purification. Nevertheless, the use of fed-batch fermentation was found to be useful for increasing 3 times more ALR protein than batch fermentation.

Table 4.2 Summary of the cell density and yield of 0ALR12 from batch and fed-batch fermentation trials.

	Batch fermentation	Fed-Batch fermentation
Max. cell density/ A_{600}	3.6	20
Yield	120 mg/L	330 mg/L

Chapter Five: Future work

Optimization of the production and purification in large scale fermentation

In order to achieve the production scale, larger scale fermentation (such as 20-L) should be carried out to investigate the process performance in different conditions. Moreover, the purification should be optimized by minimizing the purification steps in order to prevent protein loss and increase product purity.

Removal of endotoxin

Endotoxins liberated by Gram-negative bacteria such as *E. coli* contaminated frequently the protein produced from bioprocesses. As their high toxicity *in vivo* and *in vitro*, removal of endotoxins is an essential step for a pharmaceutical agent (Petsch *et al.*, 2000).

The *in vivo* half-life studies of the ALR

The half-life of a drug is the time required for the body to eliminate or biotransform half of the amount present in the body at any given point. This

suggests that elimination such as metabolism and excretion are the rate limiting factors more important than the other pharmacokinetic variables. So the animal test may be used to calculate the half-life of the drug in mouse to compare the rate of protein depletion between the native ALR and the pegylated ALR.

Optimization of pegylation

It will be useful to calculate how many PEG molecules are attached to an ALR molecule and identify the sites in the protein which are occupied. In addition, optimizing the pegylated ratio and standardizing the site of reaction can increase the efficiency of pegylation.

Chapter Six:

Conclusion

In this study, the effects of different lengths of poly-histidine tags attached to the C-terminus of recombinant hALR were studied. The derivatives were produced in a Gram-negative bacterium *E. coli*. The 0ALR0, 0ALR6 and 0ALR12 were purified and characterized. However, 0ALR18 was insoluble and was not purified. After comparing their characteristics, 0ALR12 was chosen as it is more easy to be purified than 0ALR0 and has better biological activity and sulfhydryl oxidase activity than 0ALR6. The yield was increased by about 300% when using fed-batch fermentation instead of batch (shake-flask) fermentation, from 120 mg/L to 330 mg/L, with purity over 95 %. The purification protocol for the recombinant hALR comprised of only one single step: a Chelating Sepharose affinity chromatography step. The developed protocol provides a simple and convenient method for the purification of active hALR. In order to solve the insolubility problem of the hALR, two methods were used to enhance the stability of hALR: the use of histidine solution and pegylation of the protein. After buffer exchange with histidine solution, the solubility of protein was increased by 50 times from 0.02 mg/ml to 1 mg/ml. Another solution is to increase the solubility in MilliQ water by modifying the protein with polyethylene glycol (PEG). The pegylated protein was fully active in its enzymatic and biological activities. The results of this project provide a

simple and efficient method to produce large amount of pure and active hALR.

These data will certainly facilitate the development of the recombinant hALR

as pharmacological agents in the treatment of liver failure.

References

Arun K. Mohanty and Michael C. Wiener (2004) "Membrane protein expression and production: effects of polyhistidine tag length and position" *Protein Expression and Purification.*, 33; 2: 311-325

Bang D, Kent SB. (2005) "His6 tag-assisted chemical protein synthesis" *Proc Natl Acad Sci U S A.*, 5;102: 5014-9

Barbour EK, Abdelnour A, Jirjis F, Faroon O, Farran MT. (2002) "Evaluation of 12 stabilizers in a developed attenuated Salmonella Enteritidis vaccine" *Vaccine* 22;20:2249-53

Bradford MM. (1976), "A rapid and sensitive method for the quantitation of microgram quantities of protein utilizing the principle of protein-dye binding", *Anal Biochem* 7;72: 248-54

Bowen S, Tare N, Inoue T, Yamasaki M, Okabe M, Horii I, Eliason JF. (1999) "Relationship between molecular mass and duration of activity of polyethylene glycol conjugated granulocyte colony-stimulating factor mutein" *Exp Hematol.* 27;3:425-32.

Carpenter G, Cohen S. (1979) "Epidermal growth factor" *Annu Rev Biochem.* 1;48:193-216.

Chen, X., Li, Y., Wei, K., Li, L., Liu, W., Zhu, Y., Qiu, Z.Y., and He, F. C. (2003) "The potentiation role of hepatopoietin on activator protein-1 is dependent on its sulfhydryl oxidase activity" *J. Biol. Chem.* 278; 49022-49030

Chen B, Bautista R, Yu K, Zapata GA, Mulkerrin MG, Chamow SM. (2003) "Influence of histidine on the stability and physical properties of a fully human antibody in aqueous and solid forms" *Pharm Res.* 20;12:1952-60

Cohen S. (1962) "Isolation of a mouse submaxillary gland protein accelerating incisor eruption and eyelid opening in the new-born animal" *J Biol Chem.*237:1555-62.

Cohen SN, Chang AC, Hsu L.(1972) "Nonchromosomal antibiotic resistance in bacteria: genetic transformation of *Escherichia coli* by R-factor DNA" *Proc Natl Acad Sci U S A.* 69:2110-4.

Diwan M, Park TG. (2003) "Stabilization of recombinant interferon-alpha by pegylation for encapsulation in PLGA microspheres" *Int J Pharm.* 18;252:111-22.

Fleig WE, Hoss G. (1989) "Partial purification of rat hepatic stimulator substance and characterization of its action on hepatoma cells and normal hepatocytes" *Hepatology.* 9;2:240-8.

Francavilla A, Hagiya M, Porter KA, Polimeno L, Ihara I, Starzl TE. (1994) "Augmenter of liver regeneration: its place in the universe of hepatic growth factors" *Hepatology* 20;3:747-57.

Francavilla A, Ove P, Polimeno L, Coetzee M, Makowka L, Barone M, Van Thiel DH, Starzl TE. (1988), "Regulation of liver size and regeneration: importance in liver transplantation." *Transplant Proc.* 20:494-7

Francavilla A, Ove P, Polimeno L, Coetzee M, Makowka L, Rose J, Van Thiel DH, Starzl TE. (1987) "Extraction and partial purification of a hepatic stimulatory substance in rats, mice, and dogs" *Cancer Res.* 1;47:5600-5.

Fuertges F., Abuchowski A. (1990) "The clinical efficacy of poly(ethylene glycol)-modified proteins" *J. Control. Release* 11;139-148.

Gandhi CR, Kuddus R, Subbotin VM, Prelich J, Murase N, Rao AS, Nalesnik MA, Watkins SC, DeLeo A, Trucco M, Starzl TE. (1999) "A fresh look at augmentor of liver regeneration in rats" *Hepatology* 29;5:1435-45.

Garcia-Ruiz C, Colell A, Mari M, Morales A, Calvo M, Enrich C, Fernandez-Checa JC. (2003) "Defective TNF-alpha-mediated hepatocellular apoptosis and liver damage in acidic sphingomyelinase knockout mice" *J Clin Invest.* 111;2:197-208.

Giorda R, Hagiya M, Seki T, Shimonishi M, Sakai H, Michaelson J, Francavilla A, Starzl TE, Trucco M. (1996) "Analysis of the structure and expression of the augmentor of liver regeneration (ALR) gene" *Mol Med.* 2;1:97-108.

Grivell LA. (1989) "Nucleo-mitochondrial interactions in yeast mitochondrial biogenesis" *Eur J Biochem.* 1;182:477-93.

Golovanov AP, Hautbergue GM, Wilson SA, Lian LY. (2004) "A simple method for improving protein solubility and long-term stability." *J Am Chem Soc.* 28;126:8933-9.

Gu W.F., Hu X.J., He L.M, (2003) "Analysis of the therapeutic effect of Weijia serve chronic B type viral hepatitis" *Chi. J Clin. Hepatology* 19;1: 39-40 (in Chinese)

Hagiya M., Francavilla A., Polimeno L., Ihara I., Sakai H., Seki T., Shimonishi M., Porter K.A., and Starzl T.E. (1994) "Cloning and sequence analysis of the rat augments of liver regeneration (ALR) gene: Expression of biologically active recombinant ALR and demonstration of tissue distribution" *Proc Natl Acad Sci USA* 91: 8142-46

Hans M, Shimoni K, Danino D, Siegel SJ, Lowman A. (2005) "Synthesis and characterization of mPEG-PLA prodrug micelles" *Biomacromolecules* 6;5:2708-17.

Harris JM, Chess RB. (2003) "Effect of pegylation on pharmaceuticals" *Nat Rev Drug Discov.* 2;3:214-21

Harris RC, Chung E, Coffey RJ. (2003) "EGF receptor ligands" *Exp. Cell Res.* 284, 2-13.

He F, Wu C, Tu Q, Xing G. (1993) "Human hepatic stimulator substance: a product of gene expression of human fetal liver tissue" *Hepatology* 17;2:225-9.

Higgins, G.M. & Anderson, R.M. (1931) "Experimental pathology of the liver. 1. Restoration of the white rat following partial surgical removal." *Arch. Pathol.* 12: 186-202

Hinds KD, Kim SW. (2002) "Effects of PEG conjugation on insulin properties" *Adv Drug Deliv Rev.* 17;54:505-30

Hinds KD, Campbell KM, Holland KM, Lewis DH, Piche CA, Schmidt PG. (2005) "PEGylated insulin in PLGA microparticles. In vivo and in vitro analysis" *J Control Release.* 2;104:447-60.

Hofhaus G, Lee JE, Tews I, Rosenberg B, Lisowsky T. (2003) "The N-terminal cysteine pair of yeast sulfhydryl oxidase Erv1p is essential for in vivo activity and interacts with the primary redox centre" *Eur J Biochem.* 270, 1528-35.

Hofhaus G, Stein G, Polimeno L, Francavilla A, Lisowsky T. (1999) "Highly divergent amino termini of the homologous human ALR and yeast scERV1 gene products define species specific differences in cellular localization" *Eur J Cell Biol.* 78, 349-56.

Khoo KM, Chang CF, Schubert J, Wondrak E, Chng HH. (2005) "Expression and purification of the recombinant His-tagged GST-CD38 fusion protein using the baculovirus/insect cell expression system" *Protein Expr Purif.* 40;2:396-403

Kompella U.B. and Lee V.H.L. (1991) "Pharmacokinetics of peptide and protein drugs" *Peptide and Protein Drug Delivery*, 391.

Kong XP, Yang WS, Shen GM (1989) "Experimental research about the activity of the hepatocytes stimulating factor" *Tianjin Medicine* 17;7:401

Koniaris LG, McKillop IH, Schwartz SI, Zimmers TA. (2003) "Liver regeneration" *J Am Coll Surg.* 197;4:634-59

Kurfurst MM. (1992) "Detection and molecular weight determination of polyethylene glycol-modified hirudin by staining after sodium dodecyl sulfate-polyacrylamide gel electrophoresis" *Anal Biochem.* 1;200:244-8.

LaBrecque D.R.(1991) "Hepatic Stimulator Substance. Discovery, characteristics and mechanism of action" *Digest Liver Dis* 36(5): 669-73

LaBrecque DR, Steele G, Fogerty S, Wilson M, Barton J. (1987) "Purification and physical-chemical characterization of hepatic stimulator substance" *Hepatology.* ;7;1:100-6.

LaBrecque DR, Bachur NR. (1982) "Hepatic stimulator substance: physicochemical characteristics and specificity" *Am J Physiol.* 242;3:G281-8.

LaBrecque DR, Pesch LA. (1975) "Preparation and partial characterization of hepatic regenerative stimulator substance (SS) from rat liver" *J Physiol.* 248;02:273-84.

Laemmli U.K. (1970) "Cleavage of structural proteins during the assembly of the head of bacteriophage T4" *Nature.* 227, 680-685

Lange H, Lisowsky T, Gerber J, Muhlenhoff U, Kispal G, Lill R. (2001) "An essential function of the mitochondrial sulfhydryl oxidase Erv1p/ALR in the maturation of cytosolic Fe/S proteins" *EMBO Rep.* 2, 715-20.

Lee, J.-E., Hofhaus, G., and Lisowsky, T. (2000) "Erv1p from *Saccharomyces cerevisiae* is a FAD-linked sulfhydryl oxidase" *FEBS Lett.* 477, 62-66

Li Q, Liu DW, Zhang LM, Zhu B, He YT, Xiao YH. (2005) "Effects of augmentation of liver regeneration recombinant plasmid on rat hepatic fibrosis" *World J Gastroenterol.* 28;11:2438-43.

Li, Y., Li, M., Xing, G. C., Hu, Z. Y., Wang, Q. M., Dong, C. N., Chen, J. Z., Yang, X. M., Chen, H. P., Guan, K. L., Wu, C., Zhang, C. G., and He, F. C. (2000) "Stimulation of the mitogen-activated protein kinase cascade and tyrosine phosphorylation of the epidermal growth factor receptor by hepatopoietin" *J. Biol. Chem.* 275, 37443-37447

Li Y, Wei K, Lu C, Li Y, Li M, Xing G, Wei H, Wang Q, Chen J, Wu C, Chen H, Yang S, He F. (2002) "Identification of hepatopoietin dimerization, its interacting regions and alternative splicing of its transcription" *Eur J Biochem.* 269, 3888-93.

Lisowsky T. (1992) "Dual function of a new nuclear gene for oxidative phosphorylation and vegetative growth in yeast" *Mol Gen Genet.* 232;1:58-64.

Lisowsky T. (1994) "ERV1 is involved in the cell-division cycle and the maintenance of mitochondrial genomes in *Saccharomyces cerevisiae*" *Curr Genet.* 26;1:15-20.

Lisowsky T, Weinstat-Saslow DL, Barton N, Reeders ST, Schneider MC. (1995) "A new human gene located in the PKD1 region of chromosome 16 is a functional homologue to ERV1 of yeast" *Genomics.* 10;29:690-7.

Longobardi G. P. (1994) "Fed-Batch versus Batch Fermentation" *Bioprocess Engineering*, 10, 185-194

Lu J, Xu WX, Zhan YQ, Cui XL, Cai WM, He FC, Yang XM. (2002) "Identification and characterization of a novel isoform of hepatopoietin" *World J Gastroenterol.* 8;2:353-6.

Lu C, Li Y, Zhao Y, Xing G, Tang F, Wang Q, Sun Y, Wei H, Yang X, Wu C, Chen J, Guan KL, Zhang C, Chen H, He F. (2002) "Intracrine hepatopoietin potentiates AP-1 activity through JAB1 independent of MAPK pathway" *FASEB J.* 16;1:90-2.

Michalopoulos, George K.; DeFrances, Marie C. (1997) "Liver Regeneration" *Science.* 276: 60

Michalopoulos GK, DeFrances M. (2005) "Liver regeneration" *Adv Biochem Eng Biotechnol.* 93:101-34.

Nishizuka Y. (1992) "Intracellular signaling by hydrolysis of phospholipids and activation of protein kinase C" *Science.* 258:607-14.

Osterberg T, Fatouros A, Mikaelsson M. (1997) "Development of freeze-dried albumin-free formulation of recombinant factor VIII SQ" *Pharm Res.* 14;7:892-8

Pawlowski R, Jura J. (2006) "ALR and Liver Regeneration" *Mol Cell Biochem.* 12

Pawson T. (1995) "Protein modules and signaling networks" *Nature* 373;573-580.

Petsch D, Anspach FB. (2000) "Endotoxin removal from protein solutions." *J Biotechnol.* 21;76:97-119

Polimeno L, Lisowsky T, Francavilla A. (1999) "From yeast to man--from mitochondria to liver regeneration: a new essential gene family" *Ital J Gastroenterol Hepatol. Ital J Gastroenterol Hepatol.* 31, 494-500

Polimeno L, Margiotta M, Marangi L, Lisowsky T, Azzarone A, Ierardi E, Frassanito MA, Francavilla R, Francavilla A. (2000) "Molecular mechanisms of augmenter of liver regeneration as immunoregulator: its effect on interferon-gamma expression in rat liver" *Dig Liver Dis.* 32, 217-25

Reddy KR. (2000) "Controlled-release, pegylation, liposomal formulations: new mechanisms in the delivery of injectable drugs" *Ann Pharmacother.*;34:915-23

Riddles PW, Blakeley RL, Zerner B. (1979), "Ellman's reagent: 5,5'-dithiobis(2-nitrobenzoic acid)--a reexamination", *Anal. Biochem.* 94: 75-81

Rose JP, Wu CK, Francavilla A, Prelich JG, Iacobellis A, Hagiya M, Rao AS, Starzl TE, Wang BC. (1997) "Crystallization and preliminary crystallographic data for the augmentin of liver regeneration." *Acta Crystallogr D Biol Crystallogr.* 53(Pt 3): 331-334

Sato S, Dai W, Liu XL, Asano G. (1999) "The protective effect of hepatocyte growth-promoting factor (pHGF) against carbon tetrachloride-induced acute liver injury in rats: an ultrastructural study" *Med Electron Microsc.* 32;3:184-192.

Savage CR Jr, Hash JH, Cohen S. (1973) "Epidermal growth factor. Location of disulfide bonds" *J Biol Chem.* 25;248:7669-72.

Schlessinger J, Ullrich A. (1992) "Growth factor signaling by receptor tyrosine kinases" *Neuron* 9;383-391

Schmidbauer SB, Strobel OK. (1997) "Rapid purification of histidine-tagged glutathione S-transferase fusion protein by metal chelate POROS perfusion chromatography media." *Front Biosci.* 15;2:c6-8.

Seeger M, Kraft R, Ferrell K, Bech-Otschir D, Dumdey R, Schade R, Gordon C, Naumann M, Dubiel W. (1998) "A novel protein complex involved in signal transduction possessing similarities to 26S proteasome subunits" *FASEB J.* 12;6:469-78.

Senkevich TG, White CL, Koonin EV, Moss B. (2000) "A viral member of the ERV1/ALR protein family participates in a cytoplasmic pathway of disulfide bond formation" *Proc Natl Acad Sci U S A.* 24;97:12068-73

Shiloach J, Fass R. (2005) "Growing E. coli to high cell density--a historical perspective on method development" *Biotechnol Adv.* 23;5:345-57

Sun Z, Ming L, Zhu X, Lu J. (2002), "Prevention and control of hepatitis B in China.", *J Med Virol.* 67; 3:447-50

Valdez-Ortiz A, Rascon-Cruz Q, Medina-Godoy S, Sinagawa-Garcia SR, Valverde-Gonzalez ME, Paredes-Lopez O. (2005) "One-step purification and structural characterization of a recombinant His-tag 11S globulin expressed in transgenic tobacco." *J Biotechnol.* 23;115:413-23.

Tanigawa K, Sakaida I, Masuhara M, Hagiya M, Okita K. (2000) "Augmenter of liver regeneration (ALR) may promote liver regeneration by reducing natural killer (NK) cell activity in human liver diseases." *J Gastroenterol.* 35; 2:112-9

Terpe K. (2003) "Overview of tag protein fusions: from molecular and biochemical fundamentals to commercial systems", *Appl Microbiol Biotechnol.* 60;5:523-33

Veronese FM. (2001) "Peptide and protein PEGylation: a review of problems and solutions" *Biomaterials.* 22;5:405-17

Veronese FM, Harris JM. (2002) "Introduction and overview of peptide and protein pegylation" *Adv Drug Deliv Rev.* 17;54:453-6

Weickert MJ, Pagratis M, Curry SR, Blackmore R. (1997) "Stabilization of apoglobin by low temperature increases yield of soluble recombinant hemoglobin in *Escherichia coli*", *Appl Environ Microbiol.* 63;11:4313-20

Wang Y, Lu C, Wei H, Wang N, Chen X, Zhang L, Zhai Y, Zhu Y, Lu Y, He F. (2004) "Hepatopietin interacts directly with COP9 signalosome and regulates AP-1 activity" *FEBS Lett.* 13;572:85-91.

Wong RW, Guillaud L. (2004) "The role of epidermal growth factor and its receptors in mammalian CNS" *Cytokine Growth Factor Rev.* 15;2-3:147-56

Wu CK, Dailey TA, Dailey HA, Wang BC, Rose JP (2003) "The crystal structure of augments of liver regeneration: A mammalian FAD-dependent sulfhydryl oxidase" *Protein Sci.* 12;5:1109-18

Xie Q, Guo Q, Zhou XQ (1993) "Experimental study of pHGF for treating acute liver necrosis of duck induced by DHBV" Paper collection of *the Third National Symposium on pHGF*, Guangzhou. 43 (in Chinese)

Wang G, Yang X, Zhang Y, Wang Q, Chen H, Wei H, Xing G, Xie L, Hu Z, Zhang C, Fang D, Wu C, He F. (1999) "Identification and characterization of receptor for mammalian hepatopoietin that is homologous to yeast ERV1" *J Biol Chem.* 274;274:11469-72.

Wu CK, Dailey TA, Dailey HA, Wang BC, Rose JP. (2003) "The crystal structure of augments of liver regeneration: A mammalian FAD-dependent sulfhydryl oxidase" *Protein Sci.* 12;5:1109-18

Yamada M, Ikeuchi T, Hatanaka H. (1997) "The neurotrophic action and signaling of epidermal growth factor" *Prog. Neurobiol.* 51;19-37.

Yang XM, Xie L, He H, Wei HD, Wu ZZ, He FC. (1997) "Expression and Activity of Recombinant Human Augments of Liver Regeneration" *Sheng Wu Hua Xue Yu Sheng Wu Wu Li Xue Bao* 29;4:414-418.

Yang XM, Wang AM, Zhou P, Xie L, Wang QM, Wu ZZ and He FC (1998) “Human hepatopoietin augments liver regeneration — A hepatotrophic factor for liver regeneration, and its potential antihepatitis effect *in vivo*” *Chin Sci Bull* 12; 1026-1031

Yoshikane Y, Yokochi N, Ohnishi K, Yagi T. (2004) “Coenzyme precursor-assisted cooperative overexpression of an active pyridoxine 4-oxidase from *Microbacterium luteolum*” *Protein Expr Purif.* 34;2:243-8

Zhang LM, Liu DW, Liu JB, Zhang XL, Wang XB, Tang LM, Wang LQ. (2005) “Effect of naked eukaryotic expression plasmid encoding rat augments liver regeneration on acute hepatic injury and hepatic failure in rats” *World J Gastroenterol.* 28;11:3680-5

Zhang Y, Kong X, Zheng G, Chen G, Yang E. (1995) “Evaluation of hepatocyte growth-promoting factors in treating 1687 cases of fulminant hepatitis” *Chin Med J (Engl).* 108;12:928-9.

Zhang B, Wang QM, Chen HP. (2001) “Augments liver regeneration: a novel cytokine.” *Sheng Li Ke Xue Jin Zhan.* 32: 31-34

Zhong L, Lu B, Fan Y. (2003) “Observations of the therapeutic effect of pHGF on the treating of cirrhosis of liver after hepatitis” *Chin J Regional Anat & Operative Surg* 12;1: 33-34 (in Chinese)

Zhu QH, Chen HQ, Zhang GS (1993) “Experimental study of the mechanism of pHGF produced domestically” Paper collection of *the Third National Symposium on pHGF*, Guangzhou. 33 (in Chinese)

Zimmermann A. (2004) “Regulation of liver regeneration” *Nephrol Dial Transplant*. 19 Suppl 4:iv6-10.